UNIVERSITA' DEGLI STUDI DI VERONA

DIPARTIMENTO DI BIOTECNOLOGIE

DOTTORATO DI RICERCA IN BIOTECNOLOGIE
MOLECOLARI, INDUSTRIALI ED AMBIETALI

CICLO XXIII

DISSECTING THE GENETIC HETEROGENEITY OF FAMILIAL DEMENTIAS

S.S.D. MED/26

Coordinatore: Prof. Roberto Bassi

Tutor: Prof. Gian Maria Fabrizi

Dottoranda: Dott.ssa Silvia Testi

UNIVERSITA' DEGLI STUDI DI VERONA

DIPARTIMENTO DI BIOTECNOLOGIE

DOTTORATO DI RICERCA IN BIOTECNOLOGIE
MOLECOLARI, INDUSTRIALI ED AMBIETALI

CICLO XXIII

DISSECTING THE GENETIC HETEROGENEITY OF FAMILIAL DEMENTIAS

S.S.D. MED/26

Coordinatore: Prof. Roberto Bassi

Tutor: Prof. Gian Maria Fabrizi

Dottoranda: Dott.ssa Silvia Testi

Table of contents

Abstract

Dementia is a clinical syndrome associated with progressive deterioration of intellectual functions including loss of memory, difficulties with language, simple calculations, planning and judgment, and motor skills with eventually loss of autonomy. Currently there are an estimated 36 million people worldwide with dementia and this figure is set to increase to more than 115 million people by 2050. Given the prevalence of dementia and the associated significant financial and human costs, in recent years there has been a huge burst of studies aimed to identify the causes of this disorder and its underlain pathological mechanisms, in order to define therapeutic treatments to replace the nowadays available palliative cares.

Among different subtypes of dementia, Alzheimer's Disease (AD) is the most frequent form, followed by Vascular Dementia and Frontotemporal Lobar Degeneration (FTLD) which represents the second most common form in people younger than 65 years. All three of these diseases may have a genetic component and, despite considerable progress and efforts made in recent years to clarify their molecular basis, little is known about the pathological mechanisms determining these diseases.

Three forms of dementia, which may have a genetic component, were included in this study: Alzheimer's Disease, Frontotemporal Lobar Degeneration and Cerebral Autosomal Dominant Arteriopathy with Subcortical Infarcts and Leuokoencephalopathy (CADASIL) which is a subtype of vascular dementia. The main objectives of this study included mutational analysis of the genes associated with these diseases with the dual purpose of defining their mutational frequencies in an Italian series and to evaluate the presence of possible genotype-phenotype correlations. The secondary purpose is to be able to draw diagnostic algorithms useful to clinicians in selecting which patients submit to genetic testing.

Two clinical cohorts were set up; one consisting in patients with diagnosis of AD, FTLD or related disorders, and the other made up of patients with CADASIL. The mutational analysis was performed by two main techniques: Denaturing High Performance Liquid Chromatography and direct sequencing. The analyzed genes encompassed: *Amyloid Precursor Protein (APP)*, *Presenilin1 (PSEN1)* and *Presenilin2 (PSEN2)* for Alzheimer's Disease; *Progranulin (PGRN), Microtubule Associated Protein Tau (MAPT)*, *Valosin Containing Protein (VCP)*, *Charged Multivesicular Body Protein 2B (CHMP2B)*, *TAR DNA Binding Protein (TARDBP)* for Frontotemporal Lobar Degeneration and *NOTCH3* for CADASIL.

The mutational analysis of AD- and FTLD-associated genes led to the identification of 8 mutations: three novel variations, *PSEN1* p.Ile437Asn, *PSEN2* p.Thr18Met and *PGRN* p.His400ThrfsX12 and five already described substitutions, *PSEN2* p.Arg71Trp and p.Met174Val, *PGRN* p.Phe86SerfsX170 and p.Thr272SerfsX10 and *MAPT* c.IVS10+16C>T.

The molecular data and *in silic*o analyses performed in this study argue in favour of pathogenetic nature for *Presenilins* variations even though the role of some of them is debated in literature. The substitution identified in *PGRN* and *MAPT* are mutations whose pathogenic mechanism has already been described.

The clinical phenotype associated to identified mutations was not unique and, especially mutations in the *PGRN* gene showed a marked variability in clinical presentations, even within the same family. Furthermore, the identification of a FTD-MND family linked to a locus on chromosome 9 further emphasizes the genetic heterogeneity of FTLD.

The mutational screening of *NOTCH3* gene led to the identification of 21 different mutations, including 7 novel variations, distributed unevenly along the gene. A geographical clustering was observed with mutations identified only in patients living in North-East Italy, a few in North-West and other in Central Italy. Haplotype analysis was performed to assess a possible founder

effected underlying this regionalization but, although consistent, it was not confirmed as the majority of mutations was associated with the most common haplotype.

The results of this study together were useful to define diagnostic algorithms that could help clinicians to identify patients suggestive of a molecular basis of disease to address to genetic testing.

Riassunto

La demenza è una sindrome clinica caratterizzata da declino cognitivo le cui principali manifestazioni comprendono la perdita di memoria, deficit del linguaggio, deterioramento delle capacità di pianificazione e di giudizio, cambiamenti di comportamento e, non di rado, compromissione delle funzioni motorie ed infine dell'autonomia. Oggigiorno, si stima che circa 36 milioni di persone in tutto il mondo siano affette da demenza, stime che, secondo le ultime predizioni, è destinata a crescere fino a 115 milioni nel 2050. Considerando non solo la prevalenza bensì anche l'impatto sociale ed economico che questa malattia comporta, negli ultimi anni la ricerca scientifica sta investendo molte risorse in studi finalizzati all'identificazione delle cause e dei meccanismi patologici che sottendono a questa malattia. Lo scopo ultimo è quello di riuscire ad identificare dei trattamenti terapeutici efficaci che vadano a sostituire le cure palliative, le uniche disponibili oggi per questa malattia.

Esistono diverse forme di demenza e, tra esse, la Malattia di Alzheimer (MA) è la più frequente, seguita dalla Demenza Vascolare (DV) e dalla Degenerazione Frontotemporale Lobare (FTLD), la quale, rappresenta il sottotipo più comune dopo la MA negli individui al di sotto dei 65 anni. Tutti e tre questi disordini possono presentare una componente genetica e, malgrado i notevoli

investimenti e progressi degli ultimi anni per chiarirne le basi molecolari, la conoscenza dei meccanismi patologici che li determinano è ancora limitata.

Tre forme di demenza, che possono avere una componente genetica, sono state incluse in questo studio: la Malattia di Alzheimer, la Degenerazione Frontotemporale Lobare e l'Arteriopatia Cerebrale Autosomica Dominante con Infarti Sottocorticali e Leucoencefalopatia (CADASIL), quest'ultima rappresentante un sottotipo di DV. I principali obiettivi di questo studio hanno compreso l'analisi mutazionale dei geni associati a queste malattie con il duplice intento di definirne le frequenze mutazionali in una casistica italiana e di valutare l'esistenza di eventuali correlazioni genotipo-fenotipo. Lo scopo finale era quello di definire degli algoritmi diagnostici utili ai medici specialisti nella selezione dei pazienti da sottoporre ad indagine genetica.

Sono state allestite due coorti: una comprendente pazienti con diagnosi di MA, FTLD o disordini correlati, e l'altra, pazienti con CADASIL. L'analisi mutazionale è stata eseguita mediante due principali approcci: la Cromatografia Liquida Denaturante (DHPLC) ed il sequenziamento diretto. Sono stati analizzati i seguenti geni: proteina *Precursore dell'Amiloide (APP)*, *Presenilina1 (PSEN1)* e *Presenilina2 (PSEN2)* per la Malattia di Alzheimer; *Progranulina (PGRN)*, *Proteina Tau Associata ai Microtubuli (MAPT)*, *Proteina Contenente Valosina (VCP)*, *Proteina di Modificazione della Cromatina 2B (CHMP2B)*, *Proteina Legante TAR DNA* (*TARDBP*) per la Degenerazione Frontotemporale Lobare ed il gene *NOTCH3* per il CADASIL. L'analisi mutazionale dei geni associati a MA e FTLD ha portato all'identificazione di 8 mutazioni: 3 nuove variazioni, *PSEN1* p.Ile437Asn, *PSEN2* p.Thr18Met e *PGRN* p.His400ThrfsX12 e, cinque sostituzioni già descritte, *PSEN2* p.Arg71Trp e p.Met174Val, *PGRN* p.Phe86SerfsX170 e p.Thr272SerfsX10 e *MAPT* c.IVS10+16C>T. I risultati delle analisi molecolari e delle simulazioni al computer depongono a favore di una natura patogenetica per le variazioni dei geni *Presenilina*, malgrado il ruolo di alcune di esse sia dibattuto in letteratura. Le

sostituzioni identificate nei geni *PGRN* e *MAPT* sono mutazioni il cui meccanismo patologico è già stato descritto.

Il fenotipo clinico riscontrato nei pazienti con le mutazioni identificate non era univoco e, specialmente le mutazioni nella *PGRN* erano associate ad una notevole variabilità delle manifestazioni cliniche, anche all'interno di una stessa famiglia. Inoltre, l'identificazione di una famiglia con diagnosi di FTD-MND in linkage al cromosoma 9 sottolinea ulteriormente l'eterogeneità genetica delle FTLD.

L'analisi mutazionale del gene *NOTCH3* ha portato all'identificazione di 21 diverse mutazioni, incluse 7 nuove variazioni, distribuite non uniformemente lungo il gene. Si è osservata una clusterizzazione delle mutazioni in aree geografiche diverse: la maggior parte identificate in pazienti provenienti dal nord-est Italia, alcune nel nord-ovest ed altre nell'Italia centrale. Nell'ipotesi che questa regionalizzazione rispecchiasse un effetto fondatore, si sono studiati gli aplotipi associati a queste mutazioni: i risultati, sebbene compatibili, non hanno permesso di confermare l'effetto fondatore in quanto la maggior parte di queste variazioni cadeva nell'aplotipo più frequente.

I risultati di questo studio, complessivamente sono stati utili per definire degli algoritmi diagnostici che potrebbero aiutare i clinici ad identificare i pazienti, suggestivi di una base molecolare, da sottoporre ad analisi genetica.

1. Introduction

1.1 Definition of dementia

Dementia - taken from Latin, originally meaning "madness", from *de-* "without" + *ment*, the root of *mens* "mind" - is a generic term that describes chronic or progressive dysfunction of cortical and subcortical function that results in complex cognitive decline with the substantial loss of intellectual abilities, severe enough to interfere with social or occupational functioning. The word dementia has acquired different meanings in different contexts. Originally, the term was often used synonymously with “insanity” and “madness” in general, as a clinical syndrome regardless of etiology but, in the late 19th century it was recognized that there is an organic brain defect at the bases of this disorder [1]. In the 1940s, Mayer-Gross, Guttman [2] and others identified the fundamental defects that constitute the syndrome of dementia. Memory impairment that is evident in learning, retention and recall of both new information and the distant past was considered essential to the diagnosis. However, dementia is more than just forgetfulness [3]. At least one of the following symptoms is usually required as well: impairment of thinking, reasoning, communication, orientation, practical abilities (i.e., greater difficulty maintaining learned skills or managing everyday activities) and personality changes resulting in lack of insight and judgement, disinhibition, aggressiveness, emotional bluntness and lack of empathy. Other psychiatric features, such as anxiety, depression, suspiciousness, delusions, obstinacy and anancastic-like behaviour, seem to be more related to the patient’s awareness of, and reactions and responses to, cerebral dysfunction and its consequences. These secondary or accessory symptoms are also influenced by the patient’s premorbid personality and previous experience, as well as related to better preserved brain functions [4]. However, dementia may evolve according to extraordinary, miscellaneous and variable scenarios, so that a symptom

should be interpreted cautiously. What is regarded as a primary symptom in one type or stage of dementia may be a secondary symptom in another [5, 6].

1.2 Epidemiology of dementia

Epidemiological studies define the occurrence of dementia as either *prevalence* - the proportion of people with dementia in a defined population at a given point in time - or *incidence* - the rate of new dementia cases that develop in a defined population during a specified time interval. Whereas prevalence indicates the probability that a person will have dementia at a certain point in time, incidence indicates the probability of developing the disease. Meta-analysis of several studies have led to the establishment of dementia occurrence not as a separate entity but, in relation to and influenced by other factors such as age, type of dementia, gender, geographic or ethnic factors. Considering these elements, dementia prevalence is closely related to age and, it is approximately 1% at ages 60–64, 1.5% at 65–69, 3% at 70–74, 6% at 75–79, 13% at 80–84, 24% at 85–89, 34% at 90–94 and 45% at 95 and up [7]. Alzheimer's Disease (AD) and Vascular Dementia (VaD) represent the most frequent type of dementia accounting for 60-70% and 10-20% of the total prevalence respectively. Dementia is not gender specific, but results of several epidemiological studies found a higher prevalence in women while it does not seem to be influenced by the geographic origin of patients. The incidence of dementia is also age-related, showing a rapid rate increase proportional to aging. The incidence rates of dementia per 1000 person-years is approximately 1 at ages 60–64, 3–5 at 65–69, 8–10 at 70–74, 11–18 at 75–79, 20–40 at 80–84, 30–60 at 85–89 and 50–120 at 90 and up [8, 9]. Incidence rate is even influenced by the type of dementia and, for example, it decreases in VaD dementia after age 80 while in Frontotemporal Dementia (FTD) it settles at very low levels (below 1) at any age.

1.3 Mortality and management of dementia

Due to increasing life expectancy the number of people suffering from dementia will increase rapidly in both developed and developing countries. More than 25 million people suffered from dementia in 2000. By 2030, that is expected to rise to 63 million, 65% of whom in less developed countries [10]. The increasing prevalence of dementia in the population make it one of the disease with the greatest social impact in the world (as well as for each affected individual). In fact, dementia represents a major cause of death in the elderly with an approximately double risk of dying than those without dementia and the estimated average survival time is 4.5 years from the onset of the disease [11, 12]. Given the progressive and disabling nature of dementia, patients frequently require institutional care with a consequent high demand and consumption of resources (emotional, organizational and economic). The rate of institutionalization is indeed relevant: roughly half of people with dementia move to institutions after 3 years from symptoms onset [13].

1.4 Risk factors for dementia

There are currently no drug treatments effective in fighting this disorder and this is mainly due to the fact that the underlying etiological and pathological processes are not well defined. So, considering the constant increase in the prevalence of dementia in the elderly population, the severity of this disease, its social impact, the best approach right now is to prevent or delay its onset. For this reason, many studies have focused their research on the identification of possible risk factors for the development of dementia.

The most significant risk factor for dementia is age: both the incidence and prevalence of disorders leading to dementia increase, almost exponentially, with age. Familial aggregation is a modest risk factor, valid only for Alzheimer's disease (this means that first-degree relatives of

patients with dementia have a higher risk of developing the disorder), while there are insufficient data to confirm its relevance in other forms of dementia. Moderately strong evidence argue in favour of an ApoE ε4 role as risk factor for dementia while it is a strong risk factor for AD after age-onset of 65 years [14, 15]. Smoking and moderate drinking are not risk factor for dementia while elevated blood pressure in midlife represents a moderate to strong risk factor for dementia in general and in particular for VaD and AD [16-19]. There is a positive correlation between diabetes and dementia while no significant association was identified for specific form like AD [20-23]. Also cholesterol, obesity and homocysteine are not associated with risk of develop dementia with the exception of VaD [24-29]. Association studies between antihypertensive drugs and dementia demonstrated that these treatments have protective effects in elderly people preventing the development of dementia (in particular VaD type); by contrast, an association with statin treatment or non-steroidal anti-inflammatory drugs (NSAIDs) was not supported by significant evidences [30-36]. Several findings suggest that depression may be a risk factor for dementia, but the current scientific evidence is insufficient while there are moderately strong evidence of association with low education [37-40].

1.5 Classification of dementia

Dementia is not a single nosological entity but a collection of several different syndromes that differ in clinical presentation, neuroradiological features, etiology, neuropathology and molecular genetics. The classification of dementia's subtypes has been controversial since the late 19th century and the major obstacle is represented by the different approaches of specialists (neurologists, psychiatrists, geriatricians, internists) in conceptualize the dementia syndromes without integration of various aspects of the same disorders. Current most widely used classifications are based primarily on clinical presentations or neuropathological findings and

presumed etiological factors. Clinical criteria for dementia diagnosis and classification are included in Diagnostic and Statistical Manual of Mental Disorders (DSM) 5th edition, and in the International Classification of Disease (ICD) 10th edition guidelines. ICD-10 defines four main categories of dementia: dementia of Alzheimer type (DAT), Vascular dementia (VaD), dementia in disease specified elsewhere (such as Pick's disease and Creutzfeldt-Jacob's disease), and dementia “not otherwise specified”. A Swedish consensus report from dementia research centers in Lund, Gȍteborg, Stockholm and Umeå offered a clinical classification based on predominant clinical features, as well as type and location of the brain disease [41]. Three main etiology-based categories were primary degenerative dementia, VaD and other secondary dementias.

2. Alzheimer Disease

This disorder takes its name from the German psychiatrist and neuropathologist Alois Alzheimer who described in 1906 for the first time the histopathological brain changes in a patient who was followed up and treated for five years until her death because of the onset and progressive worsening of behavioural and psychiatric symptoms, including paranoia, delusions, hallucinations and impaired memory [42]. Alzheimer identified two main brain changes, subsequently referred to as amyloid plaques and neurofibrillary tangles, that now are recognized as neuropathological hallmarks of this disorder [43].

2.1 Epidemiology

Alzheimer's Disease (AD) represents the most common form of dementia in elderly people as confirmed by data from neuropathological studies where, 50-70% of patients with an ante mortem clinical diagnosis of dementia, presented brain histopathological changes consistent with a diagnosis of AD. Estimate the occurrence of this disease is difficult because of different inclusion criteria used to define the epidemiological series. Nevertheless, the prevalence of AD is nearly 3% at age 65, with a rapid increase to around 50% of the population over 85 years [44, 45]. Incidence rate also increases with age, from approximately 0.5% per year among individuals aged 65-70 to approximately 6-8% for individuals over age 85 [46,47].

2.2 Risk factors

2.2.1 Genetic risk factor

The epsilon 4 (ε4) variant allele of *apolipoprotein-E* (*APOE*) is the only one worldwide recognized genetic risk factor for both sporadic and familial form of AD after 65 years. In a

cross-sectional study of over 65, the ε3/ε4 genotype (where ε3 is the most frequent allele in control population – normal allele) had a 3-fold increased risk to develop AD, while the ε4/ε4 genotype had a 14-fold increased risk compared with the ε3/ε3 genotype (supporting a dose-dependent effect) [48]. Indeed, longitudinal studies have shown that ε4 regulates the age of onset rather than susceptibility to the disease (the average age of onset is moved from 84 years in non-carriers of the ε4, to 68 years in ε4 homozygous) [49]. However, while *APOE* is a well-defined susceptibility factor, *APOE* ε4 is neither necessary nor sufficient for developing AD: half of individuals with apoE4 never develop AD regardless of how they live, while many patients with AD do not have ApoE4 [50]. Beyond any moral evaluation, considering the low sensitivity and specificity of the *APOE* genotyping for Alzheimer's, it can not be used as a routinary test, nor to confirm the clinical diagnosis of AD nor as a predictive test in healthy individuals.

2.2.2 Medical illness and behavioural risk factors

A family history of Down syndrome is associated with a 2-3-fold increase of Alzheimer's risk [51], also a history of depression may be associated to AD although is not clear whether it can actually represent an early stage of dementia rather than being a causal factor [52]. There is a positive association between AD and traumatic head injury even though it remains inconsistent [53]. Cardiovascular disease seems to act as a comorbidity [54, 55] and prospective studies have shown a 2-4-fold increase in AD risk, probably through with a complex interaction with cerebral vessels [56].

2.2.3 Behavioural protective factors

Mental and leisure activity (in particular frequent intellectual, passive and physical activities) as well as high education level have been associated with a lower risk to develop AD [57, 58]. Also

medications with anti-inflammatory drugs may be associated with a lower risk to develop AD, probably reducing local inflammatory response to amyloid deposition in the brain [59].

2.3 Clinical diagnosis of Alzheimer's disease

The National Institute of Neurological Disorders and Stroke-Alzheimer Disease and Related Disorders (NINCDS-ADRDA) are the most frequently used criteria for AD [60]. These criteria classify AD based on the degree of certainty of the diagnosis, and whether AD is associated with other disease processes (i.e., Probable vs. Possible AD). The criteria for probable AD include dementia established by clinical examination and documented by the mini-mental state examination (MMSE) [61], dementia test score [62] or a similar examination, and confirmed by neuropsychological tests, deficits in two additional areas of cognition, progressive deterioration of memory and other cognitive functions, no disturbance of consciousness, onset between the ages of 40 and 90, most often after 65, and absence of systemic disorders or other brain disease that could account for the progressive deficits. The diagnosis of probable AD is supported by progressive deterioration of specific cognitive functions, such as aphasia, apraxia and agnosia, impaired daily life activities and altered patterns of behaviour, family history of similar disorders, laboratory results showing normal lumbar puncture, normal or non-specific EEG changes, evidence of cerebral atrophy on CT with progression documented by serial observation. By contrast, the diagnosis of Possible AD requires a history and progression of dementia consistent with AD, but in which clinical evidence of some other disease process is present (including cerebrovascular disease or stroke, head injury, depression,..).

2.4 Clinical presentation of Alzheimer's disease

The clinical hallmark symptom of AD is impaired memory and, in particular, auditory verbal and

visual delayed recall, confrontation naming and cognitive flexibility/divided attention tests represented the best predictors of AD [63]. Actually, AD is not a unique entity starting with memory deficit and evolving with subsequent impairments in other cognitive functions, indeed, it may have different clinical presentation. Language deficits are the second most prominent cognitive manifestation of AD and in some cases they can be the initial clinical symptom. Also fluency and, to a lesser degree, auditory comprehension are usually impaired in AD [64]. In the early phases of the disease visuoconstructional and visuospatial drawing abilities are impaired, as well as problem-solving, concept formation, cognitive flexibility accompanied by ideational or ideomotor apraxia [63, 64]. Importantly, most AD patients are unaware of their cognitive deficits, or are unable to recognize the magnitude of these deficits [65].

The most common neurological, non-cognitive, signs in AD patients are myoclonic movements, and extrapyramidal signs (EPS) which manifest only with disease progresses. The characteristic EPS in AD are bradykinesia and rigidity which are often associated to a severer and faster evolution of the disease [66]. Psychotic symptoms (e.g., delusions, hallucinations) and disruptive behaviours (e.g., aggressive behaviour, psychomotor agitation, wandering) are common in AD patients while depressive symptoms can occur in up to 86% of the cases [64, 65, 67].

AD may also manifest with atypical clinical presentation, overlapping with other neurodegenerative disorders: as frontal lobe syndrome with significant behavioural or executive dysfunctions (resembling Frontotemporal Dementia); with prominent language impairment as primary symptom (resembling Primary Progressive Aphasia) or with a corticobasal syndrome (resembling Corticobasal Degeneration).

2.5 Age at onset of Alzheimer's disease and illness duration

Both age at onset and disease duration vary considerably from study to study, based on autopsy

proven cases and in families with identified AD-associated genes mutations. Nevertheless, two groups were arbitrary defined based on age of onset: Early-Onset AD (EOAD) with onset usually in the 40s or early 50s (range: 30-60 years) with a rapid progression of the symptoms lasting for nearly 5-6 years before death; and Late-Onset AD (LOAD) with onset age after 60-65 years and a 8-10 years typical disease duration.

2.6 Structural and functional neuroimaging findings in Alzheimer's disease

The first degenerative changes in the disease occur in the medial temporal lobe (MTL), including the hippocampus and entorhinal cortex (Appendix 1). A substantial number of studies have shown that Magnetic Resonance Imaging (MRI) measurements of hippocampal atrophy can distinguish Alzheimer's disease from cognitively normal elderly people with 80-90% accuracy [68]. Moreover, considering that entorhinal cortex volume might precede hippocampal atrophy, MRI measurements of its volume have a high predictive value for incipient disease in its prodromal phase [69, 70].

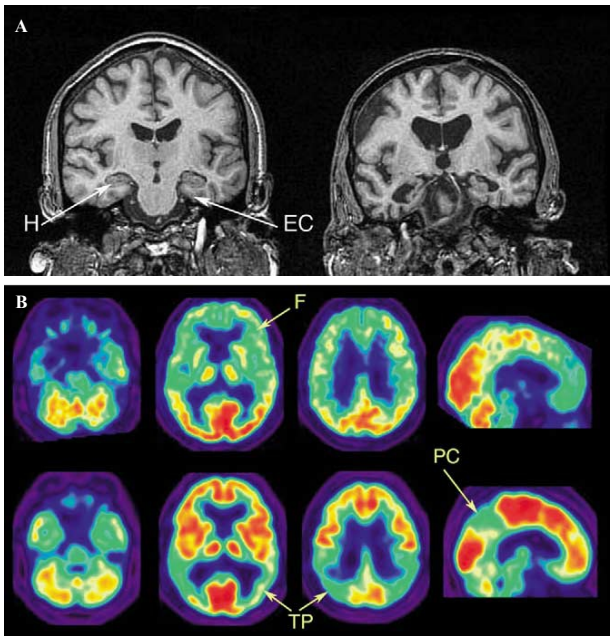

Fig. 1. MRI and FG-PET in Alzheimer's Disease
A: coronal MR images of a normal older subject (left) and a patient with Alzheimer's disease (right). Hippocampus (H) and entorhinal cortex (EC) are labeled on the normal subject and show severe atrophy in the AD patient. B: FDG-PET images of a patient with clinically diagnosed frontotemporal lobar dementia (upper row) and a patient with clinically diagnosed Alzheimer's disease (lower row). The FTLD patient shows reduced glucose metabolism in frontal cortex (F), whereas the AD patient shows reduced metabolism in temporoparietal (TP) and posterior cingulate cortex and precuneus (PC).
[Jagust W, et al. Positron emission tomography and magnetic resonance imaging in the diagnosis and prediction of dementia. Alzheimer's & Dementia. 2006;2:36–42]

Functional imaging by ^{18}F-fluorodeoxyglucose Positron Emission Tomography (FDG-PET) are useful to differentiate AD patients from normal elderly people with a 93% sensitivity and specificity [71]. FDG-PET in AD patients discloses a characteristic pattern of hypometabolism in the temporal, parietal and posterior cingulate cortex [68].

2.7 Cerebrospinal fluid (CSF) markers of Alzheimer's disease

Biological markers represent useful tools as indirect measure of disease severity and progression. In the case of AD, cerebrospinal fluid (CSF) may be considered the better source of diagnostic biomarkers given is direct contact with the extracellular space of the brain where AD pathology is restricted and biochemical changes are likely to be reflected. AD-specific biomarkers, reflecting the central pathogenic processes of amyloid β aggregation and hyperphosphorylation of tau protein, are represented by amyloid $\beta_{1\text{-}42}$ (Aβ42), total tau (t-tau) and phospho-tau (p-tau) [72-74]. In AD the concentration of Aβ42 in cerebrospinal fluid is low and that of t-tau is high compared with those in healthy controls [72, 73]. Concentrations of different phosphorylated tau epitopes may also be high [75, 76]. Noteworthy, the sensitivity and specificity of these markers are higher, reaching a elevated diagnostic value, if are combined [77, 78].

2.8 Treatments

The nowadays recognized effects of AD neuropathogenesis process are deficiencies of the brain cholinergic system and other neurotransmitters.

Drugs with symptomatic effects on behaviour and cognition have been developed, including acetylcholinesterase inhibitors such as donepezil, rivastigmine and galantamine [79]. Memantine, an NMDA receptor antagonist, has shown some effectiveness in the treatment of moderate to severe AD, leading to improvement in learning and memory processes controlled by

NMDA receptor [80]. Risperidone and olanzapine have shown efficacy in reducing the rate of common behavioural signs in AD patients, such as aggression, psychomotor agitation and psychosis [81, 82]. Other drugs treatments under investigation include the use of anti-inflammatory agents (NSAIDs), estrogens, nerve growth factors, statins, BACE inhibitors and antioxidants [83].

Disease-modifying therapy by Aβ immunisation obtained good results in AD transgenic mice models with fibrillar Aβ [84], where Aβ deposition were attenuated but, on the contrary, human trials of this approach was halted because of encephalitis in a few subjects [85].

2.9 The genetics of Alzheimer's disease

Alzheimer's disease is a classic example of a genetically complex disorder that may present in two different forms: familial (rare) versus seemingly non-familial (common) cases. Familial forms account for nearly 25% of all AD cases and, only 1% are Early-Onset Familial AD (EOFAD) with an autosomal dominant pattern of inheritance of the disease while many of the remaining familial cases have a Late-Onset (LOAD) most often not showing any overt pattern of familial segregation.

2.9.1 Early-Onset Familial Alzheimer's Disease (EOFAD)

Early-Onset Familial Alzheimer's Disease (EOFAD) is a single-gene disorder, mendenianly-inherited disorder, associated with mutations in three genes: *Amyloid Precursor Protein* (*APP*), *Presenilin 1* (*PSEN1*) and *Presenilin 2* (*PSEN2*) [86-88]. These three loci, account for different proportion of EOFAD with *PSEN1* being the most frequent mutated gene (20-70% of EOFAD) followed by *APP* (10-15%) and *PSEN2* that is the rarest cause of EOFAD. Clinical presentation of EOFAD patients do not differ from non-familial AD cases nor from LOAD.

2.9.1.1 Amyloid Precursor Protein (APP)

Amyloid Precursor Protein (*APP*) gene, located on chromosome 21q21, encodes a type-I integral-membrane protein expressed in many tissues and concentrated in the synapses of neurons. Experimental evidences implicate this protein in neural plasticity and regulation of synaptogenesis [89, 90]. The precursor protein may undergo a proteolytic cleavage by alternatively an α- or β-secretase leading to the formation of the soluble fragment amyloid-α peptide (sAPPα) and C-terminal transmembrane 10 kDa fragment in the first case, and the soluble amyloid-β peptide (sAPPβ) and C-terminal transmembrane 12 kDa fragment in the second. The 10 and 12 kDa fragments are subjected to a further proteolytic cleavage by γ-secretase, producing two different extracellular peptides: p3 and Aβ respectively, and a cytoplasmic fragment (AICD). In reality, there are two γ-secretase cleavage sites so there may be the formation of two different Aβ peptide, 40 (Aβ40) or 42 (Aβ42) aminoacids long. Aβ42 peptide represents the main component of neuritic plaques, the neuropathological hallmark of AD, and it is encoded only by exon 16 and 17 of the gene.

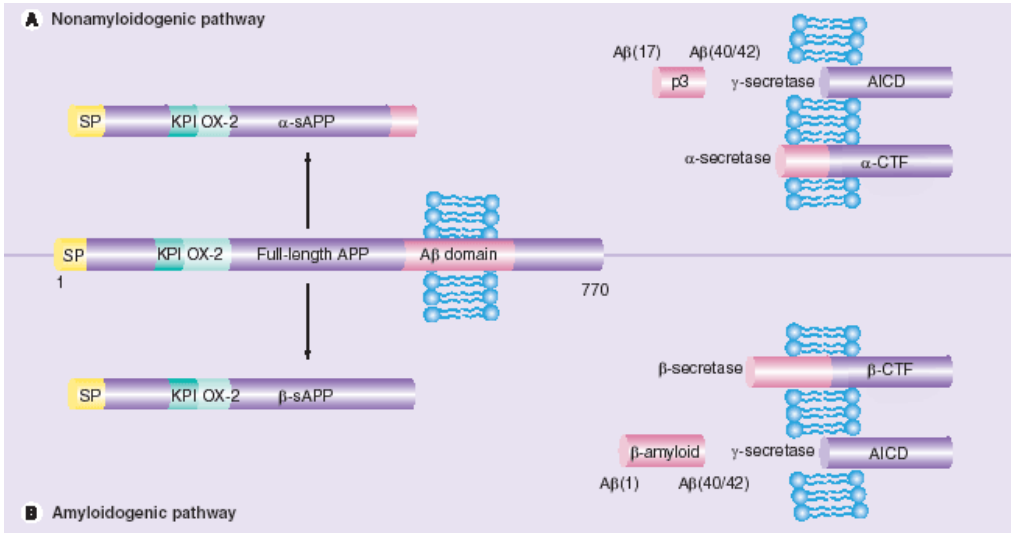

Fig. 2. The metabolism of the largest isoform of amyloid precursor protein (APP770) with amyloid-β and p3 generation.

The first 28 residues of the Aβ domain are located outside the membrane whereas the remaining 12–14 residues are in the transmembrane domain of APP. APP can be processed along two main pathways: ***(A)*** *the nonamyloidogenic pathway and* ***(B)*** *the amyloidogenic pathway.*

Aβ: Amyloid-β; AICD: APP intracellular domain; APP: Amyloid precursor protein; CTF: C-terminal fragment; KPI: Kunitz protease inhibitor domain; sAPP: Soluble APP; SP: Signal peptide.

[Portelius E, et al. Targeted Proteomics in Alzheimer's Disease: Focus on Amyloid-Beta. Expert Rev Proteomics. 2008;5(2):225-237]

Mutations in *APP* lead to an unbalance in the formation of Aβ peptides with an increase of Aβ42 isoform. There are two types of *APP* mutations:

- missense mutations, in exon 16 and 17, mostly localize near secretases cleavage sites forming mutational clusters such as Swedish, Flemish, Dutch, Florida and London mutations [91-95];
- entire gene duplication [96].

Clinical presentation associated to *APP* mutations is typical of AD, with an age at onset between 40-60 years.

2.9.1.2 Presenilin 1 (PSEN1) and Presenilin 2 (PSEN2)

Presenilin 1 and its high homologous *Presenilin 2* genes, located on chromosome 14q24.2 and 1q42.13 respectively, codify for two polytopic membrane proteins forming the catalytic subunit of γ-secretase complex involved in APP cleavage [97].

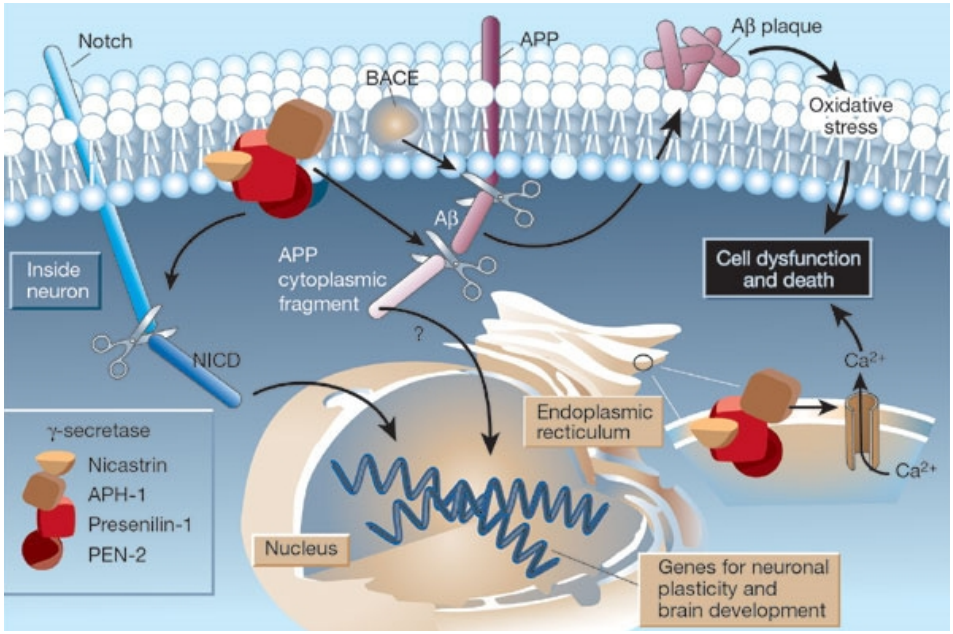

Fig. 3. PSENs and g-secretase complex in amyloid b-peptide production and neurodegeneration.
The g-secretase complex cleaves Notch (left) to generate a fragment (NICD) that moves to the nucleus and regulates the expression of genes involved in brain development and adult neuronal plasticity. The complex also helps in generating the amyloid b-peptide (Ab; centre). Mutations in presenilin-1 that cause early-onset Alzheimer's disease enhance g-secretase activity and Ab production, and also perturb the ER calcium balance. Consequent neuronal degeneration may result from membrane-associated oxidative stress, induced by aggregating forms of Ab (which create Ab plaques), and by the perturbed calcium balance.
[Mattson M, et al. Neurobiology: Ballads of a protein quartet. Nature. 2003;422:385-387]

Both proteins are expressed ubiquitously, in peripheral tissues and in the brain where they mainly localized in synaptic vesicles, synaptic adhesion site and growth cones of neurites [98]. When secreted, PSEN1 and PSEN2 undergo a proteolytic cleavage (probably by caspase3) leading to the formation of a N-terminus (NTF) and a C-terminus fragments (CTF). Released fragments interact with nicastrin (Nct), anterior pharynx defective 1 (Aph-1) and presenilin enhancer2 (PSENEN) proteins to form the γ-secretase complex [99].

Presenilins identified mutations lead to an increase in the ratio of Aβ42 to Aβ40 peptides; this change in isoforms balance seems to occur through increased Aβ42 production, decreased Aβ40 production or a combination of both changes [100]. The majority of *Presenilins* mutations are missense substitutions mostly localized in transmembrane domains.

Presenilins mutations are associated to different clinical presentation: age at onset is earlier in *PSEN1* usually in the 40s and 50s, while in *PSEN2* it ranges from 40 to 75 years; disease duration is shorten in *PSEN1* mutation carriers with a complete disease penetrance (95% in *PSEN2*).

2.9.2 Late-Onset Alzheimer's disease (LOAD)

Late-Onset Alzheimer's Disease (LOAD) is characterized by a considerable more complex pattern of genetic and non-genetic factors that remains only poorly understood. *Apolipoprotein E* (*APOE*) is the only genetic risk factor that has been demonstrated to be associated with both familial and sporadic late-onset AD [101, 102]. Since the discovery of this association, no other genetic risk factors has been found to consistently confer susceptibility to disease risk, despite intensive efforts in many laboratories worldwide [103].

2.9.2.1 Apolipoprotein E (APOE)

Apolipoprotein E (*APOE*), located on chromosome 19q13.32, codifies for an apolipoprotein playing an important role in the regulation of plasma lipid and cholesterol metabolism within many organs and cell types in human body [104].

Three major alleles occur at the *APOE* locus - ε2, ε3 and ε4 – which translate into combination of two aminoacid changes at residue 112 and 158 of the apoE protein (ε2: Cys/Cys; ε3: Cys/Arg; ε4: Arg/Arg, respectively). While the ε4 allele has been demonstrated to significantly increase the risk for AD, its minor allele - ε2 – has been associated with a decreased risk [105]. The potential pathophysiological effects of *APOE* assume that the different variant alleles directly influence Aβ-accumulation by affecting Aβ aggregation or clearance [106-108].

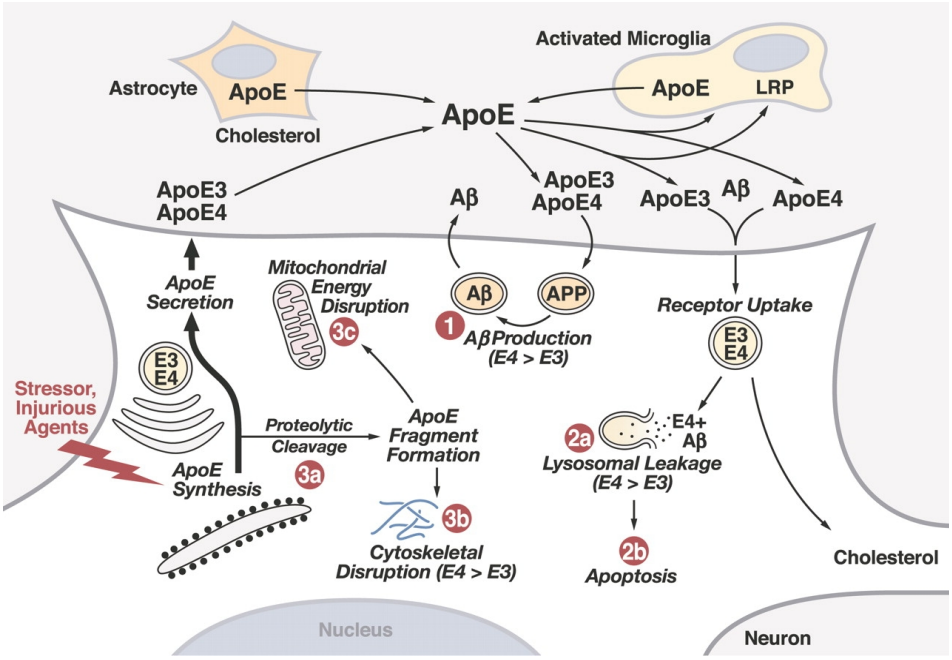

Fig. 4. Roles of apoE in lipid redistribution among cells in the CNS and apoE isoform-specific differences in neuropathology.
ApoE is synthesized by astrocytes, activated microglia, and neurons. Three potential detrimental roles for apoE4: (1) enhanced Aβ production, (2) potentiation of Aβ1–42-induced lysosomal leakage and apoptosis, and (3) enhanced neuron-specific proteolysis resulting in translocation of neurotoxic apoE4 fragments in the cytosol, where they are associated with cytoskeletal disruption and mitochondrial dysfunction.
[Mahley R, et al. Apolipoprotein E4: A causative factor and therapeutic target in neuropathology, including Alzheimer's disease. PNAS. 2006;103(15):5644-5651]

2.9.3 Other putative Alzheimer's disease loci

The association between *APP, PSEN1, PSEN2, APOE* and Alzheimer's disease was defined with the widely used candidate gene approach but was not successful in identifying other loci of potential relevance, probably because this method is focused on a preconceived functional hypothesis. To overcome this limitation recent studies have used a different approach based on large-scale genotyping technologies that enable to perform comprehensive, unbiased genome-wide association (GWA) analyses. At least fifteen Alzheimer's disease genome-wide association studies (GWAS) have been published in the last three years [109], and the most significant findings of all associative studies (study design, sample size, results, and polymorphism details, including genotype and allele frequencies) are collected and reported in AlzGen internet database (http://www.alzgene.org) maintained by Bertram *et al.* [103], where results of meta-analyses studies are also available. Nearly forty genes have shown a statistically significant association with AD in different GWAS but, none of these obtained consistent replication in the follow-up data sets except for *clusterin* (*CLU*), *complement component 3b/4b receptor 1* (*CR1*), *phosphatidylinositol binding clathrin assembly protein* (*PICALM*) [110, 111] and *bridging integrator 1* (*BIN1*) [112]. Interestingly, all four of these genes codify for proteins involved in Aβ metabolism, in particular: CLU seems involved in Aβ fibrillization[113], CR1 in amyloid clearance [114], PICALM and BIN1 in Aβ transport and clearance [115, 116].

2.10 The neuropathology of Alzheimer's disease

2.10.1 Macroscopic findings

The external appearance of the brain in AD is not a useful diagnostic tool, usually presenting mild generalized frontotemporal atrophy not greater than that observed in a number of age-matched control brains [117]. There are no pathognomonic changes on brain slices but, usually

are observed atrophy of hippocampal formation, some expansion of the third ventricle whereas the aqueduct and fourth ventricle have normal size. The white matter do not usually present visible abnormalities but, some reduction in overall volume (between 3 and 19%) [118]. In the deep grey nuclei atrophy is restricted to the caudate and putamen while globus pallidus, thalamus and substantia innominata are spared. The other consistent finding in AD is loss of pigmentation in the locus ceruleus.

2.10.2 Microscopic findings

A definite and unbiased diagnosis of AD (as well as that of other dementias) may derived only from immunohistochemical analyses of brain specimens. The major microscopic findings in AD are extracellular senile and neuritic plaques, intracellular neurofibrillary tangles, dystrophic neurites and neuropil threads.

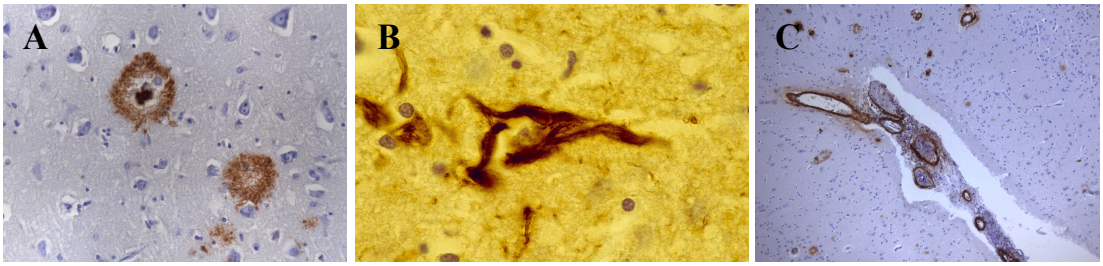

Fig. 5. Neuropathological hallmarks of Alzheimer's Disease.
A: Typical diffuse plaque with irregular outline and neuritic plaques showing the characteristic central core of amyloid surrounded by a neuritic reaction. B: neurofibrillary tangle. C: amyloid angiopathy with amyloid deposition in cerebral arteries.

Senile or *diffuse plaques* consistent of Aβ peptides, not in the β-pleated sheet conformation typical of amyloid, not associated to astrocytic and microglial cells activation and without involvement of neuropils.

Neuritic plaques are composed of a central amyloid core, constituted by β-pleated sheet Aβ peptides, with finger of fibrillary amyloid extending into the surrounding neuropil and

association with activated glial cells. Both senile and neuritic plaques are made up of 39 to 43 aminocid long Aβ peptides even though the most frequent species are Aβ1-40 and Aβ1-42 peptides. While the presence of senile plaques is visualized by Bielschowsky and MS silver stains, Congo red stain is specific for neuritic plaques.

Neurofibrillary tangles, dystrophic neurites and neuropil threads consist in accumulation of hyperphosphorilated tau protein in the form of paired helical filaments (PHF). The visualisation of all these changes requires the use of several specific stains, different from the more routine histological stains like haematoxylin and eosin, not useful to define the degree of neurofibrillary pathology.

All these microscopic findings are widespread not only in cortical regions but also and conspicuously in subcortical structures that are responsible for the clinical symptoms resulting from the loss of cholinergic, serotoninergic and noradrenergic supply.

Not infrequently, amyloid deposition in AD brains may occur in the cerebral arteries (congophilic angiopathy) as occurs in other disorders (i.e., Icelandic form of hereditary cerebral haemorrhage with amyloidosis – HCHWA).

3. Frontotemporal Lobar Degeneration

Frontotemporal Lobar Degeneration (FTLD) represents the second most common form of presenile primary cortical dementia after Alzheimer's disease. FTLD is a pathological term used to define three clinical and neuropathologically heterogeneous syndromes characterized by personality and/or behavioural changes or language dysfunctions: frontotemporal dementia (FTD), progressive nonfluent aphasia (PNFA) and semantic dementia (SD).

3.1 Epidemiology

The prevalence of FTLD is not well defined as several population-based studies have reported different estimates. Two UK and one Italian studies reported the highest prevalence of 15-22 per 100,000 inhabitants in the age group 45-64 years [119-121] while in a Dutch series the estimate was 4 per 100,000 in the same age range [122]. Two studies investigated the incidence of FTLD obtaining consistent results with incidence rate of nearly 4 per 100,000 person-years in the age-group of 45-64 years [123, 124].

3.2 Risk factors

Unlike Alzheimer's disease, only few studies have investigated risk factors of FTLD and those already reported mainly regard candidate genetic risk factors. The main difficulties in assessing this topic derived from the wide heterogeneity in clinical and neuropathological presentation of these syndromes, affecting the accuracy in patients enrollment. Some of the candidate genetic risk factors of FTLD include: 4 SNPs of *Progranulin* gene [125-127], haplotype B of *Cystatin C* [128], the allele ε4 of *apolipoprotein E* [129], heterozygosity of the codon 129 polymorphism of *Prion Protein* [130] and haplotype H1 of *Microtubule-associated Protein Tau* [131]. All these

association findings did not obtained consistent replication in the following studies. Two recently association studies have indicated *ubiquitin associated protein 1* [132] and three SNPs within the *TMEM106B* gene [133] as possible candidate risk factors, even though these results have not yet been tested in other replication analyses.

3.3 Clinical diagnosis of Frontotemporal Lobar Degeneration

Clinical diagnosis of FTLD is made according to international guidelines reported in Consensus clinical diagnostic criteria of The Lund and Manchester Groups [134] and their implementation by Nearly et al. [135]. These criteria encompass core and supportive diagnostic features that differ from one to another clinical syndrome (FTD vs PNFA vs SD) but have in common an insidious onset and gradual progression, and several supportive (onset before 65 years, positive family history of similar disorder in first-degree relative, bulbar palsy, muscular weakness and wasting) or diagnostic exclusion (clinical, biochemical, neuroimaging) features.

3.4 Clinical presentation of Frontotemporal Lobar Degeneration

Frontotemporal Lobar Degeneration encompasses three distinct clinical syndromes: Frontotemporal Dementia (FTD), Progressive Nonfluent Aphasia (PNFA) and Semantic Dementia (SD). Even though they are distinguished on the bases of predominant onset symptoms - behavioural changes in FTD and language impairment in PNFA and SD – which are associated to distinct regional pattern of brain atrophy, these clinical entities tend to overlap with the progression of the disease, as a result of atrophy spread in several brain regions.

3.4.1 Frontotemporal dementia

Frontotemporal dementia (FTD) is characterized by personality and behavioural changes which

may be revealed in an apathetic and passive state or as a disinhibited and childlike variant [136, 137]. Not uncommonly, these changes are so dramatic to be misdiagnosed as depression or mania respectively. Patients frequently show emotional shallowness, with loss of warmth and empathy towards others, appearing self-centered. There is a dramatic loss of insight, with frank denial or a very shallow recognition of the illness. Stereotyped behaviours are very common, ranging from aberrant motor behaviours (i.e., rubbing, picking, clapping, rocking) to complex compulsions (repetitive checking of clock, hygiene rituals, counting) [138]. Changes in eating behaviour (overeating, weight gait) and hyperorality (excessive drinking, alcohol intake) are highly characteristic. Patients are often perseverative, discussions focus on recurrent themes and, in later disease stages, they manifest echolalia and mutism. Behavioural changes are usually accompanied by less severe cognitive impairment mainly characterized by disorganization, difficulties in planning, problem-solving, affected executive functions, working memory, attention, abstract reasoning [139]. Unlike Alzheimer's disease, verbal and visual memory as well as temporal and spatial orientation and praxis are usually preserved in FTD.

3.4.2 Progressive Nonfluent Aphasia

The main clinical findings in Progressive Nonfluent Aphasia (PNFA) is represented by impaired speech production [140]. Patients disclose difficulties in appropriate words finding, a slow rate of speech, with agrammatisms, phonemic paraphasis errors. Repetition is impaired, reading is non-fluent and effortful while language comprehension is preserved. In contrast to FTD, PNFA is not characterized by personality or behavioural changes in the first stages, spatial skills and short-term memory are spared until late in the course. These prominent difficulties in language production make cognitive functions seem more affected than they really are, in fact, PNFA patients lead an almost normal life [141].

3.4.3 Semantic Dementia

While PNFA is a disorder of word production, Semantic Dementia (SD) is characterized by a progressive loss of knowledge about words and concepts [142]. As in the case of FTD, also SD may manifest in two different variants (depending of regional localization of brain atrophy). One variant is characterized by fluent, anomic aphasia with word-finding difficulties and naming (semantic memory), loss of words meaning even though reading and writing are preserved. SD patients often disclose inability to recognize and put objects in their correct context. Depression is another prominent finding while behavioural disturbances are uncommon in the first stages of the disease [143]. The other SD presentation is characterized by behavioural changes with flat affect, emotional blunting and alteration in social conduct [144]. Patients may exhibit excessive verbal output, hyperphagia and loss of fear. In the late stages of the disease, these patients disclosed other behavioural symptoms recalling those of FTD.

3.4.4 Frontotemporal lobar degeneration with motor neuron disease

A small number of patients with a clinical syndrome of FTLD (the most common is FTD), variable from 4 to 15%, may develop signs of motor neuron disease (MND) during the course of the illness and its presence worsens and speeds up the progression of the disease. MND is a neurodegenerative disorder characterized by degeneration of upper and lower motor neurons, leading to progressive muscle wasting, weakness and spasticity which ultimately results in profound global paralysis and death, usually due to respiratory failure. Roughly 50% of MND patients develop behavioural changes fulfilling criteria for FTLD syndrome [145]. The clinical overlapping between these two entities is also associated to a co-occurrence of neuropathologic findings of the single disorder, adding further evidences arguing in favour of a clinicopathological continuum.

3.5 Age at onset of Frontotemporal Lobar Degeneration syndromes and illness duration

Onset is most commonly in middle age between 45 and 65 years although there is a broad range in the age at onset (21-85 years) with about 20% of patients older than 65 years. Also illness duration is variable ranging from 2 to 20 years, with an average of 8 years, reduced to nearly 3 years in FTLD-MND cases.

3.6 Structural and functional neuroimaging findings in Frontotemporal Lobar Degeneration

During the first stages of the disease, there are no prominent structural brain changes detectable by MRI but, as the disease progresses, focal atrophy of frontal and anterior temporal structures is visible on T2 and T1 images (the latter are useful to detect atrophy asymmetry, very common in FTLD subjects). Distribution of atrophy among different brain regions varies according to associated FTLD clinical syndrome.

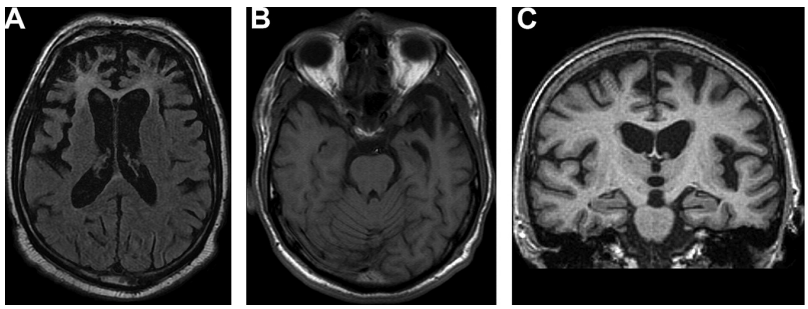

Fig. 6. Brain MRI of FTLD syndromes.
(A) Frontal atrophy on axial fluid attenuated inversion recovery MRI of a patient with behavioural variant of FTD (bvFTD). (B) Axial T1-weighted image with left temporal lobe atrophy in a patient with semantic dementia (SD). (C) Coronal T1-weighted MR image of a patient with progressive non-fluent aphasia (PNFA) and left inferior frontal and superior temporal atrophy.
[Seelar H, et al. Clinical, genetic and pathological heterogeneity of frontotemporal dementia: a review. J Neurol Neurosurg Psychiatry. 2010; Oct 22. Epub ahead of print]

In FTD atrophy mainly affects frontal and paralibic regions (anterior cingulate cortex and frontal insula) as well as hippocampus, striatum and thalamus, usually with a right-hemisphere bias [146]. Asymmetrical atrophy in the left hemisphere mostly localized in the inferior frontal lobe

and anterior insula is a common finding in PNFA patients [147]. Left hemisphere, anterior and inferior temporal lobes are usually affected by atrophy in patients with SD [148]. MRI in patients with FTLD-MND usually discloses atrophy in motor and premotor cortex, anterior temporal lobes, and middle and inferior frontal gyri [149].

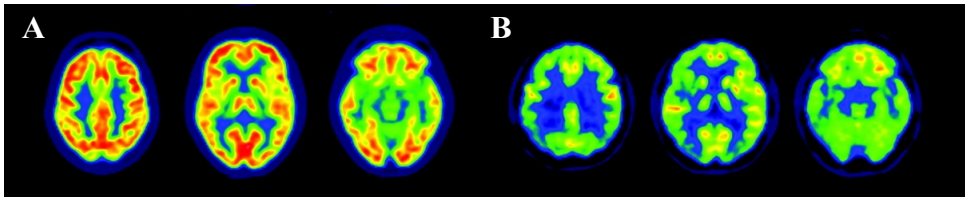

Fig. 7. 18F-FDG brain images in FTLD.
Differential glucose metabolism pattern in healthy controls (A) and FTLD patients (B).
[Koeppe RA, et al. 11C-DTBZ and 18F-FDG PET Measures in Differentiating Dementias. Journal of Nuclear Medicine. 2005;46(6):936-944.]

Functional imaging results essentially mirror the structural imaging findings for each clinical subtypes and these techniques are useful tools to differentiate FTLD from other dementias, in particular from AD. The more widely used functional imaging assays in FTLD diagnosis are ^{18}FDG-PET and ^{99m}TC-HMPAO SPECT which reveal frontal and anterior temporal lobes glucose hypometabolism or hypoperfusion [150-152].

3.7 Cerebrospinal fluid (CSF) and plasma markers of Frontotemporal dementia

Unlike Alzheimer's disease, CSF profile is not useful in making a diagnosis of FTLD in fact, several studies reported conflicting results. CSF t-tau in FTLD may settle down to normal values or it may vary widely (either increase or decrease), phosphorylated tau is normal compare to AD and also Aβ1-42 levels are often unchanged [153].

ELISA quantification of plasma, serum and CSF levels of progranulin protein are a useful tool to identify and discriminate FTLD patients harbouring a *PGRN* mutation [154], while several studies are investigating the possible diagnostic relevance of plasma or CSF TDP-43 levels for

which early results indicated an association with neuropathologically confirmed FTLD-TDP [155].

3.8 Treatments

There are currently no standard pharmacological treatments for FTLD but only symptomatic drugs therapies, focused on treating behavioural symptoms (disinhibiton, impulsiveness, depression) and compulsive and stereotypical behaviours. Moreover, most drugs are designed to settle again the balance in the neurotransmitters systems that, like AD, are highly affected in this disorder (serotonergic, glutamatergic systems) [156]. Despite these therapeutic approaches, none of these treatments delay the progression of the disease.

3.9 The genetics of Frontotemporal Lobar Degeneration

A positive family history occur in up to 40% of patients with FTLD, with an autosomal dominant pattern of inheritance in roughly 10% of cases consistent with a strong genetic component of the disease [157-159]. Actually, several studies, carried out over the past fifteen years, allowed to identify some of the molecular bases of this disorder, strongly emphasizing the genetic heterogeneity of this disorder. Mutations in two genes, *Microtubule-Associated Protein Tau* (*MAPT*) and *Progranulin* (*PGRN*) explain nearly 40% of familial cases, representing the major causes of FTLD unlike the genes *Valosin Containing Protein* (*VCP*) and *Charged Multivesicular Body Protein 2B* (*CHMP2B*) that have a low mutational frequency accounting for less than 4%. *TAR-DNA Binding Protein* (*TARDP*) and *Fused in Sarcoma* (*FUS*) genes mutations have been identified in 5% of Amyotrophic Lateral Sclerosis (ALS) subgroup of MND but occasionally also in familial cases of FTLD-MND. A locus on chromosome 9p13.2-21.3 have been associated to several families with FTLD-MND even though the causative gene has not yet been identified.

3.9.1 Microtubule-Associated Protein Tau

Microtubule-Associated Protein Tau (*MAPT*) gene, located on chromosome 17q21, codifies for a low molecular weight protein, tau, belonging to MAP family of proteins plenty expressed in central nervous system where their main function is binding and stabilization of microtubules, mantaining neuronal integrity and axoplasmic transport [160]. In adult brain, *MAPT* is expressed in six isoforms that differ in two regions: N-terminus domain for alternative splicing of exon 2 and 3, and C-terminus domain for the presence of three or four tandem repeats sequences (3R-tau or 4R-tau), codified by exon 9 to 12, involved in microtubules binding [161]. The interaction between tau and microtubules is tightly regulated by phosphorylation state of tau: nearly 80 phosphorylation sites clustered around the repeats and, hyperphosphorylation of these sites has a negative effect on proteins interaction.

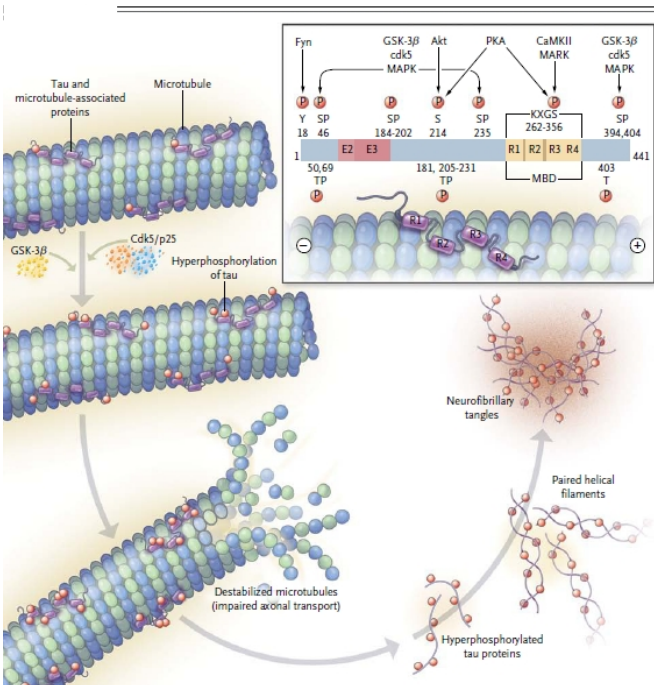

Fig. 8. Tau Structure and Function.
Four repeat sequences (R1-R4) make up the microtubule-binding domain (MBD) of tau. Normal phosphorylation of tau occurs on serine (S; inset, above horizontal bar) and threonine (T; inset, below horizontal bar) residues, numbered according to their position in the full tau sequence. Hyperphosphorylated sites specific to paired helical filament tau in Alzheimer's disease tend to flank the MBD. Tau binding promotes microtubule assembly and stability. Excessive kinase, reduced phosphatase activities, or both cause hyperphosphorylated tau to detach and self-aggregate and microtubules to destabilize.
[Querfurth HW, et al. Mechanisms of disease. Alzheimer's Disease. N Engl J Med. 2010;362:329-344.]

MAPT mutations, first associated to frontotemporal dementia with parkinsonism linked to chromosome 17 (FTDP-17) in 1998, affect exon 1 and 9 to 13 codifying for the C-terminus

domain of tau, including the microtubules binding repeats. Different mutations mechanism have been identified:

- splice-site intron 10 and few exon 10 mutations affect alternative splicing of exon 10 leading to imbalance of 3R- and 4R-tau isoforms (while in normal condition they are produced in equimolar amount) [162];
- mutations affecting the structure of protein, its ability to bind microtubules and its phosphorylation [163];
- mutations causing a direct increase of tau tendency to form aggregates into filaments [164].

FTDP-17 associated to MAPT mutations is inherited as autosomal dominant trait with high penetrance and variable clinical presentations, including behavioural and language FTLD subtypes but also other neurodegenerative disorders like Corticobasal Dementia (CBD), Progressive Supranuclear Pulsy (PSP) and Amyotrophic Lateral Sclerosis (ALS). The average age at onset is 55 years (range 45-65) and a disease duration ranging from 8 to 10 years.

3.9.2 Progranulin

Progranulin gene, located on chromosome 17q21, encodes for progranulin which is a secreted growth factor involved in inflammatory processes, wound healing and tumour progression [165, 166]. Progranulin is a precursor protein which, after protease cleavage, gives rise to 7 granulin peptides those, together with full-length protein are expressed in central nervous system and in several peripheral tissues. In the brain, *PGRN* mRNA is highly expressed in cortex pyramidal neurons, in Purkinje cells and hippocampal pyramidal cells, where it exerts its putative roles as neurotrophic factor and stimulator of neuritic outgrowth [167, 168].

PGRN mutations are mostly frameshift mutations predicted to introduce a premature stop codon

in mRNA and subsequent degradation of the messenger by a mechanism of Non-sense Mediated Decay (NMD) [169-171]. The results of degradation is the establishment of a state of haploinsufficiency that seems sufficient to trigger off a process of neurodegeneration, strengthening the role of normal progranulin in neuronal survival. In contrast to *MAPT, PGRN* mutations have incomplete penetrance (50% by age 60 years but 90% by age 70 years) Mutations in this gene are associated with variable clinical presentations, also within the same family, including the most common behavioural variant of FTD, PNFA (account for up to 25% of all cases) and 10-30% of patients disclose an AD-like amnestic presentation. Extrapyramidal features are frequent and include CBD and parkinsonism, while MND is very rare [172-174]. Also age at onset of the syndrome is variable, with an average of 60 years (range 35-89 years) and a mean illness duration of 8 years (range 3-22).

3.9.3 Valosin Containing Protein

Valosin Containing Protein (*VCP*) gene, located on chromosome 9p13, codifies for an adenosine triphosphatase functioning as molecular chaperone and involved in protein degradation in endoplasmic reticulum.

Mutations in this gene are associated to Inclusion Body Myopathy, Paget's disease of bone and Frontotemporal Dementia (IBMPFD), characterized by variable clinical presentations (inclusion body myopathy in 90% of cases; Paget's disease of bone in 45% and FTD in 38%), age at onset (range 40 to 60 years) and penetrance degree [175].

3.9.4 Charged Multivesicular Body Protein 2B

The gene product of *Charged Multivesicular Body Protein 2B* (*CHMP2B*), located on chromosome 3p11, is a component of Endosomal Sorting Complex Required for Transport III

(ESCRT-III) complex involved in the degradation of surface receptor proteins and the formation of endocytotic multivesicular bodies. Mutations in this gene have been identified only in a few FTLD cases and in only one patient with MND [176, 177].

3.9.5 Chrmosome-9p-linked FTD-MND

Several families with frontotemporal dementia associated to motor neuron disease (FTD-MND), have been associated to a locus on chromosome 9 (9p21.3-13.3) but, all attempts to identified the disease genes have not yet been successful [178].

3.9.6 TAR-DNA Binding Protein and Fused in Sarcoma

Mutations in *TAR-DNA Binding Protein* (*TARDBP*) and *Fused in Sarcoma* (*FUS*) genes, located on chromosomes 1p36.22 and 16p11.2 respectively and both codifying for DNA/RNA processing proteins implicated in transcription and splice-site regulation, are associated with MND or ALS (accounting together for nearly 10% of familial cases).

Missense variations in these genes were rarely identified in FTLD patients with or without MND but, whether these variations may represent a rare cause of FTLD is still debated, since, for some of them there is no conclusive evidence about their possible pathogenic nature [179-181].

3.10 The neuropathology of Frontotemporal Lobar Degeneration

3.10.1 Macroscopic findings

During the early phase of the FTLD clinical syndromes, there are no remarkable brain changes while with the illness progression several regions are affected by different pattern of atrophy which correlate with disease severity [182]. Gross findings in FTLD patients are represented by usually but not always symmetrical atrophy of frontal and/or temporal lobes. Depigmentation of

substantia nigra, atrophy of basal ganglia and white matter changes (axonal and myelin loss, and gliosis) are frequent.

3.10.2 Microscopic findings

The clinical and genetic heterogeneity of FTLD is also reflected at neuropathological level where the identification of distinct histological profiles led to the definition of four major neuropathological subgroups: FTLD-tau, FTLD-TDP, FTLD-FUS and FTLD-UPS [183, 184]. This classification is based on the distinct types of protein aggregates or inclusions that occur in the different categories but, this does not imply a chief role for these proteins in the pathogenesis of the disease (although this seems to be the case for some of them).

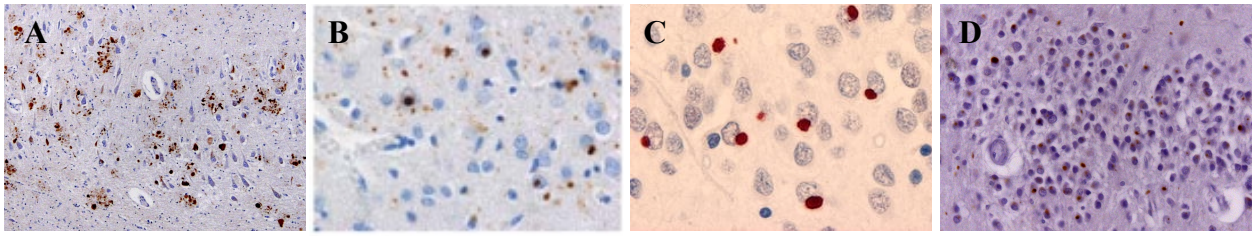

Fig. 9. FTLD neuropathological subgroups.
A: FTLD-tau with hyperphosphorylated tau deposition in neurons and glial cells; B: FTLD-TDP with cytoplasmic hyperphosphorylated, ubiquitinated and truncated TDP-43 inclusions; C: FTLD-FUS with small, round, compact neuronal cytoplasmic FUS inclusions; D: FTLD-USP with ubiquitin-positive intraneuronal inclusions.

3.10.2.1 FTLD-TDP neuropathology

FTLD-TDP is considered the most common histological profile observed in FTLD, where abnormal hyperphosphorylated, ubiquitinated and N-terminal truncated TDP-43 protein (encoded by *TARDBP*) accumulates to form cytoplasmic inclusions [185]. Depending on quantity, shape and distribution of the inclusions, four distinct FTLD-TDP pathological subgroups are recognized (named FTLD-TDP Type 1 to 4) [186]. FTLD patients with mutations in *PGRN*, *VCP* or associated to 9p21.3-13.3 locus, have displayed neuropathological findings

typical of these categories (FTLD-TDP Type 3 for *PGRN*, Type 4 for *VCP* and Type 2 for 9p21.3-13.3 locus).

3.10.2.2 FTLD-tau neuropathology

FTLD-tau represents the second most common histopathological subgroup of FTLD, characterized by aggregation and deposition of hyperphosphorylated tau protein in neurons and glial cells [187]. Actually, deposits of abnormal hyperphosphorylated tau are an hallmark not only of Alzheimer's disease (neurofibrillary tangles, neuropil threads and dystrophic neurites) but also of several other disorders named “tauopathies”. The main differences between these pathological entities are the isoforms and hyperphisphorylation degree of tau in inclusion bodies and their brain regional distribution. Several of these pathology are associated with clinical FTD (FTLD-tau), including Pick disease (PiD), progressive supranuclear pulsy (PSP), corticobasal degeneration (CBD), argyrophilic grain disease (AGS) and multiple system tauopathy with dementia (MSTD) [188-192]. FTLD-tau includes patients harbouring a *MAPT* mutation that may display a neuropathological profile typical of PiD, CBD or PSP.

3.10.2.3 FTLD-FUS neuropathology

A variable proportion of FTLD post mortem confirmed cases (5-20%) does not have deposition of abnormal protein tau, nor TDP-43 but, inclusions of ubiquitinated protein FUS similar in morphology and distribution to that observed for TDP-43 [193]. FUS aggregates have also been identified in other two rare pathologic variants of FTLD, including Basophilic Inclusion Body Disease (BIBD) and Neuronal Intermediate Filament Inclusion Disease (NIFID) [194, 195].

3.10.2.4 FTLD-UPS neuropathology

There is a fourth rare FTLD neuropathological subtype, characterized by the absence of tau,

TDP-43 and FUS deposition but, by inclusions enriched in not yet identified ubiquitinated proteins detectable only using antibody against the ubiquitin proteasome system (UPS) [196]. Mutations in *CHMP2B* gene are associated to this histopathologic profile [197], even though they do not explain all FTLD-UPS identified cases.

4. Cerebral Autosomal Dominant Arteriopathy with Subcortical Infarcts and Leukoencephalopathy

Cerebral Autosomal Dominant Arteriopathy with Subcortical Infarcts and Leukoencephalopathy (CADASIL) is a high penetrance hereditary form of vascular dementia in which occlusion of small arteries in the brain of adults results in small deep brain infarcts. The heterogeneous clinical presentation includes recurrent migraine (usually with aura), focal deficit secondary to brain infarcts and, as the disease progresses, cognitive decline and eventually dementia.

4.1 Epidemiology

Nearly 500 CADASIL families have already been reported worldwide but, the exact prevalence of this disorder is still unknown. The better estimate is 4.14 cases per 100.000 habitants, reported in an epidemiological study from Scotland, UK [198], even though this value is considered an underestimation of the real prevalence due to the occurrence of sporadic cases and difficulties in recognized family history [199].

4.2 Risk factors

Being a vascular type dementia, CADASIL is associated to the risk factors involved in vascular dementia in general. This form of dementia occurs predominantly in patients affected by cerebrovascular disease, coronary artery disease, and peripheral vascular disease, including patients with myocardial infarction, stroke, transient ischemic attacks (TIAs), cigarette smoking, diabetes mellitus, increased serum homocysteine, hyperlipidemia, hyperfibrinogenemia and hypertension (which triple the risk for vascular dementia) [200-202].

4.2.1 CADASIL molecular basis

Mutations in *Notch3* gene are the only well recognized genetic cause of autosomal dominant familial forms of CADASIL. *Notch3* genetic locus, mapping on chromosome 19, was associated with CADASIL in 1993 [203] and three years later linkage studies led to the identification of disease causing gene [204]. Since its discovery, more than 150 mutations have been identified.

4.3 Clinical diagnosis of CADASIL

The diagnosis of CADASIL should be considered in middle-aged patients showing typical clinical and neuroradiological features [205] including:

- clinically: onset in the second-third-fourth decade (but earlier or later presentations are encountered) with migraine (usually with aura), isolated or, more often, recurrent subcortical infarcts (lacunar strokes), mood changes, progressive cognitive decline or subcortical-type dementia (pseudo-bulbar palsy);
- neuroradiologically: symmetrical and periventricular white matter lesions on T2-weighted MRIs;
- positive family history for abovementioned disorders (but family history is not essential because de novo mutations are possible [199].

A definite diagnosis of CADASIL can derived by the finding of mutations in *Notch3*. Evaluation of Granular Osmiophilic Material (GOM) presence (pathological hallmark of CADASIL) in skin biopsy may be a supplementary diagnostic tool giving its high specificity (nearly 100%) but, not sufficient to exclude the clinical diagnosis due to its low sensitivity (less than 50%) [206].

As other form of dementia, clinical and neuroradiological findings in CADASIL patients may overlap with features peculiar to other diseases, in particular, those with signal abnormalities in white matter. This group includes Binswanger's disease (white matter infarcts), amyloid

angiopathy (recurrent lobar hemorrhages), multiple sclerosis (a great mimic of the disease in the first stages), familial hemiplegic migraine (migraine associated to stroke-like symptoms).

4.4 Clinical presentation of CADASIL

Clinical presentation and disease severity vary also within the same family but the main clinical symptoms include: migraine with aura, transient ischemic attack (TIAs), fixed focal neurologic deficits caused by lacunar infarcts, cognitive decline and dementia.

The most characteristic initial symptom is migraine usually with aura, reported in 20-40% of CADASIL patients with a variable mean age at onset frequently in the 20s years, associated to the appearance of punctate hyperintensities in deep hemisphere or periventricular white matter [207]. The most frequent clinical events in CADASIL are transient or fixed ischemic insults, recurrent in about two thirds of patients with first symptoms onset between 45-50 years. Lacunar associated symptoms include pure motor stroke, ataxic hemiparesis, pure sensory stroke, sensory motor stroke while, focal neurologic deficits encompass dysarthria, monoparesis, paresthesia of one limb, isolated ataxia, non-fluent aphasia [208]. Epilepsy is another common symptom, occurring in 5-10% of patients, starting usually after the onset of ischemic strokes (mean age of onset, 50 years). A variable proportion of CADASIL subjects, at least 20 to 40%, develop psychiatric disorders (usually after age 40 years in patients with previously ischemic episodes) including depression (the most common manifestation), mood disturbances, anxiety, psychotic events and rarely schizophrenia [209]. Cognitive impairment and dementia represent the second most common clinical features in CADASIL patients with onset symptom usually characterized by deficits of executive functions often associated to attention and memory disturbances. With the progression of the disease, other cognitive domains are involved, arising language dysfunctions, alterations of visuospatial abilities and loss of autonomy in daily life activities

[210]. Dementia develops in at least one third of patients, presented in about 60% of symptomatic subjects aged 60 years and reaching nearly 80% at the time of death [208, 211]. Dementia is always associated to pyramidal signs with gait problems, urinary incontinence and pseudobulbar symptoms as most frequent presentations. In advance stages of the disease, patients become bedridden and aphatetic and, they usually decease after inhalation pneumonia. Unusual clinical presentations in CADASIL may involve parkinsonism and extrapyramidal signs, deafness, visual impairment (with possible involvement of optic nerve and retina), polyneuropathy or myopathy and myocardial infarction.

4.5 Age at onset and illness duration

The heterogeneity in clinical manifestations affects the age at onset of the disease, strictly related to the type of first symptom. Nevertheless, the age of onset is usually given on the basis of the first ever stroke (not migraine that usually appears earlier) therefore, the average age at onset is 45 years and the illness duration varies between 10 and 30 years.

4.6 Structural neuroimaging in CADASIL

Magnetic Resonance Imaging (MRI) is crucial for CADASIL diagnosis. It always discloses signals abnormalities in *Notch3* mutation carriers over age 35 years and may identify brain lesions also in presymptomatic patients [212].

MRI images routinely used to confirm a clinical diagnosis of CADASIL include T2-weighted or FLAIR sequence, T1-weighted images, diffusion weighted images and SWI or gradient-echo T2* images (Fig. 10). The former show variable widespread areas of increased signal in the white matter associated with focal hyperintensities in basal ganglia, thalamus and brainstem. Detection of signal abnormalities in the external capsule and the anterior part of the temporal

lobes are useful in differentiate CADASIL from other small-vessels diseases [213]. MRI T1-weighted images disclose punctiform or larger focal hypointensities in both white matter and basal ganglia, complementary to identified T2 hyperintensities and corresponding to lacunar infarctions [212]. MRI signal abnormalities within the temporal white matter and particularly within the subcortical white matter are considered a characteristic feature of CADASIL. Silent and recent ischemic lesions are occasionally detected in CADASIL on diffusion weighted images [214] while microbleeds suggestive of microhemorrhages are detected on gradient-echo or T2*-weighted images [215].

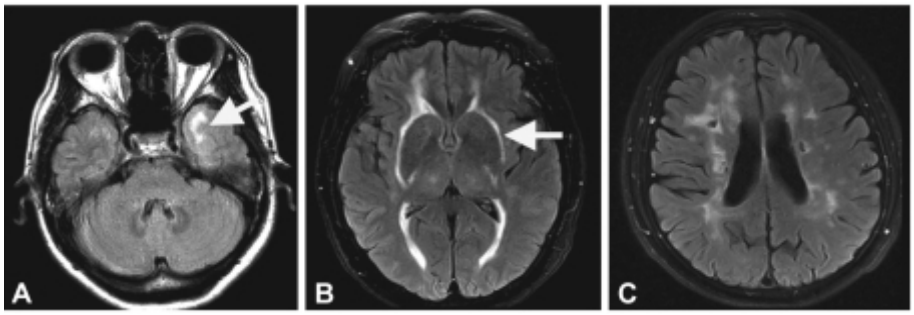

Fig. 10. Typical brain MRI findings in CADASIL.
FLAIR images demonstrate HSI lesions in the anterior temporal lobe (A) and bilateral external capsules (B). Multiple lacunar infarctions (C) are noted in bilateral periventricular and deep white matter with punctate HSI lesions. CADASIL: cerebral autosomal dominant arteriopathy with subcortical infarcts and leukoencephalopathy, FLAIR: fluid attenuated inversion recovery, HSI: high-signal-intensity.
[Choi JC, et al. Cerebral autosomal dominant arteriopathy with subcortical infarcts and leukoencephalopathy: a genetic cause of cerebral small vessel disease. J Clin Neurol. 2010;6:1-9.]

4.7 Cerebralspinal fluid (CSF) markers of CADASIL

Few studies aimed to detect biomarkers of prediction or evolution of the disease have been carried out on blood and cerebrospinal fluid but none of these succeeded in identifying significant consistent and reproducible variations correlating with the disease status [216-218]. Nevertheless, CSF levels of β-amyloid 1-42 (Aβ42), total tau protein (t-tau) and phosphorylated tau-protein (p-tau) are useful in differentiate CADASIL from other form of dementia. In particular, low CSF Aβ42 levels allow the discrimination between CADASIL and Alzheimer's

disease patients from normal values identified in healthy controls or FTD subjects moreover, unchanged CSF t-tau and p-tau are useful to differentiate CADASIL from AD where they vary significantly [219-221].

4.8 Treatments

No disease-modifying treatments are nowadays available but only symptomatic therapies. Effective treatments of migraine with aura are based on acetazolamide [222] while for acute attacks conventional analgesics and non-steroidal anti-inflammatory drugs are preferred. Administration of anticoagulants, like aspirin, in secondary prevention of cerebral ischemic events should be avoided because they may promote intracerebral hemorrhages [223]. Antihypertensive drugs could worsen hypoperfusion, the presumed mechanism of cerebral lesions in CADASIL. The only randomized controlled trial to be done in CADASIL tested the efficacy of donepezil (an acetylcholinesterase inhibitor used in Alzheimer's disease) in patients with cognitive impairment. This study did not show positive results in improving cognitive but executive functions [224]. Two other important aspects of CADASIL treatment are rehabilitation procedures following an ischemic event and, psychological support for patients and families.

4.9 The genetics of CADASIL

CADASIL is caused by mutations of *NOTCH3* gene, located on chromosome 19p13.1, which encodes a single-pass transmembrane receptor, whose expression is restricted solely to vascular smooth muscle cells (VSMC) of arterial walls [225], involved in differentiation and maturation of VSMC and probably in regulation of cerebral blood flow and vascular miogenic tone [226, 227]. The N-terminal extracellular domain of the protein consists of 34 epidermal growth factor (EGF)-like repeats, each containing six cysteine residues (Fig. 11). All CADASIL mutations

occur in exons 2-23 encoding for the EGF-like repeats. They are mainly missense mutations, although in-frame deletions or insertions may occur [228], that lead to the gain or loss of one cysteine. Whether the mutations cause a loss or a gain of the *NOTCH3* signaling function [229, 230], or abnormal misfolding [231] remains unclear.

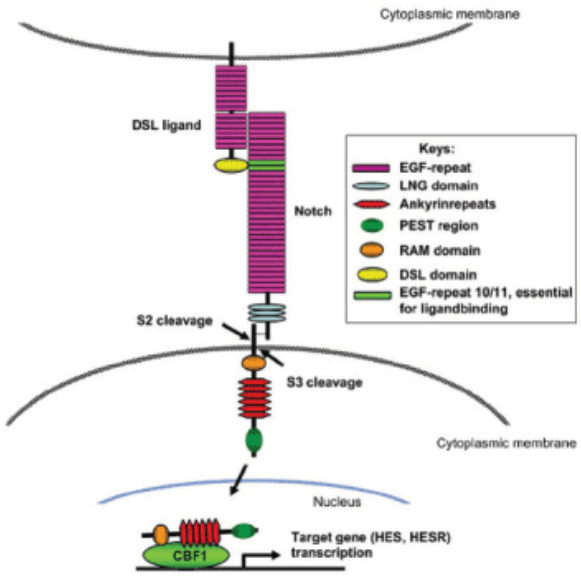

Fig. 11. The classic NOTCH signaling pathway.
The Notch receptor locates at cell surface as a heterodimer following protease cleavage (S1) during protein maturation. The extracellular domain (NECD) – containing up to 36 EGF-repeats and three cysteine-rich Notch/LIN-12 repeats (LNG domain) – associates non-covalently with a membrane-tethered intracellular domain (NICD) – with a RAM domain, six tandem ankyrin repeats and a praline-, glutamate-, serine, threonine-rich sequence (PEST domain). The interaction between the DLS-ligand and the Notch receptor leads to two additional proteolytic cleavages – S2 (mediated by a metalloproteinase family protein TNFa-converting enzyme, TACE) and S3 (within the transmembrane domain, by a g-secretase) – resulting in the release of the NICD, which then translocates to the nucleus, where it interacts with CBF1/RBP-Jk to activate transcription of target genes HES and HESR (or HRT).

4.10 The pathology of CADASIL

4.10.1 Neuropathological macroscopic findings

Macroscopic examination of the brain shows a diffuse myelin pallor and rarefaction of the hemispheric white matter predominating in periventricular areas and centrum semiovale. These lesions are associated with lacunar infarcts located in the white matter and basal ganglia. In the cortex there is the widespread of neuronal apoptosis [232, 233].

4.10.2 Neuropathological microscopic findings

Microscopic investigations show a thickening of cerebral and leptomeningeal arterioles wall, with a reduction of the lumen and, a stenosis of penetrating arteries in the cortex and white matter [234]. A distinctive feature is the presence of a PAS-positive granular material within the media extending into the adventitia. On electron microscopy, the smooth muscle cells appear swollen and often degenerated. There is a granular, electron-dense, osmiophilic material (GOM) within the media, located close to the cell surface of smooth muscle cells [235].

4.10.3 Skin biopsy

The granular, electron-dense, osmiophilic material is present not only in the brain but also in the media of arteries located in the spleen, liver, kidneys, muscle and skin. The presence of GOM in the skin vessels now allows confirmation, in the living patient, of the diagnosis of CADASIL using skin-punch biopsies (Fig. 12) [236].

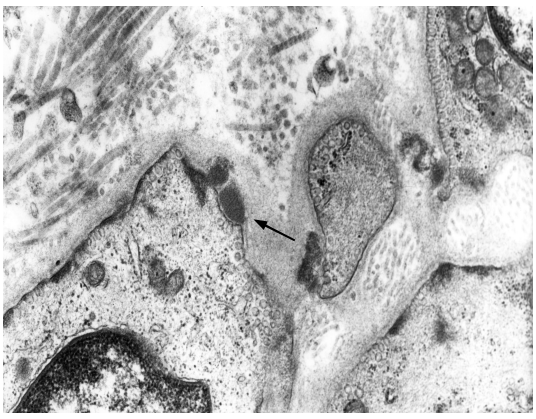

Fig. 12. Osmiophilic granules seen on electron microscopy.
Electron microscopy (EM) of NOTCH3 mutation carrier skin biopsy revealing granules osmiophilic material (GOM) embedded within the

This diagnostic method is useful in predicting and confirming *Notch3* mutation carriers but,

considering that skin biopsies are still an invasive approach and that the absence of GOM does not exclude the disease (in same cases the vessel changes may be focal, requiring a thorough evaluation of the biopsy specimen), this technique can not be considered a gold standard in CADASIL diagnosis. A promising alternative to electron microscopy GOM identification, may be represented by an immunohistochemistry by anti-*NOTCH3* antibody to identify the accumulation of the small aggregates that NOTCH3 ectodomain forms around the degenerating vascular smooth muscle cells in proximity to GOM deposits. This method seems to have not only high specificity (100%) but also high sensitivity (96%) [237].

5. Aims of the study

Whereas Alzheimer's Disease and Frontotemporal LobarDegeneration are both neurodegenerative disorders while CADASIL is a form of vascular dementia, the latter will be dealt separately from other.

In the mutational analysis of Alzheimer's Disease and Frontotemporal Lobar Degeneration associated genes, four main aims have been pursued:

- development of optimal experimental conditions (primer design, PCR amplification profiles, DHPLC analysis conditions and MLPA);
- evaluation of mutational frequency of AD and FTLD associated genes in an Italian series;
- identification and definition of possible correlations between genotype and clinical/pathological presentations of these disorders;
- definition of possible diagnostic algorithm for genetic testing.

In the mutational analysis of *NOTCH3*, three main aims have been pursued:

1) evaluation of mutational frequency of *NOTCH3* in an Italian series of CADASIL patients;
2) definition of distribution of *NOTCH3* mutations along the gene in order to define a possible useful diagnostic approach;
3) adding more data to reinforce the correlation between the presence of a *NOTCH3* mutation and the typical CADASIL pathological findings (deposition of GOM).

6. Patients and Methods

Mutational, microsatellites and haplotype analyses were performed on DNA samples extracted from peripheral blood samples or from frozen brain tissues, and stored at -20°C for subsequent uses.

6.1 Patients

Enrolled patients were visited by neurologists and neuropsychiatrists in dementia medical clinic at G.B. Rossi Hospital in Verona or referred from centers in North- and Central-Italy. After obtaining informed consent for genetic analysis, patients underwent venous blood sampling for DNA extraction.

6.1.1 Patients with AD or FTLD

AD- and FTLD-associated genes were analyzed in 210 patients and the whole series is summerized in two tables which distinguish cases whose DNA was extracted from peripheral blood (Table 1) and those with DNA extracted from frozen brain tissue (Table 2). The series was subdivided according to clinical diagnosis and, for each subtypes are given, the number of index cases, age of onset of the disease and data about family history. The neuropathological diagnosis has been reported for autopsy cases. Noteworthy, these informations were not available for all patients, especially those enrolled in hospitals or care facilities outside G.B. Rossi Hospital where this study was performed. In addition, this study included even patients with clinical diagnosis suggestive of possible atypical presentations of AD and FTLD (as stated in the introduction); among this group there were also Mild Cognitive Impairment (MCI) that is considered to represent the prodromal phase of AD and the Creutzfeldt-Jacob Disease (CJD)

which is a form of rapidly progressive subacute dementia that can sometimes be misdiagnosed instead of an Alzheimer's with rapid clinical evolution.

Diagnosis	*N. of index cases*	*Mean age at onset (n)*	*Inheritance*		
			Familial	*Sporadic*	*Unknown*
MCI	13	66,5 ± 9,49 (8)	5	1	7
DEMENTIA	48	65,5 ± 8,04 (8)	11		37
DEMENTIA + EPS	5	47,5 ± 3,54 (2)	1		4
AD	41	63,96 ± 9,81 (24)	17	1	23
FTD	59	59,65 ± 7,6 (23)	12	6	41
PNFA	7	53,83 ± 4,4 (6)	2		5
FTD + MND	5	55 ± 7,55 (3)	1	1	3
LBD	2	72,5 ± 10,61 (2)			2
CBD	4	56 (1)			4
PSP	7	69 (1)		1	6
PSP/CBD	2				2
CAA	2	54 (1)	1		1

Table 1. Clinical series with DNA samples extracted from peripheral blood.
Abbreviations: MCI, Mild Cognitive Impairment; EPS, Extrapyramidal Signs; AD, Alzheimer's Disease; FTD, Frontotemporal Dementia; PNFA, Primary Non-fluent Aphasia; MND, Motor Neuron Disease; LBD, Lewy Body Dementia; CBD, Corticobasal Dementia; PSP, Progressive Supranuclear Pulsy; CAA, Cerebral Amyloid Angiopathy; Unknown, data not available; (n), number of index cases whose age of onset was available

Clinical Diagnosis	*Case index*	*Mean age at onset (n)*	*Inheritance*			*Pathological diagnosis (n)*
			Familial	*Sporadic*	*Unknown*	
AD	3	72,33 ± 2,52 (3)		2	1	Tauopathy (1); AD (2)
DEMENTIA	3			1	2	AD (3)
FTD	2	80 (1)		1	1	Tauopathies (2)
PSP	1	65 (1)		1		Tauopathy (1)
CBD	1	73 (1)		1		FTLD-UPS (1)
CJD	5				5	AD (3); LBD + AD (2)

Table 2. Clinical series with DNA samples extracted from frozen tissue.
Abbreviations: AD, Alzheimer's Disease; FTD, Frontotemporal Dementia; PSP, Progressive Supranuclear Pulsy; CBD, Corticobasal Dementia; CJD, Creutzfeldt-Jacob Disease; UPS, Ubiquitin Proteosome System.; Unknown, data not available; (n), number of index cases whose age of onset was available

The choice of samples extracted from postmortem brain tissue was driven by the pathological diagnosis (performed by histological and immunohistochemical studies) of AD or FTLD. Otherwise, samples extracted from peripheral blood were mainly selected by the outcome of clinical and neuropsychological tests according to diagnostic criteria for either dementia subtypes. Nevertheless, the clinical picture is not always plain or well defined to drawing up with certainty the clinical diagnosis of a particular form of dementia. In these cases, informations about familial aggregation of the disorder plays an important role. In this study 50 out of 210 were familial cases of dementia, 16 were apparently sporadic while for remaining informations were not enough to rule out or support a positive family history. The terminology “familial case” means that in a patient family one or more cases of dementia or related illnesses occur but this not necessary imply a genetic cause which actually is the basis for defining a character as inheritance. The terminology “apparently sporadic” means that family history informations seem to exclude a disease familiarity but, this is not always true considering the difficulties in

collecting this type of data from patients and their relatives and possibility of *de novo* mutations. "Unknown inheritance" is often regarding outpatients examined in other hospitals, for whom a detailed history is not available.

6.1.2 Patients with CADASIL

Six hundreds twenty-eight patients overlapping clinical and/or radiological criteria for CADASIL were referred to Neuropathology laboratory at G.B. Rossi Hospital for molecular screening of *NOTCH3*. Five hundreds seventy-seven were unrelated index cases while fifty-one were family members belonging to twenty-two families.

6.1.3 Controls series

For mutational analysis (of either AD and FTLD associated genes or NOTCH3) and the study of NOTCH3 haplotypes, it was necessary to establish two series of cognitively normal control subjects. Patients referred to Neuropathology laboratory at G.B. Rossi Hospital with clinical and/ or molecularly confirmed diagnosis for other disorders of central or peripheral nervous system, with a normal cognitive profile and without positive family history for dementia, were included in this group of controls after obtain informed consent.

In particular, 492 unrelated subjects were selected to define the frequency of identified non-synounimous nucleotide variations, to confirm or rule out their possible pathogenetic role while, for NOTCH3 haplotypes analysis a cohort of other 50 cognitive normal subjects was enrolled in order to define the frequency of different haplotypes in our population.

6.2 DNA extraction from peripheral blood leukocytes

DNA extraction from peripheral blood leukocytes was performed starting from a 5 to 10 ml of

whole blood collected in a anticoagulant Ethylenediaminetetraacetic Acid (EDTA) tube by Salt-in-out protocol, as following:

- all blood volume was transferred in 50 ml sterile falcon;
- 3 volumes of 1X cold hemolysis solution (155 mM NH_4Cl, 10 mM $KHCO_3$, 1 mM EDTA, pH 7.4) were added and, after vigorous inversions, the tube was placed on ice for 20 min;
- the tube was spinned at 2000 rpm for 10 min at 4°C in a Beckman GS-6R refrigerated centrifuge;
- the supernatant was aspirate with vacuum and the pellet washed with 15 ml of 1X cold hemolysis solution and incubated on ice for 20 min;
- the tube was spinned at 2000 rpm for 10 min at 4°C, the supernatant was aspirate with vacuum and the pellet resuspended in 3 ml of 1X lysis solution (10 mM TriHCl, 75 mM NaCl, 24 mM EDTA, pH 8);
- entire volume was transferred in a 15 ml sterile falcon and 450 µl of 10% SDS and 300 µl of Pronase (1g/50ml) were added. The tube was placed in water bath at 37°C for 1-2 days;
- after digestion, 1.5 ml of saturated NaCl solution (35g/100ml) was added and tube shaked vigorously for a few sec and then spinned at 2500 rpm for 15 min at room temperature;
- the supernatant was transferred to a new tube and DNA was precipitated with 2 volumes of 100% ethanol;
- two 70% ethanol were carried out and then, DNA precipitate was transferred to a 1.5 ml eppendorf tube letting to dry ethanol excess;
- 1 ml of 1X TE (100 mM Tris, 0.1 mM EDTA, pH 7.5) was added to dry DNA left to completely dissolve at 4°C for a few days and then stored at 20°C.

6.3 DNA extraction from frozen brain tissue

DNA extraction from frozen brain tissue was performed with DNA Isolation Kit for Cells and Tissue (Roche Applied Science), starting from 400 mg frozen tissue, according to manufacturer's instructions. DNA yields were determined via spectrophotometry.

6.4 DNA amplification

For each gene included in the study, a genomic clone was selected from the GenBank database:

4) *Progranulin* (*PGRN*): NM_002087.2;
5) *Microtubule-Associated Protein Tau* (*MAPT*): NM_001123066.3;
6) *Valosin Containing Protein* (*VCP*): NM_007126.3;
7) *Charged Multivesicular Body Protein 2B* (*CHMP2B*): NM_014043.3;
8) *TAR DNA Binding Protein* (*TARDBP*): NM_007375.3;
9) Amyloid Precursor Protein (APP): NM_000484.3;
10) *Presenilin1* (*PSEN1*): NM_000021.3;
11) *Presenilin2* (*PSEN2*): NM_000447.2;
12) *Apolipoprotein E* (*APOE*): NM_ 000041.2;
13) *NOTCH3*: NM_000435.2

Pairs of oligonucleotides were designed for each coding exon using Primer3 software (http://frodo.wi.mit.edu/primer3/) following a few criteria: amplicons maximum of 400-600 bp in length, intron-exon boundaries included in the amplicon, similar melting temperatures for primer pair, avoiding primer sequences prone to form secondary structures or dimers (Table 2-12). For each exon, the best amplification conditions were tested in order to obtain specific PCR products, including the choice of DNA polymerase, the right concentration of salts, organic

compounds like DMSO (to facilitate double strand separation), primers and the optimal amplification cycle.

PCR reactions were run on GeneAmp 9700 thermocycler (Applied Biosystems) or Mastercycler ep gradient S (Eppendorf) and, after amplification, analysis of PCR products was performed by agarose gel electrophoresis (1% agarose).

PCR standard mix reactions (per sample):

5X Colorless GoTaq Reaction Buffer (Promega)	1X
2 mM mix dNTPs	40 µM
primer forward	0.2 µM
primer reverse	0.2 µM
GoTaq DNA Polymerase (Promega)	1 unit
DNA sample	200 ng
H_2OmQ	(to adjust total volume to 10 µl)
TOTAL	30 µl

10X PCR Gold Buffer (Applied Biosystems)	1X
25 mM $MgCl_2$ Solution	2.5 mM
2 mM mix dNTPs	40 µM
primer forward	0.2 µM
primer reverse	0.2 µM
AmpliTaq Gold (Applied Biosystems)	2 units
DNA sample	200 ng
H_2OmQ	(to adjust total volume to 10 µl)
TOTAL	30 µl

10X Reaction Buffer (Transgenomic)	1X
25 mM $MgSO_4$ Solution	2.5 mM
2 mM mix dNTPs	40 µM
primer forward	0.2 µM
primer reverse	0.2 µM
Optimase Polymerase (Transgenomic)	0.75 unit
DNA sample	200 ng
H_2OmQ	(to adjust total volume to 10 µl)
TOTAL	30 µl

PCR amplification profiles:

APP, PSEN1, PSEN2, PGRN

94°C	5 min	
94°C	30 sec	40 cycles
T annealing	30 sec	
72°C	30 sec	
72°C	2 min	
16°C	∞	

MAPT

94°C	5 min	
94°C	30 sec	40 cycles
T annealing	35 sec	
72°C	40 sec	
72°C	2 min	
16°C	∞	

VCP, CHMP2B

94°C	5 min	
94°C	30 sec	40 cycles
T annealing	30 sec	
72°C	30 sec	
72°C	2 min	
16°C	∞	

TARDBP

94°C	5 min	
94°C	30 sec	35 cycles
T annealing	30 sec	
72°C	30 sec	
72°C	2 min	
16°C	∞	

APOE

94°C	7 min	
94°C	30 sec	38 cycles
T annealing	30 sec	
72°C	30 sec	
72°C	2 min	
16°C	∞	

NOTCH3

94°C	7 min	
94°C	30 sec	38 cycles
T annealing	30 sec	
72°C	30 sec	
72°C	2 min	
16°C	∞	

Table 3: *PGRN* primers

Exon	Primer sequence (5' → 3')		amplicon length (bp)	Annealing Tm (°C)	DNA polymerase	Oven Temperature (°C)
	Forward	Reverse				
1	CCCACCTCTATATTGATAAGTAGCC	TTCTTCTGTTGTCTCCGGCT	256	62*	Gold	62 / 63 / 64
2	TGGCGTGGGCTTAAGCAGTT	TCTGGCCAATCCAAGATGAC	263	60	Go Taq	62.7 / 63.7
3	ATCTTGGATTGGCCAGAGGA	AGGTGGTAGAGTGCAGGAAA	263	60	Go Taq	60.7 / 61.7
4	GCTTTTCCTGCACTCTACCA	GTTCCAGACTCCACATGCTG	211	60	Go Taq	63.2 / 64.2
5	CCACCAGCTCCTTGTGTGAT	TGGTCCTGACTCCGTCTTCA	279	64	Go Taq	61.1 / 62.1
6	GTATGTGGAGGGAAGTGGGG	AACTTTTTCCTACACTTGGAGTC	286	60	Go Taq	63.3 / 64.3
7	CCTCATTGACTCCAAGTGTAGG	CCCCTGTAAGGTGCGTGTCA	253	62*	Go Taq	63.7 / 64.7
8	GAGCCTGGAAGTGACAAAGA	ACCTTGCAGTGATCCTAAGG	248	60	Go Taq	63.1
9	CAAAGGGTTGATACCCCTGA	TGTGGTCCTCACAGCACACA	276	62*	Go Taq	62.4 / 63.4
10	TGAGCACAGTGTGGCAGGCA	GCAGAAAGCAATAGGAGCTTGG	373	64	Go Taq	62.3 / 62.7
11	CACATAGTGGCTACCTACAACG	TGGCATTATGTTCCTGTCCC	347	60	Go Taq	64.3 / 64.9

Table 3: PGRN primers

Exon	Primer sequence (5' → 3')		amplicon length (bp)	Annealing Tm (°C)	DNA polymerase	Oven Temperature (°C)
	Forward	Reverse				
12	AGCTAAGCCCAGTGAGGGGA	TTGGACGAGGTGGGACCTGG	352	64	Go Taq	63.9 / 64.3
13	ATCCTGGGGCTGGGTATGGC	AGGTGCTAGGGAGGCCTGAG	273	64	Go Taq	64.6 / 65.6

Table 4: *MAPT* primers

Exon	Primer sequence (5' → 3')		amplicon length (bp)	Annealing Tm (°C)	DNA polymerase	Oven Temperature (°C)
	Forward	Reverse				
1	CAACACTCCTCAGAACTTATC	CAGTGATCTGGGCCTGCTGTG	229	53.5	Gold	59.5 / 61.5 / 62.5
9	CGAGTCCTGGCTTCACTCC	CTTCCAGGCACAGCCCTACC	370	65.5	Go Taq	64.3 / 65.3
10	GGTGGCGTGTCACTCATCC	CGCACTCACACCACTTCC	198	60	Gold	59.1 / 60.1 / 61.1
11	CTTCTCATTGAGTTACACCC	CTCACCAGGACTCCTCCAC	256	57	Gold	59.4 / 60.4
12	AGATGCTCTTGTGTGTGTTGTG	CAGCATCCAACCCACCCTAC	170	62*	Gold	58.4 / 59.4
13	CTTTCTCTGGCACTTCATCTC	CCTCTCCACAATTATTGACCG	299	60	Gold	62 / 63 / 64

Table 5: *VCP* primers

Exon	Primer sequence (5' → 3')		amplicon length (bp)	Annealing Tm (°C)	DNA polymerase	Oven Temperature (°C)
	Forward	Reverse				
1	AAGCCGCTTGCGGGTTTGTC	GGTCTCCACCTCTCTGACGC	261	64*	Go Taq	67.6/68.6
2	GGGACAGCTTCATCTATTCA	CCCACTCTATCTGCAGTCAC	319	58	Go Taq	57.9/58.9
3	TGACTGCAGATAGAGTGGGG	GACAGGTGCCAAGAACTTGG	381	62*	Gold	57.7/58.7
4	TATCAGCTATCTGTGCCAGG	AATAAATAAATACAGGGGAAAAGC	359	54*	Gold	55.6/59.6
5	GGGCACTATCTAATGAGCTTGG	CTCCCAAAGTACTGGGATTACAG	365	61*	Gold	59.7/60.2
6	GCACACTAGGTAGTGGAATGAT	CAATAATGAAAGCCATGCAT	327	58	Gold	56.8/58.8
7	TTGAAGCCTGATTCTCACCC	CATGGGTGCAAAAAGGATGT	296	58	Go Taq	58.1/59.1
8	CCTGTCTCTGGGCCAAACAA	TGAGTCTGCCAGAACAGGATG	312	58	Go Taq	57.6/58.6
9	ATGCCATCGCTCCCAAAAGA	CCAATCACTGTGAAGGGCTTC	340	58	Go Taq	59.5/61.5
10	GGACAATCCTGTGCTGGCTG	CAAAACCCATCTCCTCACATC	314	58	Go Taq	58.8/59.8
11	GGACCCAGGGATAGCAGTCA	TCTGGCTCAAGGCCCACTAG	373	58	Go Taq	60.1/61.1

Table 5: *VCP* primers

Exon	Primer sequence (5' → 3')		amplicon length (bp)	Annealing Tm (°C)	DNA polymerase	Oven Temperature (°C)
	Forward	Reverse				
12	ACTTCCGGGTAAGGACCACA	GCTCTCACAACTCTTGCAGC	323	58	Go Taq	60.4/61.4
13	CCATTGGGTACACCATGAAA	TGAGCAGCCAGCACTAAGAA	418	58	Go Taq	57.4/59.4
14	TGAGCCACCACGTTTGCCTA	AAGAGCACTCCGTACCAGCC	442	58	Go Taq	61/63
15	AAAGAAGGGGCAAACTGTAG	CTTTCCAACAGCTTCTACTCTC	355	62*	Gold	60.4/61.4
16	ATTGGAAGGGCAAGGAGACC	CACAACTACCCCTCTAGCTTCC	355	62*	Gold	59.1/60.1
17	CAAAAGGGATGGGAGTCCTA	TGTTCAGACTGGAGAATGGAG	329	62*	Gold	61.9/92.9

Table 6: *APOE* primers

Exon	Primer sequence (5' → 3')		amplicon length (bp)	Annealing Tm (°C)	DNA polymerase	Oven Temperature (°C)
	Forward	Reverse				
16	TGGGTAGGCTTTGTCTTACAG	TAGCACAGGATGAACCAGAG	218	65	Gold	67.4/68.4

Table 7: *CHMP2B* primers

Exon	Primer sequence (5' → 3')		amplicon length (bp)	Annealing Tm (°C)	DNA polymerase	Oven Temperature (°C)
	Forward	Reverse				
1	CCTGTCCTTTGCCAGCGTT	TGTGGGACCACTTGATCCAG	219	62*	Go Taq	64.4/65.1
2	CGCCCAGCCAATATAAGATTT	CCATGTGCCTTCTTCCTAGTTAG	294	62*	Go Taq	53.8/55.8
3	GGACAAAGGGTCTGTTATGT	GGAGGTGCTTTTAAATCTGCT	386	62*	Go Taq	53.3/54.3
4	CGGCAGGATGGATATCTTTT	CTTCGTGAATGAGAATATGAGAC	312	62*	Go Taq	52.9/54.9
5	TTCACTGAGTTTGCCTTCTG	CCATGCACCTCCTAGTAAAAA	313	62*	Go Taq	54.8/55.8
6	CAGACCTCTTTACAGCACATC	TAGCCATGGGTTAGGAAACA	340	62*	Go Taq	55.2/57.2

Table 8: *TARDBP* primers

Exon	Primer sequence (5' → 3')		amplicon length (bp)	Annealing Tm (°C)	DNA polymerase	Oven Temperature (°C)
	Forward	Reverse				
2	TTCTGACATGAATGTTGTTCAT	GACACACACCTGAACACACTT	347	57.5	Go Taq	56.8/57.8
3	TGCTTCTCATTTCTAGATGTAGG	TGCTAGATACTCATTCACATGGTA	306	57.5	Go Taq	55.6/56.6
4	GGAACTATGATTTGGGAATGG	CCTGCCGCTATCTTTTCTAAG	308	57.5	Optimase	56.6/57.6
5	CTATCCAAGGCGAATGATTT	TCCAAAGTGCTGGGATTGTA	341	57.5	Optimase	55/60
6A	GCTTGTAATCTAAGTTTTGTTGCT	CATCATGGCTGGATTAATGC	339	57.5	Optimase	55.4/58.4
6B	TCAAGGTAGTAATATGGGTGGTG	TGAATTCCCACCATTCTATACC	383	57.5	Optimase	59.6/60.6

Table 9: *APP* primers

Exon	Primer sequence (5' → 3')		amplicon length (bp)	Annealing Tm (°C)	DNA polymerase	Oven Temperature (°C)
	Forward	Reverse				
16	TGGGTAGGCTTTGTCTTACAG	TAGCACAGGATGAACCAGAG	263	55	Go Taq	54.5 / 55.5
17	TCCCCTGCATTTAAGAAATG	CTAAGCCTAATTCTCTCATAGTCT	310	53	Go Taq	56.6 / 58.6

Table 10: *PSEN1* primers

Exon	Primer sequence (5' → 3')		amplicon length (bp)	Annealing Tm (°C)	DNA polymerase	Oven Temperature (°C)
	Forward	Reverse				
3	ATTGTAGTGCACAAAGTTCTGT	AGGTGAGGGGAGATGATAAG	244	55	Go Taq	57.9 / 58.9
4	CTGCTGAGAATCTGATTTACTG	TGTAAAGAAAAGCCACACTG	351	56.6	Gold	56.9 / 60.5
5	GGTGATCTCCATTAACACTG	CAACCATAAGAAGAACAGGG	244	55	Go Taq	57.9 / 58.9
6	GTACTTTTTAAGGGTTGTGGG	TCATCAACAAAGTACATGGC	213	55	Go Taq	54.1 / 55.1
7	TGGTGAAAATTATTGTACATCT	AAAGAAAACACTCCAGTGGG	330	53	Go Taq	57 / 58
8	CCATTTACAAGTTTAGCCCA	GTTACATGTGCTTCAGTTCC	228	56.6	Gold	52.7 / 53.7
9	ATGGCTTGTTGTTGTCTATG	GACCAAAGAAAGACGATAAAAAC	248	53	Go Taq	54.1 / 55.1 / 56.1
10	CAGCTAGTTACTGTTTCCATGTA	AAAAGGTTGATAATGTAGCTACC	325	53	Go Taq	55.9 / 58.9 / 60.9
11	GTGAAATCATAGCAAAGAGTGAC	ACAGAACTGCCTTAAAGGGA	256	55	Go Taq	55.7 / 56.7
12	GAGTTTTGCCTGAAAATGCT	CAGGAAAATCACCTTTGTCC	300	55	Go Taq	56.1

Table 11: *PSEN2* primers

Exon	Primer sequence (5' → 3')		amplicon length (bp)	Annealing Tm (°C)	DNA polymerase	Oven Temperature (°C)
	Forward	Reverse				
4	CACAGGAAAGTGGAACAAGG	TAAGGTACAGTAGCCGCAGG	260	58	Go Taq	62.2 / 63.2
5	TTACATGGATAGGCTGCCGT	AGTGACCAACACAGGCTGCT	360	58	Go Taq	61.2 / 62.2
6	GGTCCAGAATCACTCAAGGTG	CTAAAGGCGGCTGTTTCACG	307	58	Go Taq	63.2 / 63.4
7	CCTAATGAAGAGCATTCAGGC	CTCATGCCCATGTCCACTTGT	245	58	Go Taq	58.4 / 59.4
8	GCTGTAATGCCTCCACTGAG	TGCAGCACTGGGGACGATTT	343	62	Go Taq	61.5 / 62.5
9	CAGGGCAGGCTCTTCTTCAG	AAAGCCACGGCCAGGAAGCA	252	62	Go Taq	59.7
10	CTTTCTGGGACGCAGACTGG	TCCTGAACTCATGCCTCTCAG	280	58	Go Taq	62.9
11	GTAACACTCTGACCAGCTGTTG	GAGCCTCCACCCTCTGTCTC	256	58	Go Taq	61.3
12	TTCTGGGCCAGAGTTTCTCT	ATCCCTAGGGATCCTGAGAC	287	58	Go Taq	61.5 / 62.5
13	ACCATGACTCACAGCTCCTG	AACTATACAACTGCATCCAATG	286	58	Go Taq	61.8 7 62.8

Table 12: *NOTCH3* primers

Exon	Primer sequence (5' → 3')		amplicon length (bp)	Annealing Tm (°C)	DNA polymerase	Oven Temperature (°C)
	Forward	Reverse				
1	GGAAGGAGGGAGGAGGGGAGG	CACTCCCCCTCTGCCGCCCT	205	65.5	Gold	67.5/68.5
2	GGGCACCTGGCTGATCCTCCA	CACACACAGGGCCCACTGGTG	162	65.5	Gold	65.2/66.2
3	TGTGCTGCCCAACCAAGCCATC	TGTGCTGCCCAACCAAGCCAT	252	66*	Gold	65
4	TAGTCGGGGGTGTGGTCAGT	GGAAGGGGGCAAGGATGG	474	66*	Gold	65.1/66.1
5	CCCTACTCAGGAGAGTCAGAG	GTCCAAGCCACCTGGCGCATG	272	64*	Gold	62.8/63.8
6	CCAGGTGGCTGGACTGCTGC	CAAGTCAGACTTCTTATTTGCC	308	62.5*	Gold	63.6/64.6
7	ATGGAGTGCGATCGGTGTGG	CTTTCCCAGCCCATTCACAG	283	62.5*	Gold	62/63
8	TGTGAATGGGCTGGGAAAGA	CCCACTTACACCCCATTCTG	359	61	Gold	65/66
9	CCATAGGGTAGCCCCCG	TGCCCCTTCCCAGACATG	209	58	Gold	62.7/63.7
10	GTGTACTGCTCTCACCCTTTC	CAAGTCTGTTATTGGCCCTG	181	58*	Gold	64.5/65.5
11	TGGGCAGGCCCCTGGCAAGT	CCCAAACCCTCTGTGCCCCT	341	66*	Gold	63.6/64.6

Table 12: *NOTCH3* primers

Exon	Primer sequence (5' → 3')		amplicon length (bp)	Annealing Tm (°C)	DNA polymerase	Oven Temperature (°C)
	Forward	Reverse				
12	GAATGGTGCATCTAGTGGG	GACTTCACCCTCGATCTAGG	221	62	Go Taq	60.4/61.4
13	TTGTCCCTGCTGACTTTGTTC	GTCAGGCCAGGGAGGTG	305	62	Gold	62.2/64.2
14	CTTCTCAGCCTCAGACACTG	GGGAGGAGAGAGTAGAGGAG	301	62	Go Taq	63.6/64.6
15	TCAATCATTTCCCTCCAGGA	CCCAGCATCATCCCTGATAG	320	58	Go Taq	62.3/63.3
16	CCCTGCTCTGTACCCTGTAA	AGGCACACAGTTCAAGCTTAT	276	62	Gold	62.4/63.4
17	CCAAGGCATATCCCAGTCAG	CGTTGCTGTCCCCACTTCGT	382	58	Go Taq	64.2/65.2
18	ACTCAGGAAGGAGGGCAGGG	AGAAACTGTGCCCCGACTTG	302	62	Go Taq	64.4/65.4
19	CAAGTCGGGGCACAGTTTCT	AGCAGGAGGTACGTGCATGA	285	58	Go Taq	63.7/64.7
20	TGAATGATCTGTGTGATGGA	GCCCAGACGCACCCAAGCAT	322	58	Go Taq	63.1/64.1
21	GTATGTCCAGGTGGGTCTGT	GGTCAAGAGGGAATGAAGAC	255	55	Go Taq	61.6/62.6
22	GATGAGAGGCTGTCTTCATT	GCATGTAGATCAGCCACAAT	379	55	Go Taq	62.6/64.6

Table 12: *NOTCH3* primers

Exon	Primer sequence (5' → 3')		amplicon length (bp)	Annealing Tm (°C)	DNA polymerase	Oven Temperature (°C)
	Forward	Reverse				
23	AGGTAAGCGTTGGCGAAGGG	CACGCCCCTACTACTCCAGA	269	58	Go Taq	63.4/64.4
24 A	CTCCCCACCCTCATTTTTAT	TGTTGCACTCGCGGTCGCAG	429	58	Go Taq	68.7/69.7
24 B	CCTTCTTCCGCTGCGCTTGC	CTGGGATGGATGCATAGACA	382	58	Go Taq	67.1/68.1
25	TTGTCTCCTCTGACCCCTGA	TGAAACACACAAGACCTGGA	464	58	Go Taq	64.3/65.3
26	CTTGGTACCAGGGGGTGCAT	TTTGGCCTCAGGCGGGGCTT	292	65.5	Go Taq	63.3/64.3
27	AAGCCCCGCCTGAGGCCAAA	TCAAGGCGGGGTCCAGGGTT	354	65.5	Go Taq	65.2/65.7

Table 13: Real-Time PCR primers

Gene	Exon	Primer sequence (5' → 3')	
		Forward	Reverse
B2M	2	TTACTGAAGAATGGAGAGAGAATTGAAA	GACCAGTCCTTGCTGAAAGACA
UBC	1	GGGTCAATATGTAATTTTCAGTGTTAG	TTGTCTAACAAAAAAGCCAAAAACG
PGRN	3	ATGCAGGTTTCTCTGTGTTCCA	CCCAGCTGCACCTGATCTTT
	8	TCCTCTCTGCTTCCCTCACAGT	TGTAGACGGCAGCAGGTATAGC
	11	GCTGGCTACACCTGCAACGT	GGGCAGAGACCACTTCCTTCT
APP	5	ATGACTACGGCATGTTGCTG	CACATTGTCACTTTCTTCAGC
	11	CCCCATGGACATATGTGTTT	TTCCACTCTGGCCATGTGTG
	18	GCTCTCCTCTTGTTTTTCAGG	ATCTGCTCAAAGAACTTGTAG

6.5 PCR products purification by ethanol precipitation

If used in direct sequencing, PCR products were purified from primers and salts excesses which can interfere with the reaction. Ethanol precipitation was carried out as following:

- entire PCR volume was transferred to a 1.5 ml eppendorf tube and 2 volumes of 100% cold ethanol and 1/10 of final volume of 3M Sodium Acetate (pH 5.2) were added and mixed throughly;
- the tube was spinned at 14000 rpm for 16 min at 4°C in a Eppendorf 5417R refrigerated centrifuge;
- the supernatant was discarded and 200 µl of 75% cold ethanol were added to the pellet and mixed throughly;
- the tube was spinned at 14000 rpm for 11 min at 4°C;
- the supernatant was discarded and 200 µl of 75% cold ethanol were added to the pellet and mixed throughly;
- the tube was spinned at 14000 rpm for 6 min at 4°C;
- the supernatant was discarded and the pellet was air- or vacuum-dried and then, dissolved in 10-20 µl of H_2OmQ and stored at -20°C until usage.

6.6 Mutational analysis

Mutational screening of AD, FTLD and CADASIL associated genes was performed by two main techniques: the Denaturing High Performance Liquid Chromatography (DHPLC) and direct sequencing.

6.6.1 Denaturing High Performance Liquid Chromatography

The DHPLC technology allows the identification of sequence variations in DNA fragment or

PCR products. It is mostly used for the identification of single nucleotide polymorphisms (SNPs), point mutations, small deletions and insertions. This technology is based on heteroduplex detection whose chromatographic profile is easily distinguishable from homoduplex peaks and, therefore, provides a good method for the identification of new mutations. The choice to use DHPLC for mutation screening in this study arises from its high degree of sensitivity. In this study Transgenomic WAVE ® 3500 HT System was used and its basic principle is as follows. Wildtype and tested allele are amplified separately, mixed, heated at 94°C for 5 min and then cooled at room temperature promoting the formation of homoduplexes and heteroduplexes (if a nucleotide variation is present). When a mutation is present, there are four possible configurations: wildtype homoduplex, mutant homoduplex and two heteroduplexes. The samples are placed on a 96-well plate and injected into a DNASep separation cartridge containing hydrophobic beads. The cartridge is located inside an oven which controls and maintains a constant temperature fixed by the operator. Negatively charged phosphate backbone of DNA fragments interact with the positively charged ammonium group of triethyammonium acetate (TEAA) present in the buffer flow path injected in the cartridge with the samples. As a result of these interactions, the DNA will be indirectly bound to the hydrophobic beads of the cartridge from which it will be subsequently removed by increasing concentration of an organic solvent, acetonitrile (ACN), which competes with TEAA: the outcome is the release of the DNA fragments from the cartridge. Heteroduplexes, with mismatched base pairs, elute off of the cartridge first followed by the homoduplexes. The fragments pass through the UV detector which detects the absorbance over time. This information is sent to Navigator Software on PC and translated into a chromatogram characterized by a variable number of peaks, depending on the genotype of analyzed DNA fragments. If no nucleotide variation is present, homoduplexes DNA fragments elute off of the

cartridge at the same time producing a single peak on the chromatogram on the contrary, if there is a nucleotide variation two or more peaks will be visible. The ideal analysis conditions (melting profiles, analysis temperatures and TEAA and ACN concentrations) closely depend on the nucleotide sequence. For this reason, fragment specific methods are created by WAVE Navigator software (Transgenomic) which predicts (and controls) both the oven temperature and the ACN gradient analyzes through algorithms generated on the basis of the studied nucleotide sequence. Oven temperatures used to perform mutational analysis of each exons are reported in Tables 2-12.

6.6.2 Direct sequencing

Direct sequencing is a variant of "di-deoxynucleotide sequencing method" developed in 1977 by Frederick Sanger. This technique consists in the elongation of a template DNA starting from a short oligonucleotide primer complementary to a specific region. In this reaction a DNA polymerase incorporates deoxynucleotide bases present in solution in high concentration, and chain terminating nucleotides (di-deoxynucleotides) present in low concentration. Limited random incorporation of di-deoxynucleotides results in a series of related DNA fragments that differ in length (the ending point is strictly related to the di-deoxynucleotide insertion site). In Sanger method radioisotopes were used to label the primer and four separate incorporation reactions, one for each di-deoxynucleotide, were performed. Once elongation reactions were finished, the fragments were size-separated by polyacrylamide gel electrophoresis and individual bands were detected by autoradiography. The template complementary sequence was reconstructed by reading the gel bands from the bottom up (in order of increasing molecular weight).

The automated direct sequencing follows the same basic principle of the Sanger method, but no

longer includes the use of radioisotopes labelled primers but di-deoxynucleotides conjugated with a separate fluorescent dyes (which fluoresce at different wavelength). The variant allows to perform a single amplification reaction. The different fluorophores are excited with a laser beam and, each fluorescent signal (corresponding to different conjugated di-deoxynucleotides) is translated by a software in chromatographic peaks of a particular colour, occurring in the reconstructed sequence in positions corresponding to the associated di-deoxynucleotides. According to the peaks order cthe software reconstructs the nucleotide sequence. If the software is unable to discriminate, for the same nucleotide position, between two peaks of different colours, none of the four DNA bases (A, G, C, T) are attributed.

In this work automated direct sequencing was carried out using Capillary Array Electrophoresis Sequencer CEQ™ 8800 (Beckman Coulter) and the GenomeLab Dye Terminator Cycle Sequencing (DTCS) with the Quick Start Kit (Beckman Coulter). Each sequence reaction were performed in duplicate (once with the forward primer and one with the reverse), shrewdness useful in confirming possible ambiguities in the sequence or identify mutations.

DNA sequencing reaction per sample was prepared as follows:

DTCS	2 µl
primer Forward (or Reverse)	10 pmol
purified PCR	30-50 ng
H_2OmQ	(to adjust total volume to 10 µl)
TOTAL	10 µl

and the sequencing reaction program is run on GeneAmp 9700 thermocycler (Applied Biosystems) or Mastercycler ep gradient S (Eppendorf) with the following conditions:

96°C	20 sec	30 cycles
50°C	20 sec	
60°C	4 min	
4°C	∞	

After thermal cycling program, the sample was purified by ethanol precipitation as follows:

- a fresh Stop Solution/Glycogen was prepared for each sample and transferred in a 1.5 ml labeled eppendorf tube: 2 µl of 3M Sodium Acetate (pH 5.2), 2 µl of 100 mM Na_2-EDTA (pH 8.0) and 1 µl of 20 mg/ml of glycogen;
- the 10 µl of sequencing reaction and 60 µl of 100% cold ethanol were added to the Stop Solution and mixed throughly;
- the tube was spinned at 14000 rpm for 16 min at 4°C in a Eppendorf 5417R refrigerated centrifuge;
- the supernatant was discarded and 200 µl of 75% cold ethanol were added to the pellet and mixed throughly;
- the tube was spinned at 14000 rpm for 11 min at 4°C;
- the supernatant was discarded and 200 µl of 75% cold ethanol were added to the pellet and mixed throughly;
- the tube was spinned at 14000 rpm for 6 min at 4°C;
- the supernatant was discarded and the pellet was air- or vacuum-dried and then, dissolved in 35 µl of Sample Loading Solution (Beckman Coulter) and stored at 4°C until usage.

Nucleotide changes were numbered starting from the A of the ATG initiation codon of the GenBank cDNA clones.

6.7 Phylogenetic conservation and *in silico* analysis

Presenilins phylogenetic study was performed by Blastp program (http://expasy.org/tools/blast/) which inputs protein sequences to sequence databases and returns an output file containing a list of potentially matching sequences (chosen on the bases of calculated statistical significance).

In silico analysis was carried out by SIFT (http://sift.jcvi.org/) and PolyPhen2 (http://genetics.bwh.harvard.edu/pph/) amino-acid-substitution (AAS) prediction methods, which predict the possible impact of a particular aminoacid substitutions on protein structure and function. SIFT uses an analysis algorithm based only on sequence homology (scores are calculated using position-specific scoring matrices with Dirichlet priors); PolyPhen2 refers to sequence conservation as well as it considers SWISS-PROT annotations (such as transmembrane domains and secondary structures) and informations from protein-structure database in order to model the position of amino acid substitution.

6.8 PCR products cloning

Frameshift nucleotide deletions or insertions are difficult to be directly interpreted on PCR-sequence. In these cases one of the strategies that will overcome this difficulty, is the cloning of affected gene portion into a vector. Nucleotide sequencing of separate alleles enables to identify the type and the position at which this change is occurred.

In this study cloning reactions were carried out using the commercial kit pSTBlue-1 AccepTor Vector Kit (Novagen) following manufacture's protocol.

Briefly, the procedure requires:

- preparation of the insert by PCR amplification with a non-proofreading DNA polymerase

[the GoTaq polymerase (Promega)] ;

- purification of insert (chloroform: isoamyl alcohol treatment);
- ligation reaction at 16°C for 2 hours;
- transformation of NovaBlue Singles™ Competent Cells, followed by an outgrowth step at 37°C for 45 min, shaked at 200-250 rpm;
- plating of transformed cells on LB agar medium containing ampicillin (or kanamycin), X-gal and IPTG;
- incubation overnight at 37°C;
- transformants and recombinants selection: pSTBlue-1 vector containing a dual kanamycin/ampicillin resistance and the open reading frame (ORF) codifing for a functional *lacZ* α-peptide located in the polylinker. The antibiotic resistance is necessary for the transformed cells to survive when plated on agar containing the appropriate antibiotic. The *lacZ* α-peptide complements the *lacZ* ω-fragment expressed by the competent cells forming an active β-galactosidase which can cleave the chromogenic substrate X-gal to yield a blue colony phenotype. Inserts are cloned within *lacZ* α-peptide ORF preventing the production of functional α-peptide, which results in white colony phenotype when plated on X-gal/IPTG indicator plates. Whereby, pSTBlue-1 vector provides for blue/white screening of recombinants.
- Insert checking: a variable number of transformed colonies (white phenotype) were dissolved in 30 µl of H_2OmQ and used as template

PCR mix for colonies DNA amplification (per sample):

5X Colorless GoTaq Reaction Buffer (Promega)	1X
2 mM mix dNTPs	40 µM
primer forward	0.2 µM
primer reverse	0.2 µM
GoTaq DNA Polymerase (Promega)	0.75 units
dissolved colony	10 µl
H_2OmQ	(to adjust total volume to 10 µl)
TOTAL	30 µl

The appropriate PCR cycle was run on GeneAmp 9700 thermocycler (Applied Biosystems) or Mastercycler ep gradient S (Eppendorf) and PCR products were separated by agarose gel electrophoresis (1% agarose). The dissolved colonies actually containing the insert were used for subsequent direct sequencing reactions (according to 5.6.2 procedures).

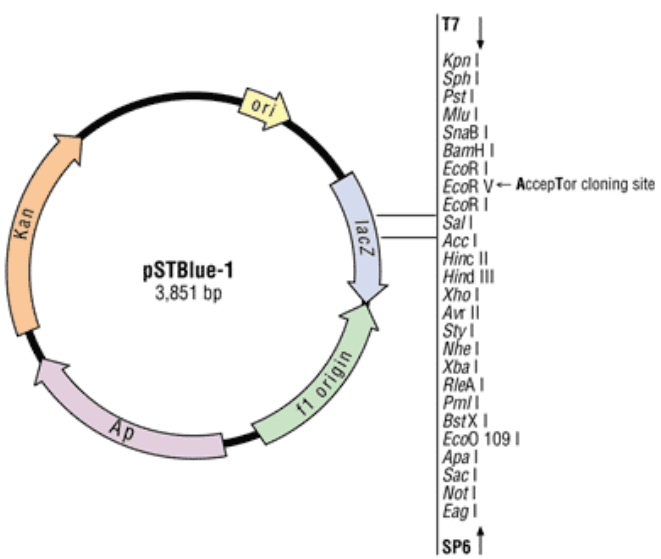

Fig. 13. pSTBlue-1 Vector.
The pSTBlue Vector is a general purpose vector with dual opposed promoters, both ampicillin (Ap) and kanamycin (Kan) resistance, and a wide array of flanking restriction sites.

6.9 Gene copy number variations analysis

Complete *APP* duplication and *PGRN* deletion have been reported in literature [238-240] to be associated with Alzheimer's disease and Frontotemporal Lobar Degeneration respectively. In this study, gene copy number variations (CNV) of *APP* and *PGRN* were investigated by Real-Time PCR and/or Multiplex Ligation-dependent Probe Amplification (MLPA) assay of MRC Holland.

6.9.1 Real-Time PCR

Real-Time PCR is an assay in which the progression of PCR reaction is monitored as it occurs, not at the end of the process; this allows to detected the PCR product as it accumulates each cycle and not the final amount at the end-point step. In this study Real-Time PCR was carried out on a 7300 Real-Time PCR System (Applied Biosystem) by SYBR Green I chemistry, using iTaq™ SYBR® Green Supermix With ROX 2X (BIO-RAD), and performing a relative quantitation. A relative quantitation (RQ) determinates the change in expression of a target DNA (RNA) sequence in a test sample relative to the same sequence in a calibrator sample. Relative quantitation is commonly used to compare expression levels of wild-type (calibrator) with mutated (test sample) alleles or the expression levels of a gene in different tissues. Besides target sequence, in a RQ assay an endogenous control is also essential because it is used as an active reference (usually a gene present at a consistent expression level in all experimental samples, both test and calibrator) to normalize quantitation of a target DNA for differences in the amount of DNA added to each reaction. Indeed, SYBR Green I is a double-stranded DNA Binding dye which binds nonspecifically to all double-stranded DNA sequences. For this reason, in this study, a singleplex PCR method was used where target sequence and endogenous control are amplified separately. A pair of primers for three exons of target *PGRN* and *APP* genes and one exon of endogenous *Beta-2-microglobulin* (*B2M*) and *Ubiquitin C* (*UBC*) genes were designed using

Primer3 software (http://frodo.wi.mit.edu/primer3/) [Table 13] in order to define amplicon 80-120 bp long. A DNA sample of a patients with trisomy 21 (*APP* maps on chromosome 21) was available as positive control for *APP* duplication.

PCR reaction mix (per sample):

2X iTaq™ SYBR® Green Supermix With ROX	1X
primer forward	450-600 nM
primer reverse	450-600 nM
DNA template	100 ng
H_2OmQ	(to adjust total volume to 25 µl)
TOTAL	25 µl

Real-Time PCR cycle:

95°C	10 min	
95°C	15 sec	40 cycles
60°C	1 min	

At the end of PCR reaction, contamination of DNA samples was excluded by a dissociation stage consistent in a gradually slow temperature elevation over several minutes in order to determine the melting temperature of the target DNA sequence and rule out the presence of nonspecific PCR products.

6.9.2 Multiplex Ligation-dependent Probe Amplification (MLPA)

MLPA consists of a multiplex PCR method detecting abnormal copy numbers of genomic DNA and it is able to distinguish sequences differing in only one nucleotide. In contrast to a standard multiplex PCR, a single pair PCR primers is used for amplification, with a mixture of MLPA probes that hybridise to the target sequence. The resulting amplification products (usually

ranging between 130 and 480 nt in length) can be analysed by capillary electrophoresis. Comparing the peak pattern obtained to that of reference samples indicates which sequences show aberrant copy numbers.

The MLPA reaction can be divided in five major steps:

1) DNA denaturation and hybridisation of MLPA probes: the DNA is denatured and incubated overnight with a mixture of MLPA probes, which consist of two separate oligonucleotides, each containing one of the PCR primer sequences. The two probe oligonucleotides hybridise to immediately adjacent target sequences.
2) ligation reaction: only when the two probe oligonucleotides are both hybridised to their adjacent targets can they be ligated during the ligation reaction.
3) PCR reaction: only ligated probes will be exponentially amplified during the PCR reaction thus the number of probe ligation products is a measure for the number of target sequences in the sample.
4) separation of amplification products by capillary electrophoresis.
5) data analysis. Probe oligonucleotides that are not ligated only contain one primer sequence. As a consequence, they cannot be amplified exponentially and will not generate a signal.

In this study, the SALSA P275-B1 MAPT-PGRN and SALSA P170-B2 APP kits (MRC Holland) were used according to the manufacturer's protocol. Two hundreds ng of genomic DNA for each patients were used. MLPA amplification products were analyzed using a Capillary Array Electrophoresis Sequencer CEQ™ 8800 (*Beckman Coulter*). Raw data analysis was performed by Fragment Analysis software (*Beckman Coulter*) while normalisation of the electrophoresis results and interpretation of data were carried out using MRC Coffalyser software (http://old.mlpa.com/coffalyser/download.html).

6.10 Microsatellites Analysis

Microsatellites DNA (also called Simple Sequence Repeats – SSR) are 1-4 nucleotide-long tandem repeat sequences. The number of repeats in a given microsatellite can be highly variable, a characteristic that makes them genetic useful markers, used for mapping, linkage analysis and to trace inheritance patterns. When used to identify a specific chromosome or locus (i.e. associated to a definite disorder), the difference in the number of repeats between alleles are evaluated. A disease inheritance pattern within a family may be traced by microsatellites analysis which allows the identification of mutant allele by comparing the alleles of affected and unaffected individuals.

In this study, the association to the 9p21.3-13.3 chr9 locus was evaluated for a family with FTD-MND and a neuropathological patter compatible with the FTLD-TDP subtype. The SSRs analysis (performed genomic DNA samples of 2 affected and 1 unaffected family members) was done in collaboration with the Neurodegenerative Brain Disease Group, VIB-Department of Molecular Genetics, University of Antwerp, Belgium where the assay was carried out by the group of Christine Van Broeckhoven and Marc Cruts. The analysis involved the following markers: D9S285, D9S157, D9S1684, D9S1846, D9S1870, D9S171, D9S1679, D9S1833, D9S1121, D9S259, chr9_7, D9S319, D9S1853, D9S43, D9S304, W1226, D9S1845, D9S165, D9S1804, D9S1859, D9S772, ATA124G, D9S273, D9S1799, D9S1837, D9S175, D9S1780. Polymerase chain amplification reactions and analysis was performed as described [241, 242].

6.11 Protein serum quantification by ELISA assay

Progranulin levels in serum or plasma were demonstrated to be a predictor of *PGRN* mutation carriers, both in symptomatic patients and asymptomatic family member, vice versa, the analysis may be useful to interpret the pathological meaning of unclear variations (not frameshift

mutations).

In this study, progranulin serum levels were quantified both in patients affected by FTLD and in control subjects using Progranulin (human) ELISA Kit (*AdipoGen*). Serum protein assay was performed according to the manufacturer's protocol. Duplicate serum PGRN levels for each sample were averaged.

6.12 Haplotype analysis

6.12.1 *NOTCH3* mutation carriers

Genotyping was performed on 134 individuals including 103, affected (64) or healthy (39), individuals from 22 available families, and 31 unrelated probands for whom no additional pedigree members were available (Table 14).

Mutation	Families			N. Unrelated
	N.	Affected	Unaffected	
R90C				3
C108S				1
R133C	1	2		1
R141C	2	3	2	1
C146R	3	12	6	1
R169C				1
C174Y	1	5		
C201R	1	2	1	
R207C				3
C251R				1
C271F	1	2		
C366W				1
S396C	5	11	4	5
G528C	1	3	1	1
R592C	1	2	1	
C606R				1
R607C	1	5	1	
C939R				1
R1006C	5	17	23	7
G1013C				1
R1231C				2

Table 14. Pedigree and unrelated index cases included in genotype and haplotype analyses. *For each mutation the number of available families and unrelated index cases is reported. The total number of analyzed affected and unaffected family members is also reported.*

6.12.2 Tagging SNPs of *NOTCH3* gene

A set of single nucleotide polymorphism (SNP) was selected from the HapMap database (caucasoid population, http://www.hapmap.org, rel#24) by a tag selection algorithm that searches for the marker subset presenting maximum entropy (http://www.well.ox.ac.uk/rmott/SNPS/running.shtml). The following 5 SNPs were selected to tag the most common *NOTCH3* haplotypes in the Caucasian population: rs3815188, rs10423702, rs10426042, rs4809030 and rs1044009 (Fig. 14). Each SNP was analysed by DHPLC, nucleotide sequencing and Illumina ASPE Assay.

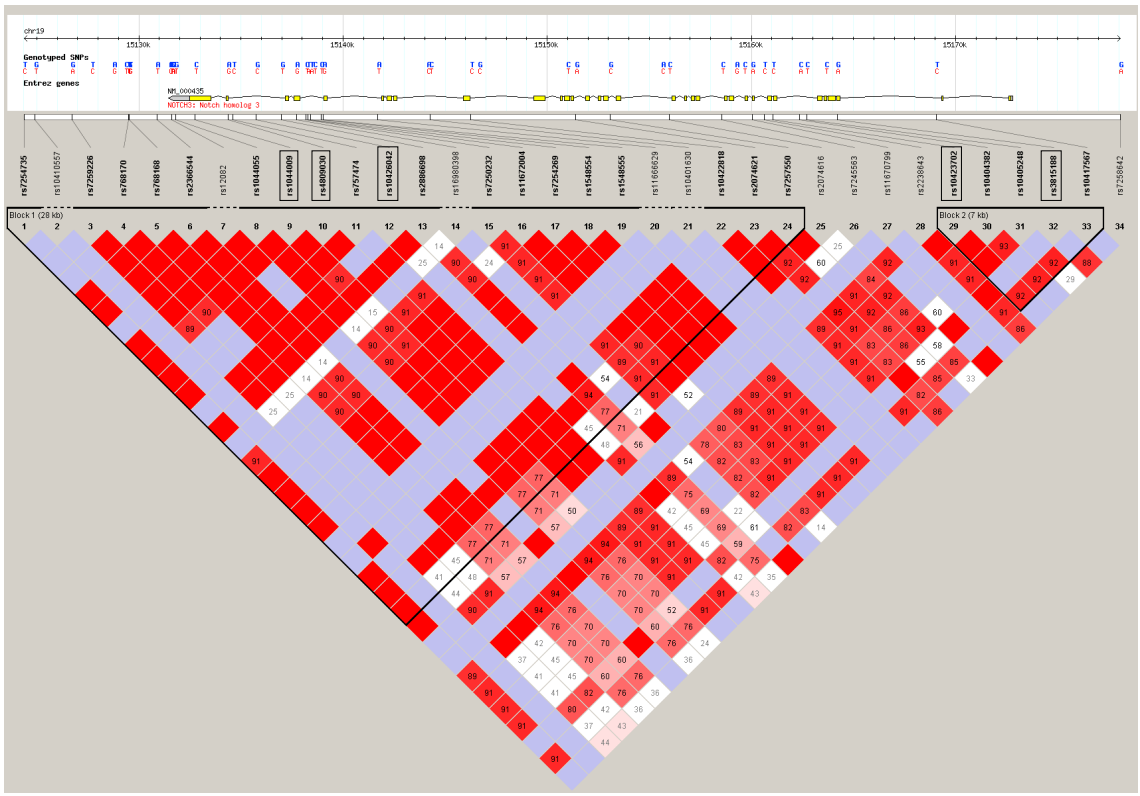

Fig. 14. Block structure for NOTCH3 from HapMap Genome Build 36.
The linkage disequilibrium (LD) plot was obtained using Haploview and HapMap Build 36. The scale at the top of the figure depicts the HapMap region for NOTCH3 (Chromosome 19: 15,131,445 to 15,172,792), and roughly 7 kb upstream and downstream of this region. Single nucleotide polymorphisms (SNPs) genotyped by HapMap are identified in blue (minor alleles) and red (major alleles). Gene regions with the direction of their respective reading frame, exons, and introns, are also given. 5 SNPs in boxes are the tagSNPs selected in this gene region. The r2 LD color scheme is depicted. Two blocks are delineated using the default block definitions from Haploview [Gabriel SB, et al. The structure

6.12.3 SNPs Genotyping by Illumina ASPE Assay

The set of five selected SNPs was analyzed using Illumina VeraCode Universal Capture Beads technology by ASPE (Allele-Specific Primer Extension) chemistry combined with Illumina BeadXpress Reader System. ASPE is a low plex genotyping assay based on the use of two different sets of oligonucleotides: PCR-primers (forward and reverse) for amplification of genomic DNA region with SNP of interest and, ASPE-probes (a pair for each SNP) composed of three parts: 5'- capture sequence (used in subsequent hybridization reactions) - genomic sequence (complementary to genomic region preceding the SNP) - wildtype or variant allele SNP -3'. Each ASPE probe is associated to a unique VeraCode capture sequence, different between wildtype and variant allele. PCR-primers and ASPE-probes were designed using Primer3 software (http://frodo.wi.mit.edu/primer3/) taking in consideration the criteria reported in VeraCode Assay Guideline: melting temperature of nearly 60°C and 100-200 bp amplicon length for PCR-primers; melting temperature of nearly 50°C, wildtype and variant allele ASPE-probes design from the same strand with a 20-30 bp length (Tables 15-16). For each pairs of primers and probes formation of secondary structure, dimers or crosshybridization were rulled out. All five selected SNPs were amplified in a multiplex PCR carried out in a 15 µl reaction volume containing, 150 ng of genomic DNA template, 1X TAQ Buffer, 1.67 mM MgCl, 200 µM dNTPs, 10 pmol each PCR-primer, 0.75 units of Platinum TAQ (Invitrogen). PCR amplification was performed by a GeneAmp 9700 thermocycler (Applied Biosystems) with the following PCR program: 95°C hot start denaturation for 5 min; 30 cycles including a denaturation step at 95°C for 30 sec, annealing step at 58°C for 30 sec and extension step at 72°C for 30 sec. After amplification, PCR products underwent a single-step enzymatic clean-up to eliminate unincorporated primers and dNTPs. ExoSAP-IT® (usb) was added directly to the reaction products after amplification and the following thermocycler program was run: incubation at 37°C for 45 min and enzyme inactivation

at 99°C for 15 min. After this treatment, PCR products were incubated with both wildtype and variant ASPE probes and underwent multiple rounds of oligonucleotide extension incorporating biotin. ASPE elongation reaction was carried out in a 20 µl reaction volume containing, 1X TAQ Buffer, 1.58 mM MgCl, 5 µM dATP, dGTP, dTTP and Biotin 14-dCTP, 5 pmol ASPE-probes premix, 1 unit of Platinum TAQ (Invitrogen) and 3 µl of PCR/ExoSAP-IT reaction. The ASPE thermocycler program was as following: 96°C hot start denaturation for 2 min; 40 cycles including a denaturation step at 94°C for 30 sec, annealing step at 54°C for 30 sec and extension step at 74°C for 30 sec. During this program, there is the preferentially extension of either probe or both, depending on genotype (homozygous for wildtype or variant allele in the first case or heterozygous in the second). After probes extension, products were hybridized to the VeraCode Beads (that have been previously kitted into a 96-well polypropylene plate) and labeled with a streptavidin-fluorophore conjugate according to the manufacture's protocol. After this step, the VeraCode Bead Plate was scanned by BeadXpress Reader and, only streptavidin-labeled biotinylated extension products will produce a fluorescent signal. The automatic allele calling was performed by the Illumina BeadStudio Data Analysis Software with a GeneCall threshold of 0.25. The genotype of the SNP was determined by the ratio of the relative fluorescent levels of the two bead type. ASPE genotyping accuracy was evaluated and validated comparing the SNP genotype obtained using ASPE Assay with available results of direct sequencing and DHPLC analysis.

Table 15: oligonucleotide sequences for PCR-amplification of SNPs

SNP	PCR-Primer sequence (5' → 3')	
	Forward	Reverse
rs3815188	GGACAGGGTGAGTTTAGGA	GTGTCTGCCAGAGTTCAGT
rs10423702	CCATTTGCACCTGTCCT	AGCCCATTCACAGACGA
rs10426042	CTGTGCAACCACTGATTTG	GGGTGAACCTTGAGAACATA
rs4809030	ACACACACACAGACACAAAGTG	CCAGTGTAAGGCTGATTTCC
rs1044009	CTCGTTCCTGCTGCCACT	CAGGTAAGGGTGCTCACTG

Table 16: probe sequences for ASPE-elongation of the SNPs

SNP	ASPE-probes sequence (5' → 3')	
	Allele 1	Allele 2
rs3815188	CATGAGAATCGGGCA	ATGAGAATCGGGCG
rs10423702	CCCATTCACAGACGAC	CCCATTCACAGACGAT
rs10426042	CAGACAAAAAAGACCACC	CAGACAAAAAAGACCACG
rs4809030	CTCTCTCCCCTTCAC	CTCTCTCCCCTTCAT
rs1044009	AGGAGTACCCGGC	GAGGAGTACCCGGT

6.12.4 Haplotypes reconstruction

In 20 pedigrees haplotypes were reconstructed using the computer program Genehunter (http://www.broad.mit.edu/ftp/distribution/software/gh2.1/). For each of the 20 families the haplotype segregation proposed by the computer program was verified by a researcher to evaluate possible alternative segregation patterns involving different haplotype configurations,

according to haplotype frequency estimated on the entire family set. Segregation of the mutation was linked to a precise haplotype in all the families (Appendix 2.

In 31 unrelated probands without testable pedigree members haplotypes were reconstructed by a maximum-likelihood computation computation based on a expectation-maximization algorithm as implemented in the computer program Gerbil [243].

6.13 Skin biopsy and electron microscopy

Sixteen patients belonging to 13 families harbouring 8 distinct mutations of *NOTCH3* underwent skin biopsy upon signing an informed consent. Scalpel skin biopsies, carried out at our hospital by a singleton operator (S.F.) after patients examination, were taken from the deltoid region and included derma and subderma. Skin biopsy specimens 6-8 mm thick were processed for histological and ultrastructural examination according to standard techniques. Skin biopsies from CADASIL patients and 50 unrelated patients with a leukoencephalopathy of undetermined etiology, not associated with mutations of *NOTCH3* were analysed. In each case, 2 pathologists (T.C. and N.R.), blinded to clinical and genetic data, evaluated the presence of GOM by examining the ultrastructure of at least 10 vessels surrounded by smooth muscle cells.

6.14 Formalin-fixed Paraffin-embedded immunohistochemistry (IHC)

Brains of patients with clinical diagnosis of dementia (Alzheimer's disease, Frontotemporal Lobar Degeneration) were collected post-mortem in line with Local Ethical Committee approval and after obtain informed consent from deceaseds parents. After collection, they were immediately fixed in 10% buffered formalin for 3-4 weeks. Standard blocks of frontal cortex, temporal pole, parietal cortex, occipital cortex, hippocampus and amygdala, caudate nucleus and putamen, globus pallidus and thalamus, cerebellum and dentate nucleus, substantia nigra and

locus caeruleus, were cut from the fixed brains and processed routinely into paraffin wax.

In this study, Formalin-Fixed Paraffin-Embedded (FFPE) brain tissue blocks were cut in a Autocut 2040 Microtome (Reichert-Jung) at a thickness of approximately 9 microns, and immunostained using a conventional avidin-biotin peroxidase method.

The primary polyclonal rabbit anti-ubiquitin (Dako, Ely, UK), anti-human PHF-TAU monoclonal (Thermo Scientific) and TARDBP monoclonal (ABnova) antibodies were used at a dilution of 1:200, 1:1000 and 1:1000 respectively.

Briefly:

- slides preparation: cut sections were affixed onto Superfrost Plus slides (Thermo Scientific) and dried at 37°C for 24 hours.
- Deparaffinization and hydration of tissue sections: the slides were put into a vertical slide rack for IHC and dipped into 2 consecutive staining jars containing xylene (Carlo Erba Reagents) for 5 minutes each step. Then, the rack was dipped in 100% and 95% ethanol for 5 minutes each step.
- Quenching the peroxidase: the rack was dipped in 30 volume H_2O_2 + 8% methanol for 30 minutes. The slides were then dipped into 4 consecutive staining jars containing 70%, 50% and 30% ethanol and distillate H_2O for 5 minutes every step.
- Retrieving antigen: an additional step was performed when using primary anti-human PHF-TAU and TARDBP antibodies. For the former, an extra treatment in formic acid for 5 minutes and repeated washing in distillate H_2O, for the latter, an autoclaving in 0.1M citrate buffer (pH 7.6) at 121°C for 5 minutes letting the slides drying at room temperature. After these treatments, the slides were washed with PBS buffer (pH 7.4).

The slides that were going to be treated with a monoclonal or a polyclonal antibody were preincubated with 2% Normal Horse Serum, NHS (Vector) or Normal Goat Seruma, NGS

(Dako, Ely, UK) respectively, in PBS for 30 minutes at room temperature and in a wet chamber.

- Primary antibody incubation: the rack was dipped three times in PBS, 5 minutes each ones and the sections were encircled with a PAP pen. Antibody solution (with the proper dilution in NHS or NGS) was dropped to cover the section and incubated overnight at 4°C.
- Secondary antibody incubation: the rack was dipped three times in PBS, 5 minutes each ones and secondary antibodies (diluted 1:200 in PBS), anti-mouse IgG biotinylated (Vector) for primary monoclonal antibody or anti-rabbit IgG biotinylated (Vector) for primary polyclonal antibody were dropped to each slides and incubated for 1 hour at room temperature in a wet chamber. Three PBS washings were performed, 5 minutes long. ABC elite standard (Vector), prepared in PBS as manufacturer's data sheet 45 minutes before usage, was dropped to each slide and incubated for 45 minutes. One washing in PBS and two in distillate H_2O, each 10 minutes long, followed this step.
- Colorimetric detection: this step was carried out using NovaRED Substrate Kit (Vector) following manufacturer's protocol. The detection reaction was stopped dipping slides in tap water followed by a washing in distillate H_2O.
- Counter staining: the slides were quickly dipped into a staining jar containing Mayer hematoxylin and rinsed with distillate H_2O. The rack was then dipped 5 times in 70%, 100% ethanol and xylene consecutively.
- Mounting: Entellan (Merck) was dropped onto the sections and a cover glass was put onto the slides.

7. Results

7.1 Alzheimer's Disease and Frontotemporal Lobar Degeneration

During the mutational analysis of AD- and FTD-associated genes, eight non-synounimous nucleotide variations were identified, those already reported in literature and considered pathogenic mutations and others first identified in this study that represent putative novel mutations (See Table 17). Clinical and genetic findings for each of these substitutions are separately detailed below.

Table 18 reports many intronic and exonic nucleotide variations identified with high recurrence in the series, already reported in literature as single nucleotide polymorphisms (SNPs).

SNPs frequencies were calculated on the entire series and, out of this list another *PSEN2* nucleotide variation was identified, p.Arg62His (frequency, 1,4%), for which there is a debate in literature about its possible pathogenic role in Alzheimer's Disease due to conflicting findings.

Table 17: DNA nucleotide variations with definite or probable pathogenic nature

Patient id	*Clinical Diagnosis*	*Gene*	*Exon*	*Genome*[1]	*Predicted RNA*[2]	*Predicted Protein*[3]
F1	FTD	*PGRN*	3	g.9420	c.378delC	p.Phe86SerfsX170
F2	FTD		8	g.11019_11022	c.813_816delCACT	p.Thr272SerfsX10
F3	**PNFA**		**11**	**g.11910**	**c.1197delC**	**p.His400ThrfsX12**
F4	FTD	*MAPT*	IVS10	g.120998	c.2002+16 C>T	
A1	**AD**	*PSEN1*	**12**	**g.87725**	**c.1310 T>A**	**p.Ile437Asn**
A2	**AD**	*PSEN2*	**4**	**g.16389**	**c.53 C>T**	**p.Thr18Met**
A3	AD		5	g.18203	c.211 C>T	p.Arg71Trp
A4	AD		7	g.22541	c.520 A>G	p.Met174Val

Table 17-18.

[1] Numbering according to the largest isoforms with GenBank Accession Number [NG_007886.1 for PGRN, NG_007398.1 for MAPT, NG_007887.1 for VCP, NG_007386.2 for PSEN1 and NG_007381.1 for PSEN2].

[2] Numbering according to the largest isoforms with GenBank Accession Number [NM_002087.2 for PGRN and NM_001123066.3 for MAPT, NM_007126.3 for VCP, NM_000021.3 for PSEN1 and NM_000447.2 for PSEN2] and starting at the translation initiation codon.

[3] Numbering according to the largest isoforms with GenPept Accession Number [NP_002078.1 for PGRN and NP_001116538.2 for MAPT, NP_009057.1 for VCP, NP_000012.1 for PSEN1 and NP_000438.2 for PSEN2].

Novel probable mutations are reported in bold.

Table 18: DNA polymorphisms

Gene	Exon	Genome[1]	Predicted RNA[2]	Predicted Protein[3]	SNP	frequency
PGRN	3	g.9450	c.264+21 G>A		rs9897526	27,7%
	5	g.10115	c.359 C>A	p.Ser120Tyr	rs63750043	0,5%
	5	g.10140	c.384 T>C	p.Asp128Asp	rs25646	3,6%
	5	g.10242	c.462+24 G>A		rs850713	29,0%
	10	g.11464	c.970 G>A	p.Ala324Thr	rs63750541	0,5%
	12	g.12349	c.1533 G>C	p.Gly515Ala	rs25647	0,5%
MAPT	1	g.72904	c.1-13 A>G		rs17650901	30,4%
	1	g.73077	c.133+28 C>A			30,4%
	9	g.106953	c.1562-26 G>A		rs117200923	38,4%
	9	g.107022	c.1605 C>T	p.Pro200Pro		46,5%
	9	g.107103	c.1686 A>G	p.Ala227Ala	rs1052553	39,7%
	9	g.107187	c.1770 T>C	p.Asn255Asn	rs17652121	40,2%
	9	g.107232	c.1815 G>A	p.Pro270Pro	rs11568305	5,4%
	11	g.124781	c.1921-42 T>C			9,8%
	11	g.124938	c.2002+34 G>A		rs75534191	14,7%
	13	g.134785	c.*+26 T>C		rs118104841	4,5%
VCP	2	g.9539	c.129+47 G>A		rs10972300	38,0%
	7	g.14768	c.811+3 G>A		rs514492	30,3%
	12	g.16785	c.1360-35 A>G		rs2258240	32,2%
	12	g.16994	c.1482+52 T>C		rs562381	32,2%
	13	g.17438	c.1695+8 A>G		rs684562	47,8%
PSEN1	4	g.39343	c.104 G>A	p.Arg35Gln	rs63750592	0,5%
	8	g.66540	c.770-21 T>C		rs3025786	10,7%
	8	g.66675	c.868+16 G>T		rs65932	40,6%
	9	g.75000	c.953 A>G	p.Glu318Gly	rs17125721	4,0%
PSEN2	4	g.16405	c.69 T>C	p.Ala23Ala	rs11405	53,6%
	4	g.16465	c.129 C>T	p.Asn43Asn	rs6759	53,1%
	5	g.18092	c.142-42 G>A		rs1295643	18,3%
	5	g.18105	c.142-29 T>C		rs1295644	32,1%
	5	g.18253	c.261 C>T	p.His87His	rs1046240	31,7%
	6	g.20138	c.498+30 G>C		rs2236910	34,4%
	10	g.25683	c.887-24 T>C		rs2802267	36,1%
	12	g.28578	c.1191+24 G>A		rs2855562	13,4%

7.1.1 Alzheimer's Disease

Seventeen out of 50 unrelated index cases with clinical and/or neuropathological diagnosis of AD, presented family history for dementia (FAD cases).

Four non-synonymous nucleotide variations were identified in four independent FAD cases including, two novel substitutions one in each *Presenilin* gene, and two already reported *PSEN2* variations (Table 17).

These variations together account for 23,52% of FAD and for 8% of all analyzed AD patients.

No *APP* mutations or gene duplication were detected.

7.1.1.1 A1 case

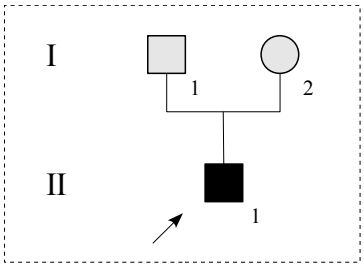

Fig. 15. A1 pedigree.
The arrow indicates the proband; circles, females; squares, male; black symbols, affected family members; grey symbols, affected status not available; slashed symbols, deceased family members.

7.1.1.1.1 Clinical presentation and neuroradiological features

At the moment in which this study has been draft no detailed clinical and radiological data were available about this seventy-three year-old man examined at Bellaria Hospital, with a clinical diagnosis of AD. The only known informations included a positive family history and a late onset of the disease.

7.1.1.1.2 Molecular genetics

DHPLC analysis disclosed an abnormal chromatographic profile for exon 12 of *PSEN1* which was further characterized by direct sequencing leading to the identification of the novel c.1310

T>A heterozygous transversion (Fig. 16). This nucleotide variation is predicted to cause the substitution of aminoacid isoleucine with an asparagine at codon 437 (p.Ile437Asn), affecting a residue localized in putative transmembrane domain IX (TM-IX) of the protein.

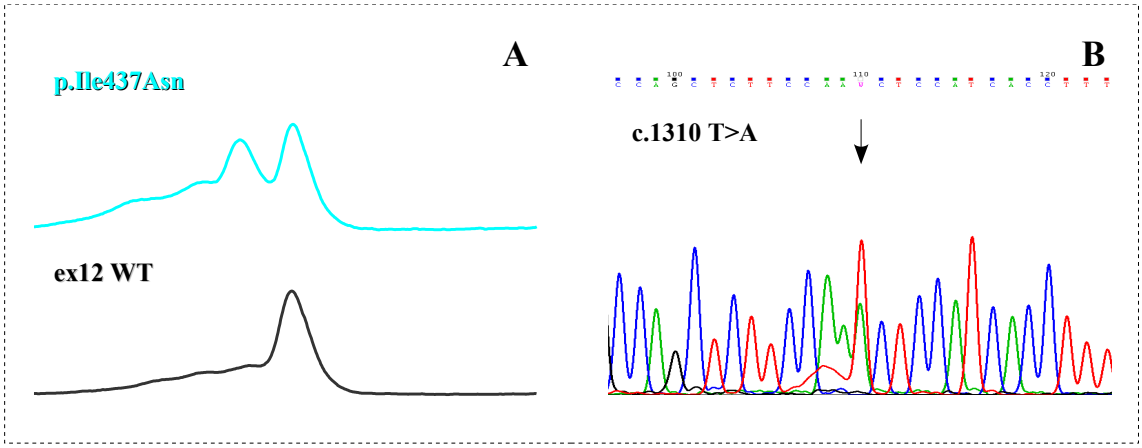

Fig. 16. A1 case: DHPLC and sequencing analysis results.
A: PSEN1 ex12 chromatographic profiles in A1 patient (upper) and wild-type control (lower). B: direct sequence of ex12 in A1 patients disclosing the c.1310 T>A heterozygous nucleotide transversion (arrow).

This *PSEN1* nucleotide variation was excluded in 492 cognitively healthy control subjects.

7.1.1.1.3 Phylogenetic and *in silico* analysis

Multiple alignment of presenilins disclosed high phylogenetic conservation of the affected residue (Ile 437) among different species, both in PSEN2s and PSEN1s (Fig. 17). The effects of this aminoacid substitution on protein function was predicted to be not tolerated and probably deleterious.

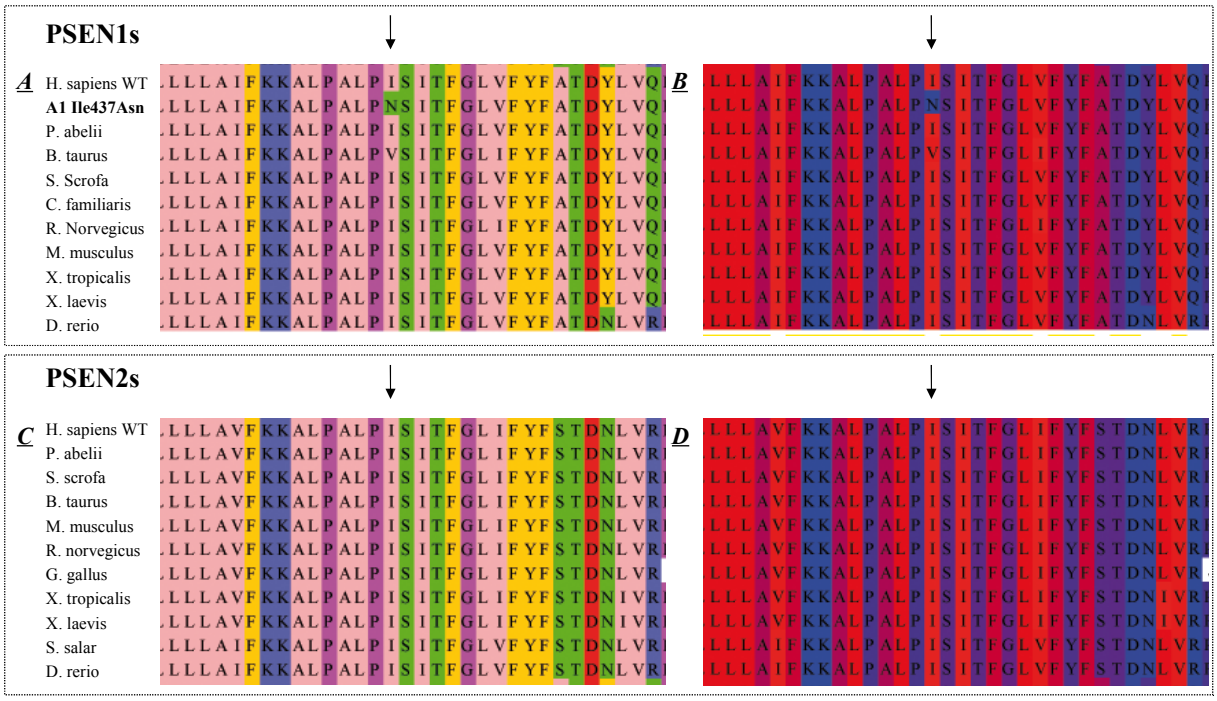

Fig. 17. Phylogenetic conservation of PSEN1 Ile437 among different PSEN1s and PSEN2s species.
The Isoleucine residue at codon 437 is highly conserved among PSEN1s and PSEN2s of different species.
Panels A and C differentiate aminoacids according to their physicochemical properties [pink, aliphatic/hydrophobic residues; green, hydrophilic residues; red, negative charged aminoacids; blue, positive charged aminoacids; yellow, cysteines; orange, aromatic residues; cyclamen, conformationally special].
Panels B and D differentiate aminoacids according to their hydrophobicity properties [the most hydrophobic residues are reported in in red while the more hydrophilic in blue].

7.1.1.2 A2 case

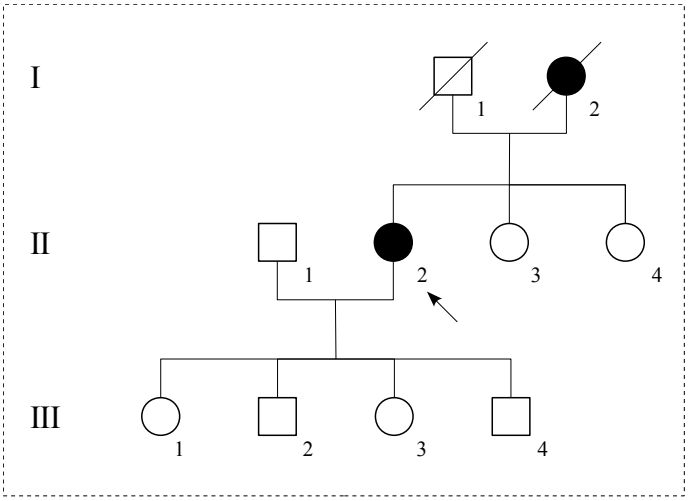

Fig. 18. A2 pedigree.
The arrow indicates the proband; circles, females; squares, male; black symbols, affected family members; slashed symbols, deceased family members. I.2: died at the age of 80 years with clinical diagnosis of Alzheimer's disease, began when she was 70. II.3 and II.4, respectively 68 and 60 years old asymptomatic proband's sisters. III.1-2-3-4, respectively 48, 47, 45 and 40 years old asymptomatic proband's offspring.

7.1.1.2.1 Clinical presentation and neuroradiological features

The proband, a 74 years old female (individual II.2 in Fig.17) came to the attention of neurologists at G.B. Rossi Hospital one year after onset of symptoms (age 72) consisting of social withdrawal, mood deflection, short-term memory deficit and anomie. During her first neuropsychological examination she scored 21/30 to MMSE, disclosing mild deficit of short-term memory and word production. She preserved daily self-care and instrumental activities [Activities of Daily Living (ADL): 6/6; Instrumental Activities of Daily Living (IADL): 8/8]. At age 73 years she underwent a brain CT scan disclosing an accentuation of Cerebral Spinal Fluid (CSF) and cisternal spaces. Eighteen months after symptoms onset the patient underwent a second neuropsychological assessment that showed no significant changes except for a worsening of long-term memory. Six months later she was subjected to a further neuropsychological examination revealing a consistent worsening of cognitive functions (MMSE: 11/30): severe memory deficits, impaired word production and a modest decline in executive functions affecting her skilfulness of daily life and reducing her autonomy (ADL: 5/6 and IADL: 4/8). Two years after symptoms onset a brain MRI disclosed white matter hyperintensity, enlargement of third and lateral ventricules, CSF and cisternal spaces (Fig. 19). At the same time she performed a brain SPECT which revealed slight hypoperfusion of temporal cortex, most marked in the left hemisphere.

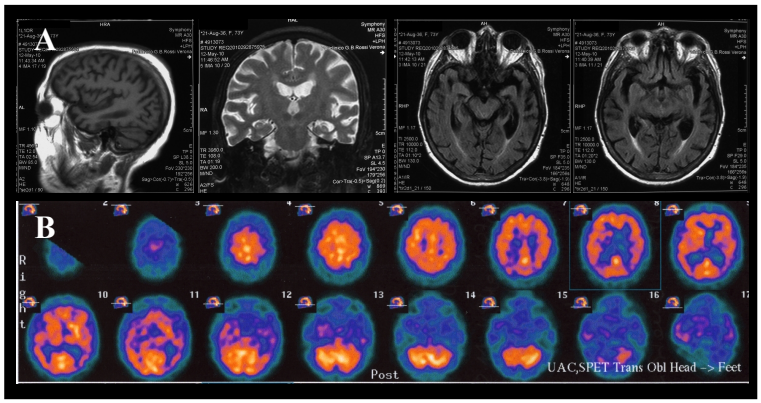

Fig. 19. A2 proband neuroradiological findings.
A: Magnetic Resonance Imaging scan: saggital and coronal sections.
B: ^{18}F-Fluorodeoxyglucose (^{18}FDG) positron emission tomography (PET).

7.1.1.2.2 Molecular genetics

DHPLC analysis disclosed an abnormal chromatographic profile for exon 4 of *PSEN2* which underwent direct sequencing displaying the novel c.53 C>T heterozygous transition (Fig. 20). This nucleotide variation is predicted to cause the substitution of aminoacid threonine with a methionine at codon 18 (p.Thr18Met), affecting a residue localized in the putative N-terminal domain of the protein.

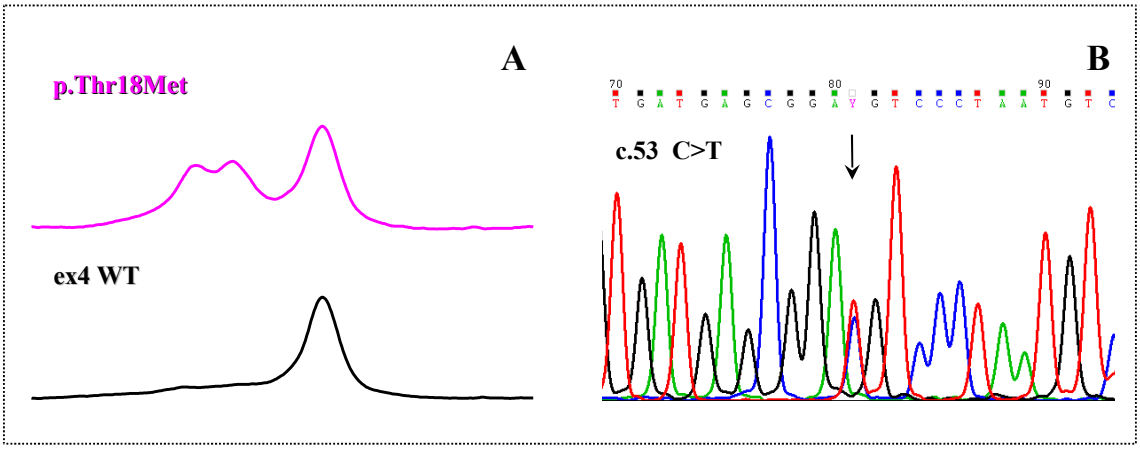

Fig. 20. A2 case: DHPLC and sequencing analysis results.
A: PSEN2 ex4 chromatographic profiles in A2 proband (upper) and wild-type control (lower). B: direct sequence of ex4 in A2 proband disclosing the c.53 C>T heterozygous nucleotide transition (arrow).

This *PSEN2* nucleotide variation was excluded in 492 cognitively healthy control subjects.

7.1.1.2.3 Phylogenetic and *in silico* analysis

Multiple alignment of presenilins disclosed high phylogenetic conservation of affected residue (Thr 18) in PSEN2s of different species not in PSEN1s (Fig. 21). The effects of this aminoacid substitution on protein function was predicted as not tolerated and probably damaging by SIFT and PolyPhen *in silico* analyses.

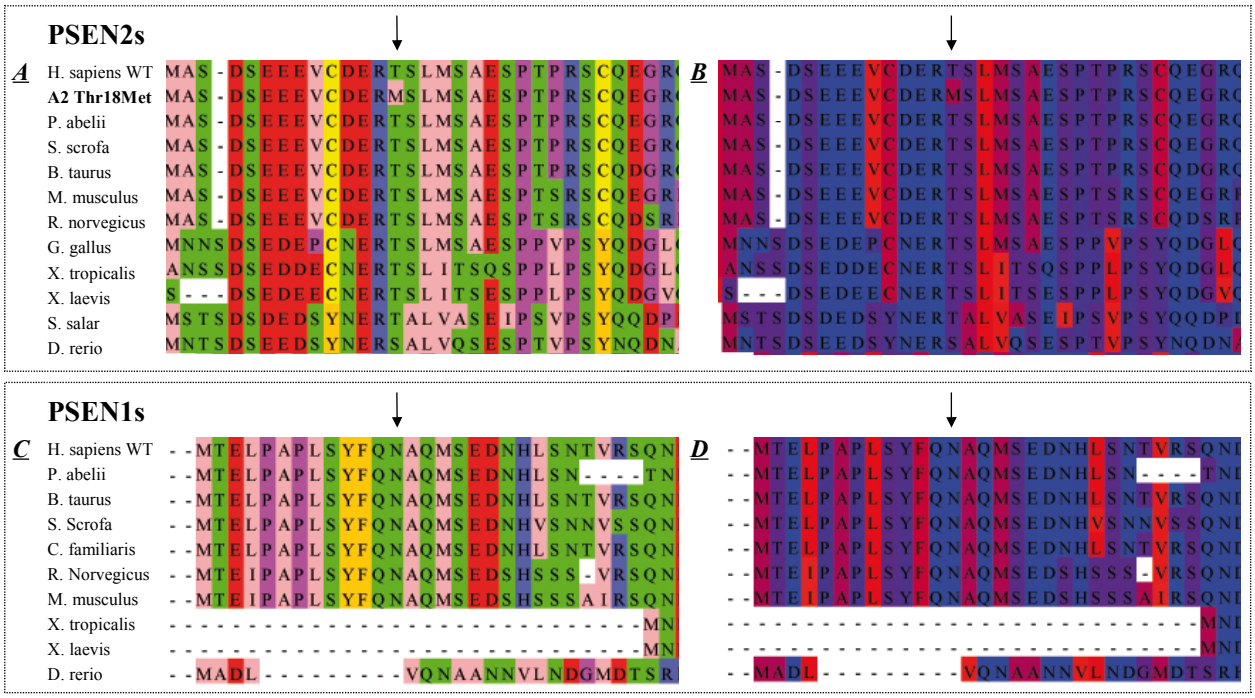

Fig. 21. Phylogenetic conservation of PSEN2 Thr18 among different PSEN2s and PSEN1s species.
The Threonine residue at codon 18 is highly conserved among PSEN2s of different species, not in PSEN1s.
Panels A and C differentiate aminoacids according to their physicochemical properties [pink, aliphatic/hydrophobic residues; green, hydrophilic residues; red, negative charged aminoacids; blue, positive charged aminoacids; yellow, cysteines; orange, aromatic residues; cyclamen, conformationally special].
Panels B and D differentiate aminoacids according to their hydrophobicity properties [the most hydrophobic residues are reported in in red while the more hydrophilic in blue].

7.1.1.3 A3 case

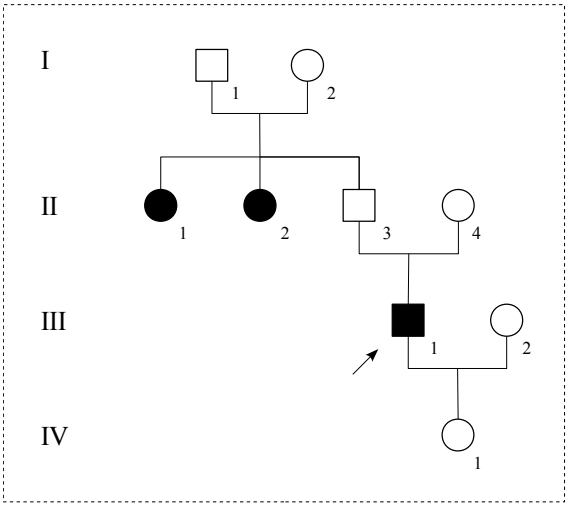

Fig. 22. A3 pedigree.
The arrow indicates the proband; circles, females; squares, male; black symbols, affected family members; slashed symbols, deceased family members.

7.1.1.3.1 Clinical presentation and neuroradiological features

This proband (III.1) is a 63 years old male with a four-year history of behaviour changes and multiple cognitive decline. A SPECT scan, carried out at age 59 years, demonstrated mild hypoperfusion in both temporal and parietal cerebral cortex, more pronounced on the right side. Neuropsychological evaluation, two years after his initial referral, revealed a prominent worsening of cognitive functions with a fair impairment of daily living activities (MMSE: 16/30; IADL: 3/5 and ADL:6/6). Over the following year he developed substantial behavioural and personality changes characterized by an alternation between a state of apathy and restlessness, disinhibition, verbal and physical aggression, foul language. Also his memory (especially long-term verbal memory) and attentional functions have undergone a further deterioration, associated to impaired executive functions, deficits of written comprehension, constructive apraxia, agraphia. He underwent a further neuropsychological examination which confirmed a progressive global cognitive impairment (he scored 7/30 to MMSE, 1/5 to IALD and 5/6 to ADL).

7.1.1.3.2 Molecular genetics

DHPLC analysis disclosed an abnormal chromatographic profile for exon 5 of *PSEN2* which, after direct sequencing revealed the already reported c.211 C>T heterozygous transition (Fig. 23). This nucleotide variation is predicted to cause the substitution of aminoacid arginine with a tryptophan at codon 71 (p.Arg71Trp), affecting a residue localized in the putative N-terminal domain of the protein.

This *PSEN2* nucleotide variation was excluded in 492 cognitively healthy control subjects.

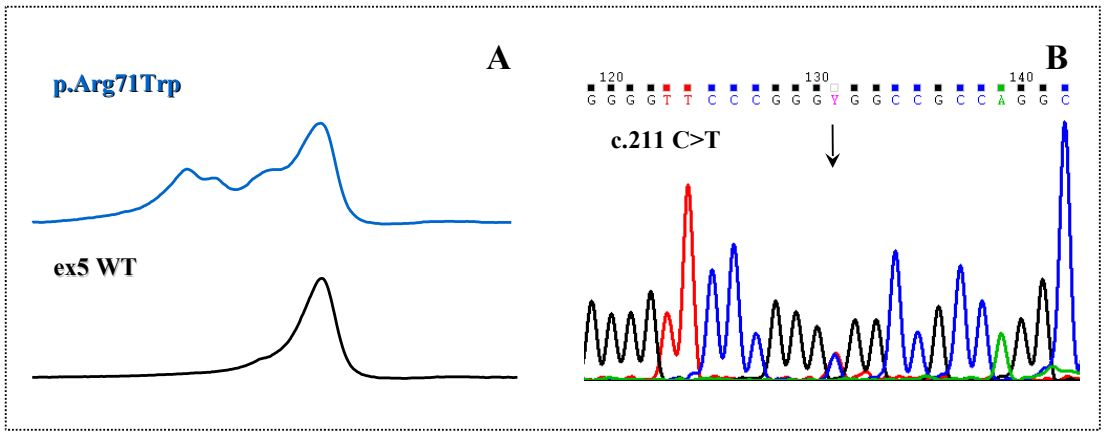

Fig. 23. A3 case: DHPLC and sequencing analysis results.
A: PSEN2 ex5 chromatographic profiles in A3 patient (upper) and wild-type control (lower). B: direct sequence of ex5 in A3 patient disclosing the c.211 C>T heterozygous nucleotide transition (arrow).

7.1.1.3.3 Phylogenetic and *in silico* analysis

Multiple alignment of presenilins showed affected residue (Arg 71) to be phylogenetic conserved among PSEN2s of many different species not in PSEN1s (Fig. 24). The effects of this aminoacid substitution on protein function was predicted as not tolerated and probably damaging by SIFT and PolyPhen *in silico* analyses.

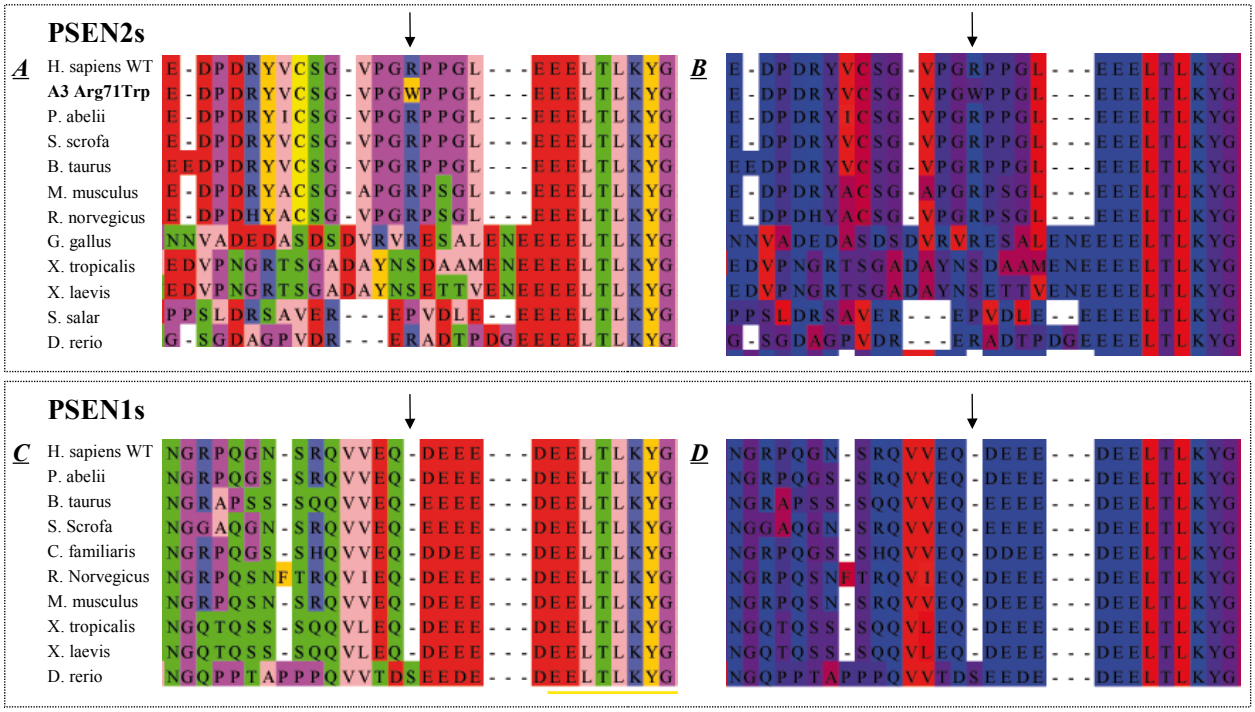

Fig. 24. Phylogenetic conservation of PSEN2 Arg71 among different PSEN2s and PSEN1s species.
The Arginine residue at codon 71 is conserved among PSEN2s of many different species, not in PSEN1s.
Panels A and C differentiate aminoacids according to their physicochemical properties [pink, aliphatic/hydrophobic residues; green, hydrophilic residues; red, negative charged aminoacids; blue, positive charged aminoacids; yellow, cysteines; orange, aromatic residues; cyclamen, conformationally special]. Panels B and D differentiate aminoacids according to their hydrophobicity properties [the most hydrophobic residues are reported in in red while the more hydrophilic in blue].

7.1.1.4 A4 case

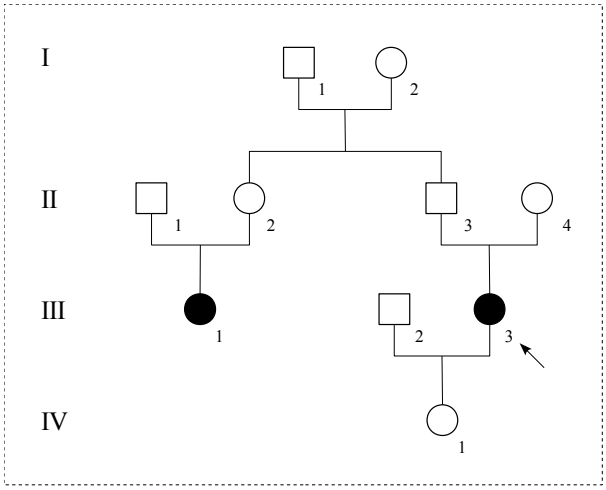

Fig. 25. A4 pedigree.
The arrow indicates the proband; circles, females; squares, male; black symbols, affected family members; slashed symbols, deceased family members.

7.1.1.4.1 Clinical presentation and neuroradiological features

The proband (III.3) disclosed behavioural impairment by the age of 75. She became increasingly apathetic, with personal and daily workhouses neglect. Over the first year after symptoms onset she developed mnesic and attentional deficits, temporal disorientation, anomie and ideo-motor slowing. Repeated neuropsychological assessments showed no significant alterations of cognitive functions. Three years after her first evaluation, she underwent a further neuropsychological examination (MMSE: 20/30) which revealed temporal disorientation associated to deficits of long- and short-term verbal memory, impairment of phonemic and semantic verbal fluency, with deficits of attentional and frontal executive functions. Her ideo-motor slowing worsened in association with a remarkable impairment of quality and autonomy of daily living (IADL: 1/8 and ADL: 3/6) accompanied by depressive symptoms. A brain MRI and SPECT, performed at age 78 years, showed respectively a mesial temporal atrophy and, an hypoperfusion of both temporal and frontal parieto-occipital cortex, worse in the left hemisphere

with an asymmetric uptake at basal ganglia (Fig. 26). The patient died at age 79 years, four years after onset of symptoms. No post-mortem examination was undertaken.

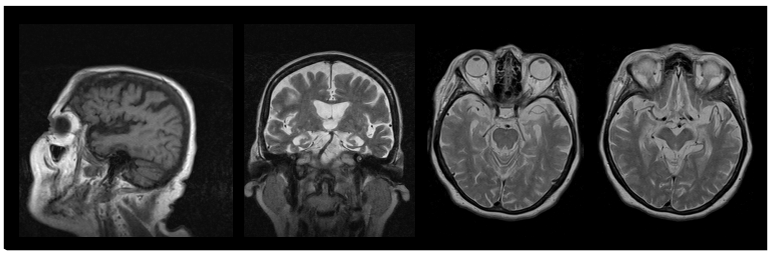

Fig. 26. A4 proband neuroradiological findings.
Magnetic Resonance Imaging scan: saggital and coronal sections.

7.1.1.4.2 Molecular genetics

DHPLC analysis disclosed an abnormal chromatographic profile for exon 7 of *PSEN2* which, after direct sequencing revealed the already reported c.520 A>G heterozygous transition (Fig. 27). This nucleotide variation is predicted to cause the substitution of aminoacid methionine with a valine at codon 174 (p.Met174val), affecting a residue localized in the putative transmembrane domain III (TM-III) of the protein.

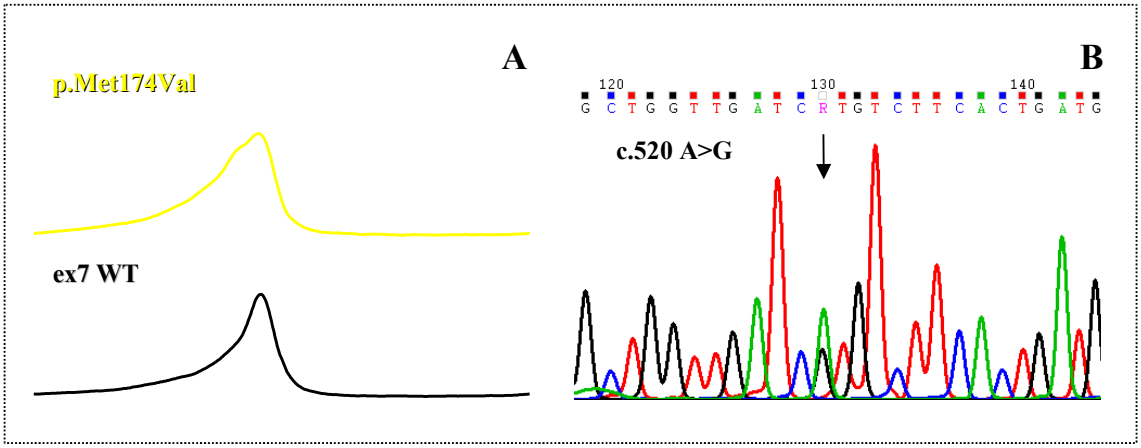

Fig. 27. A4 case: DHPLC and sequencing analysis results.
A: PSEN2 ex7 chromatographic profiles in A4 proband (upper) and wild-type control (lower). B: direct sequence of ex7 in A4 patient disclosing the c.520 A>G heterozygous nucleotide transition (arrow).

This *PSEN2* nucleotide variation was excluded in 492 cognitively healthy control subjects.

7.1.1.4.3 Phylogenetic and *in silico* analysis

Multiple alignment of presenilins showed that the affected residue (Met 174) was phylogenetic conserved among PSEN2s of only few different species but it was not conserved in PSEN1s (Fig. 28). The effects of this aminoacid substitution on protein function was predicted as tolerated and probably not damaging by SIFT and PolyPhen *in silico* analyses.

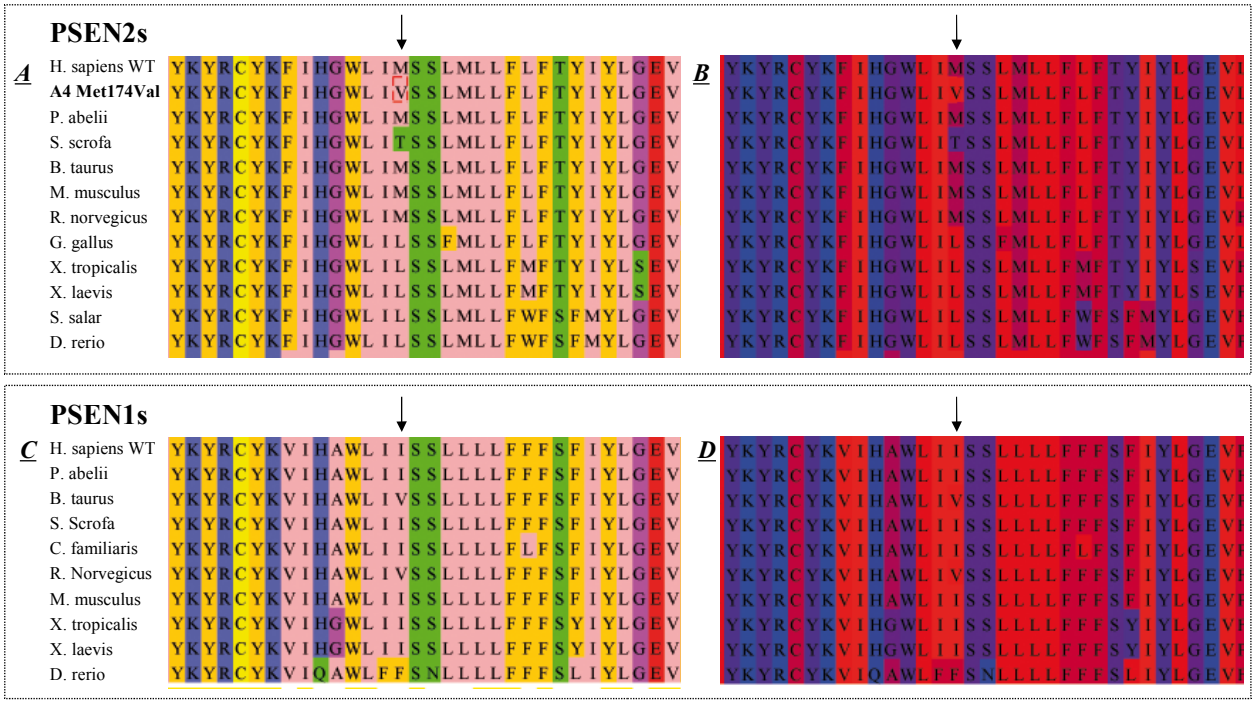

Fig. 28. Phylogenetic conservation of PSEN2 Met174 among different PSEN2s and PSEN1s species.
The Methionine residue at codon 174 is conserved in PSEN2s of few different species, not in PSEN1s.
Panels A and C differentiate aminoacids according to their physicochemical properties [pink, aliphatic/hydrophobic residues; green, hydrophilic residues; red, negative charged aminoacids; blue, positive charged aminoacids; yellow, cysteines; orange, aromatic residues; cyclamen, conformationally special].
Panels B and D differentiate aminoacids according to their hydrophobicity properties [the most hydrophobic residues are reported in in red while the more hydrophilic in blue].

7.1.2 Frontotemporal Lobar Degeneration

Fifteen out of 76 unrelated index cases with clinical and/or neuropathological diagnosis of FTLD syndromes, presented family history for dementia.

Four non-synonymous nucleotide variations - two already reported and one novel frameshift *PGRN* and one already reported splice-site *MAPT* mutations - were identified in four independent familial FTLD cases (Table 17).

Together these four variations account for 26,66% of familial FTLD cases and for 5,26% of all analyzed FTLD cases.

No *PGRN* deletion or *VCP*, *CHMP2B* and *TARDBP* mutations were detected.

7.1.2.1 F1 case

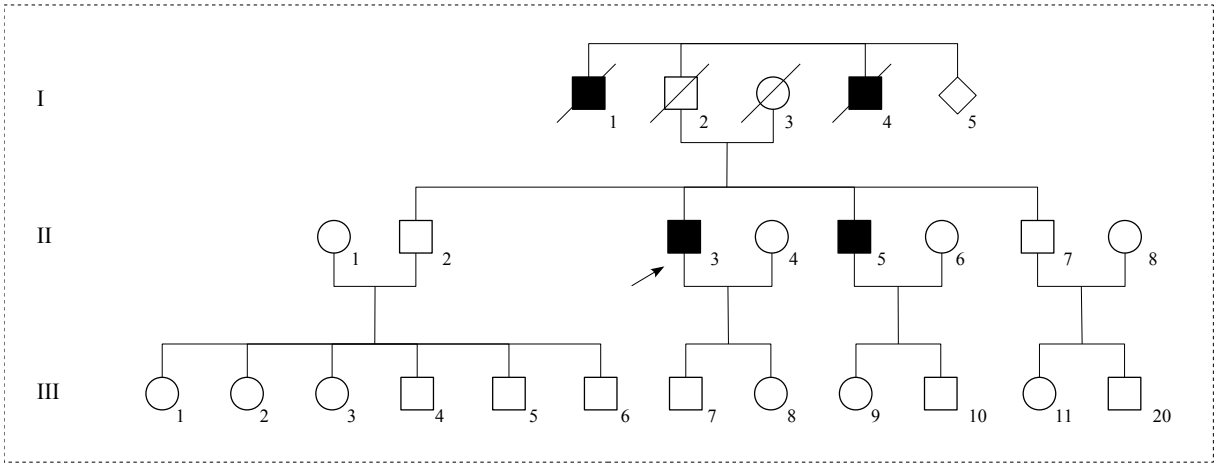

Fig. 29. F1 pedigree.
The arrow indicates the proband; circles, females; squares, male; black symbols, affected family members; slashed symbols, deceased family members. The proband's father (I.2) died of myocardial infarction at age 72 whereas his mother (I.3) died of old age. His oldest uncle (I.1) was affected by FTD instead the youngest (I.4) received clinical diagnosis of AD. One of the younger brother (II.5) is affected by FTD.

7.1.2.1.1 Clinical presentation and neuroradiological features

The proband (II.3), a 70 years old man, was examined by clinicians at Girolamo Fracastoro Hospital, where he performed neuropsychological and neuroimaging assessments.

He was first referred at the age of 65 years with a 7-months history of phonetic verbal fluency deficits, verbal apraxia with preserved ability in word finding, accompanied by mood and behavior change. Neuropsychological examination revealed deficits in solving problems and abstract reasoning (MMSE: 21/30). A brain MRI carried out a year and a half after the onset of the symptoms, revealed a moderate bilaterally symmetrical cerebral atrophy, most pronounced in the frontal lobes. The clinical and neuroradiological findings led to a clinical diagnosis of FTD.

7.1.2.1.2 Molecular genetics

DHPLC analysis disclosed an abnormal chromatographic profile for exon 3 of *PGRN* which revealed the presence of a frameshift mutation after direct sequencing. The subcloning of this exon allowed to identified the already reported c.378delC single nucleotide deletion, predicted to introduce a premature stop codon (p.Phe86SerfsX170) leading to the formation of an unstable mRNA, degradated by a mechanism of Non-sense Mediated Decay (NMD) [170, 171].

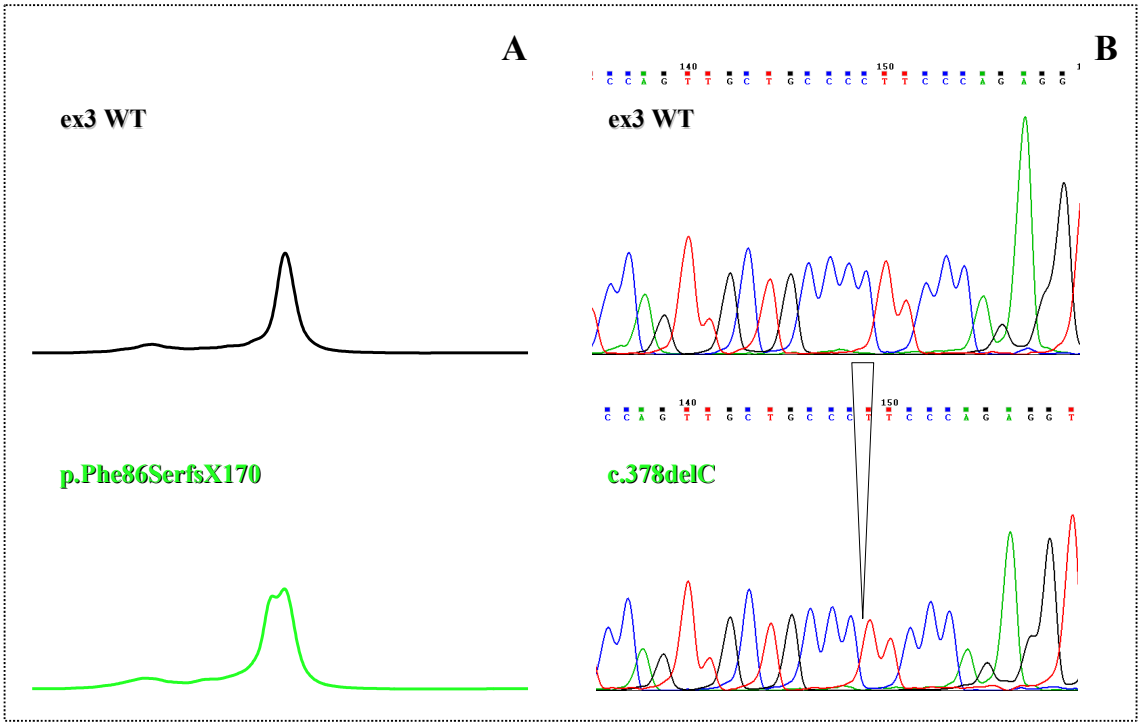

Fig. 30. F1 case: DHPLC and sequencing analysis results.
A: PGRN ex3 chromatographic profiles in a wild-type control (upper) and F1 proband (lower). B: direct sequence of wild-type (upper) and mutated (lower) alleles of F1 proband, disclosing the c.378delC heterozygous single nucleotide deletion.

7.1.2.2 F2 case

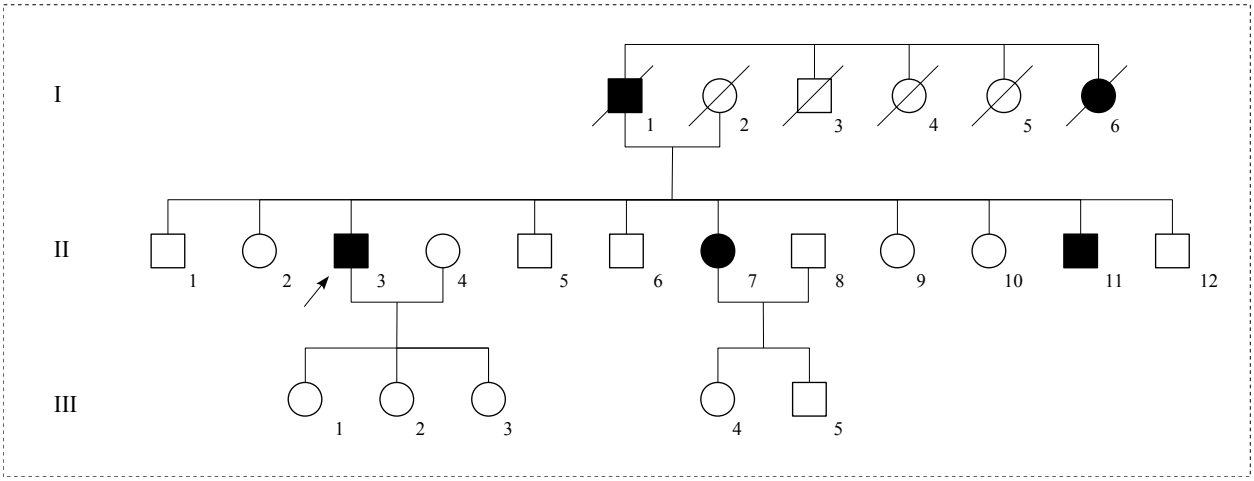

Fig. 31. F2 pedigree.
The arrow indicates the proband; circles, females; squares, male; black symbols, affected family members; slashed symbols, deceased family members. The proband's father (I.1) died at age 74 after 19-years history of Parkinson disease; his affected aunt (I.6) developed both memory and cognitive deficits. One of his sister (II.7) has a diagnosis of FTD with severe cognitive deficit and, one brother (II.11) with a progressive worsening of Parkinson disease.

7.1.2.2.1 Clinical presentation and neuroradiological features

The proband (II.3), a 79-year-old male, was hospitalized in Neurology Department of G.B. Rossi Hospital at the age of 74 years to carry out surveys on a clinical picture, reported slowly evolving (first symptoms onset at age 68 years) and characterized by abnormal gait with postural instability and slight deficits in working memory and attention. On the basis of these symptoms, the patient was previously subjected to neurological examination which revealed ideo-motor slowing and bradykinesia, associated with attentional and mnesic decline. He has also undergone a brain MRI that showed a triventricular hydrocephalus (Fig. 32A). During this hospitalization he performed a cranial CT scan which confirmed the dilatation of lateral and third ventricles. At the same time, he underwent a further neuropsychological assessment which showed a normal cognitive profile without deficits in attentional or executive functions and the preservation of language functions with fluent speech devoid of anomie or paraphasias and intact comprehension. One year after the first investigation at G.B. Rossi Hospital, he repeated neuropsychological evaluation that revealed a slight worsening with the appearance of hint of

temporal and spatial disorientation and perseveration in speech. His language skills were preserved as well as comprehension.

A brain SPECT scan, carried out seven months later, demonstrated a reduction in global perfusion of the cerebral cortex, widespread at mid-inferior frontal and parietal, occipital and temporal cortex (more consistent in the left hemisphere). Moreover, tracer uptake was homogeneously reduced in the cerebellum. The following year the patient performed a brain SPECT scan with receptor tracer that showed an initial damage to presynaptic dopaminergic system at the right putamen. He performed a brain PET scan at the age of 77 years that showed global and moderate hypometabolism of associative temporal-parietal-occipital cortex, slightly more evident on the left, in the superior frontal area and in cerebellum with modest bilaterally sparing of primary sensory-motor cortex (Fig. 32B). CINE phase-contrast MRI (CINE-MRI) was used to measure cerebrospinal fluid (CSF) flow through the ventricolar system, brain parenchyman and subarachnoidal spaces in order to exclude the presence of a normotensive hydrocephalus. The study of endo-cranial CSF circulation showed a steady flow at the aqueduct of Sylvius (Fig. 32C).

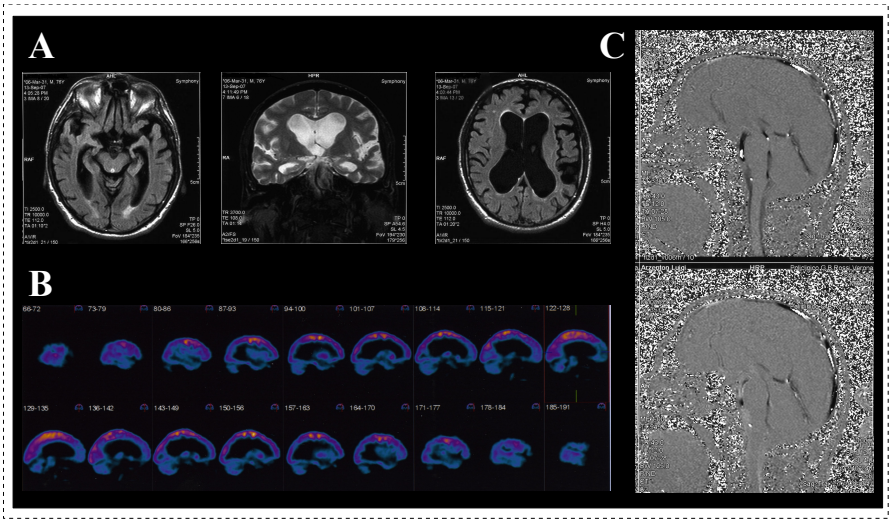

Fig. 32. F2 proband neuroradiological findings.
A: MRI shows a large frontotemporal atrophy and a triventricular hydrocephalus "ex-vacuo" with slight asymmetry (>left side). B: 18-F FDG cerebral PET displays a global and moderate hypometabolism of associative temporal-parietal-occipital cortex (>left side). C: kinetic MRI for the study of endo-cranial CSF circulation shows regular flow at the aqueduct of Sylvius.

The patient underwent to a further neuropsychological assessment that displayed a broad worsening of cognitive profile, characterized by intellectual impairment with deficits of long-term verbal memory, mild attentional deficits and impaired deductive logic. He also exhibited deficits of executive functions and his language skills were impaired with problems of phonemic verbal fluency. Test results, assessing life's quality, disclosed the presence of frontal behaviour symptoms including apathy, carelessness, logopenia, disorganization, loss of spontaneity and stereotypes behavior. At the present, four years after the first neurological assessment, the patient scored 20/30 at MMSE although he did not show spatial or temporal disorientation observed in previous evaluations. He has also obtained a pathological score at tests assessing autonomy in daily activities (IALD: 1/5 and ADL: 2/6).

7.1.2.2.2 Molecular genetics

DHPLC analysis disclosed an abnormal chromatographic profile for exon 8 of *PGRN* which, after direct sequencing revealed the presence of a frameshift mutation (Fig. 33).

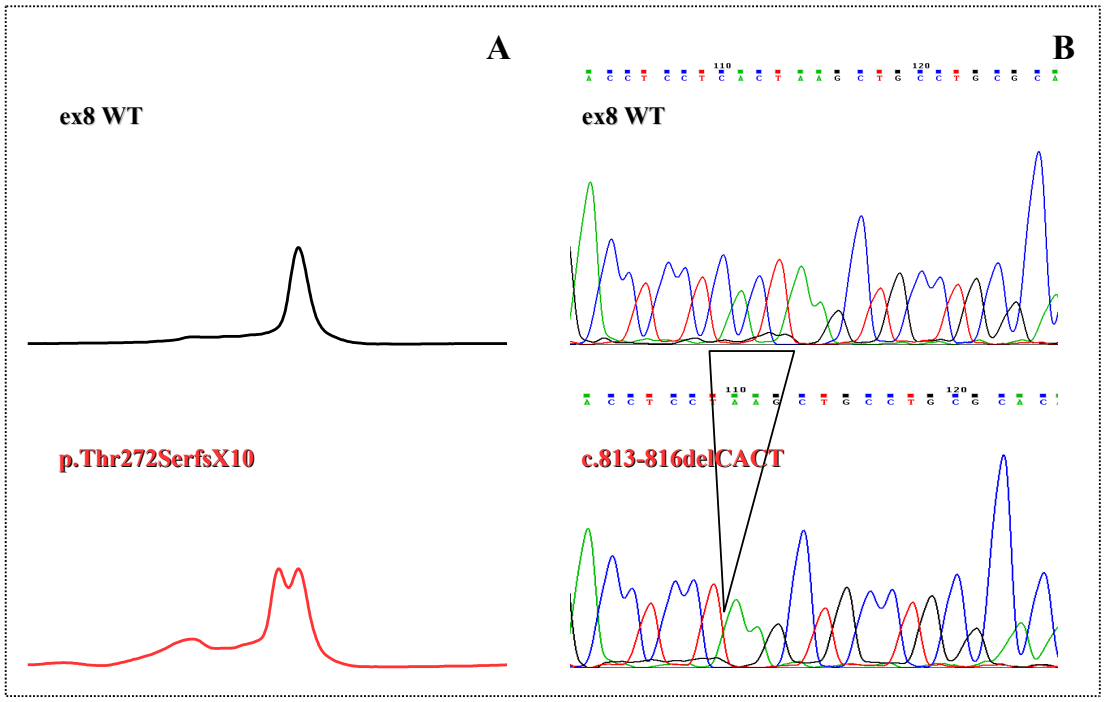

Fig. 33. F2 case: DHPLC and sequencing analysis results.
A: PGRN ex8 chromatographic profiles in a wild-type control (upper) and F2 proband (lower). B: direct sequence of wild-type (upper) and mutated (lower) alleles of F2 proband, disclosing the c.813-816delCACT heterozygous four-nucleotides deletion.

The subcloning of this exon allowed to identified the already reported c.813-816delCACT four-nucleotides deletion, predicted to introduce a premature stop codon (p.Thr272SerfsX10) leading to the formation of an unstable mRNA, degradated by a mechanism of Non-sense Mediated Decay (NMD) [170, 171].

7.1.2.2.3 Biochemical study

For this patient was also available a serum sample that was used in a biochemical ELISA assay to test whether this mutation (like already reported *PGRN* frameshift mutations, which are predicted to introduce a premature stop codon in mRNA with the demonstrated establishment of a state of haploinsufficiency [170, 171]) was able to cause a reduction in PGRN protein levels [154, 244]. Measured PGRN serum values turned out to be strongly reduced compared to those seen in healthy control subjects, indirectly confirming the degradation of mutant allele by NMD mechanism (Fig. 34)

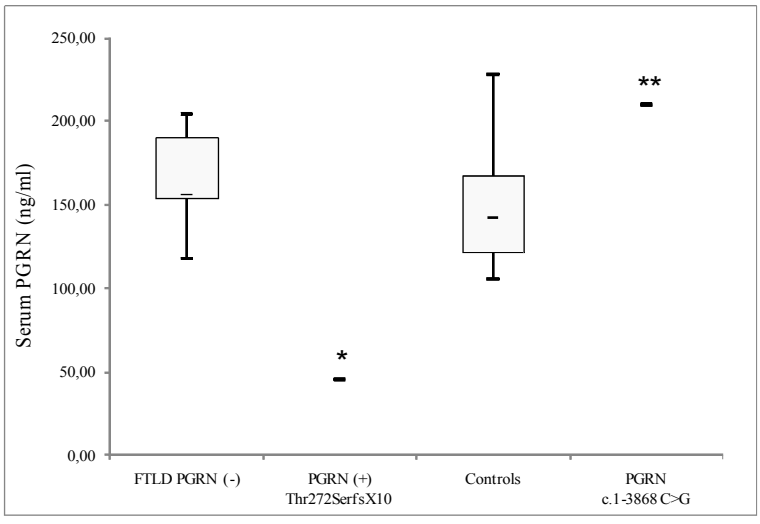

Fig. 34. F2 proband serum progranulin levels (ng/ml).
FTLD PGRN (-): affected unrelated FTLD patients without PGRN mutation; PGRN (+) Thr272SerfsX10: affected F2 proband with Thr272serfsX10 mutation; Controls: healthy control subjects; PGRN c.1-3868 C>G: FTLD-MND affected patient with PGRN non-coding exon 1 variation.
** Serum progranulin levels are decreased in affected carrier of PGRN Thr272SerfsX10 mutation with respect to PGRN (-) patients with FTLD and Controls [mean values ± SD: PGRN (+) Thr272SerfsX10 carrier 45,42 ng/ml; PGRN (-) FTLD affected patients 165,44 ± 30,59; Controls 147,29 ± 37,08].*
*** Serum progranulin levels are not decreased in a FTLD patient with a nucleotide variation in PGRN non-coding exon 1, representing the regulatory region of the gene.*

7.1.2.3 F3 case

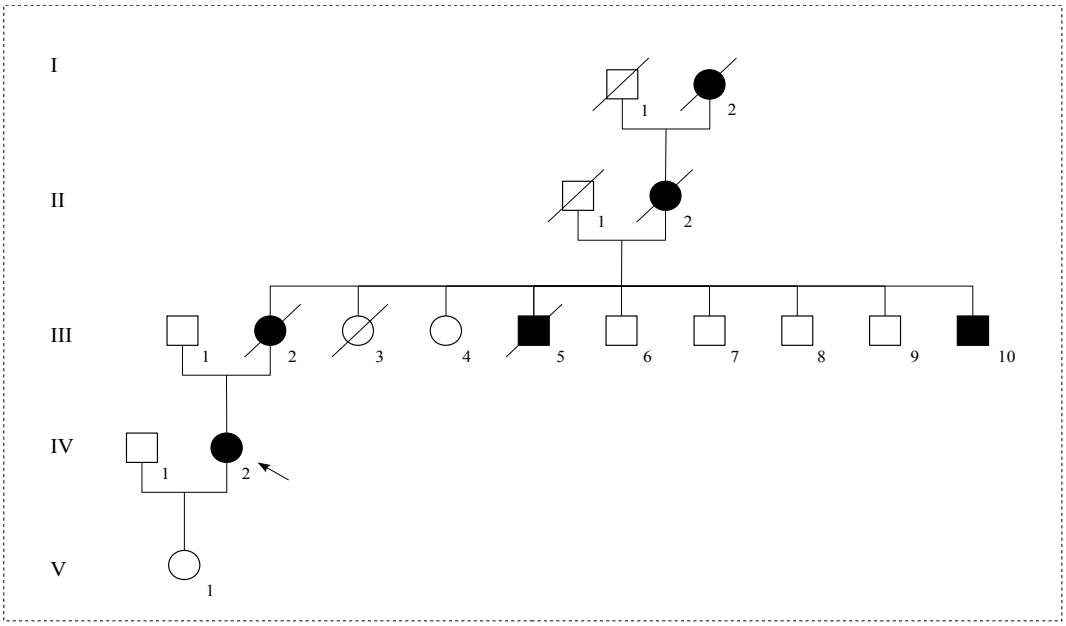

Fig. 35. F3 pedigree.
The arrow indicates the proband; circles, females; squares, male; black symbols, affected family members; slashed symbols, deceased family members. Individuals I.2 and II.2 were affected by late onset dementia, individuals III.5 and III.10 were both affected by early onset dementia with language dysfunctions first and then memory deficits (III.5 died after a disease's duration of 7 years). Individual III.2 started to manifest language disorders before 50 years, followed by dementia. She died at age 57.

7.1.2.3.1 Clinical presentation and neuroradiological features

The proband (IV.2), a clerk woman, began to exhibit language dysfunctions at age 49. During the following year there was a progressive language deterioration: her spontaneous speech was non-fluent, mildly agrammatically, with occasional phonemic and semantic paraphasias. Language comprehension and also memory functions were preserved. She developed an apathetic state with reduction of initiative, loss of interests and lack of personal care. Brain MRI, performed one year after symptoms onset, showed supratentorial cortical atrophy with light right frontal predominance (Fig. 36). Brain perfusion SPECT revealed significant hypoperfusion in the right frontal cortex. After neuropsychological assessment (MMSE score of 26.99/30), she received a clinical diagnosis of progressive non–fluent aphasia (PNFA).

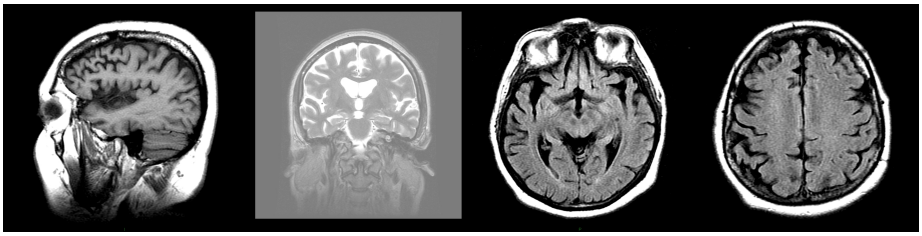

Fig. 36. F3 proband neuroradiological findings.
Magnetic Resonance Imaging scan: saggital and coronal sections.

One year later, at age 51, neuropsychological tests disclosed a progressive decline of language functions, attention degree and memory. In particular, she developed both sequential and phonological errors in repeating words and phrases. Her phonemic fluency performance was reduced, while semantic fluency was normal. Objects naming performance was within normal limits, while verbs naming was compromised. Comprehension of single words was normal, but she had difficulty understanding syntactically complex sentences. The patient scored abnormally in frontal functions test (the attention and the ability to inhibit irrelevant information were reduced); she produced more errors in spatial intelligence and her performance on non-verbal reasoning test was poor. The neuropsychological evaluation revealed prominent deficits of language and executive functions. No abnormalities were detected in constructive praxis, non-verbal intelligence ability and visual memory; her verbal memory performance was patchy, being poorest for verbal tasks. This profile was consistent with frontal lobe dysfunction , PNFA variant. Later on, her spontaneous language was reduced and the comprehension was scarce. Her occupational functioning was significant impaired and personal hygiene was poor. Three years after the onset of symptoms the patient developed behavioural changes which included irritability, verbal aggressiveness, apathy and hyperorality. She also began to disclose behaviour automatism (such as grinding teeth and blow) and she got uninhibited. She continued to worsen until the complete loss of any ability, critical assessment and finally, of autonomy. She died after a disease duration of 4 years.

7.1.2.3.2 Molecular genetics

DHPLC analysis disclosed an abnormal chromatographic profile for exon 11 of *PGRN* which, after direct sequencing revealed the presence of a frameshift mutation (Fig. 37). The subcloning of this exon allowed to identified the novel c.1197C single nucleotide deletion, predicted to introduce a premature stop codon (p.His400ThrfsX12) leading to the formation of an unstable mRNA, possibly degradated by a mechanism of Non-sense Mediated Decay (NMD).

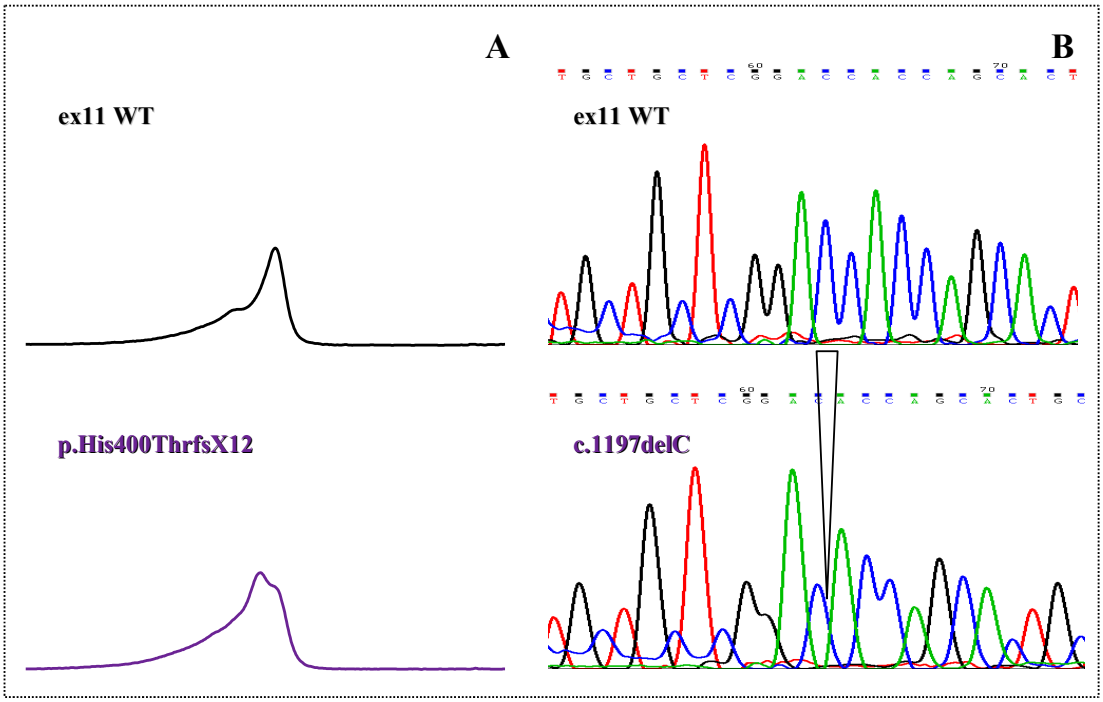

Fig. 37. F3 case: DHPLC and sequencing analysis results.
A: PGRN ex11 chromatographic profiles in a wild-type control (upper) and F3 proband (lower). B: direct sequence of wild-type (upper) and mutated (lower) alleles of F3 proband, disclosing the c.1197delC heterozygous single nucleotides deletion.

7.1.2.4 F4 case

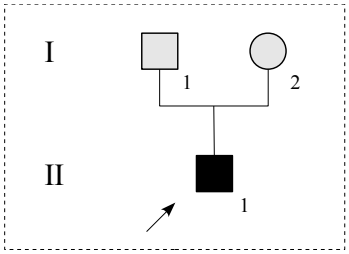

Fig. 38. F4 pedigree.
The arrow indicates the proband; circles, females; squares, male; black symbols, affected family members; grey symbols, affected status not available; slashed symbols, deceased family members.

7.1.2.4.1 Clinical presentation and neuroradiological features

No detailed clinical and radiological data were available about this sixty-four years old man who was examined by clinicians in Bellaria Hospital where he performed neuropsychological and neuroimaging assessments which led to a clinical diagnosis of FTD syndrome. The only known informations included a positive family history and a symptoms onset at age 59 years.

7.1.2.4.2 Molecular genetics

DHPLC analysis disclosed an abnormal chromatographic profile for exon 10 of *MAPT* which was further characterized by direct sequencing which led to the identification of the intron 10 (IVS10) c.2002+16 C>T nucleotide transition. This substitution has already been reported in literature as a pathological mutation affecting the stoichiometric ratio between four- and three-repeats tau isoforms, sufficient to trigger off a process of neurodegeneration of FTLD-tau subtype [245, 246].

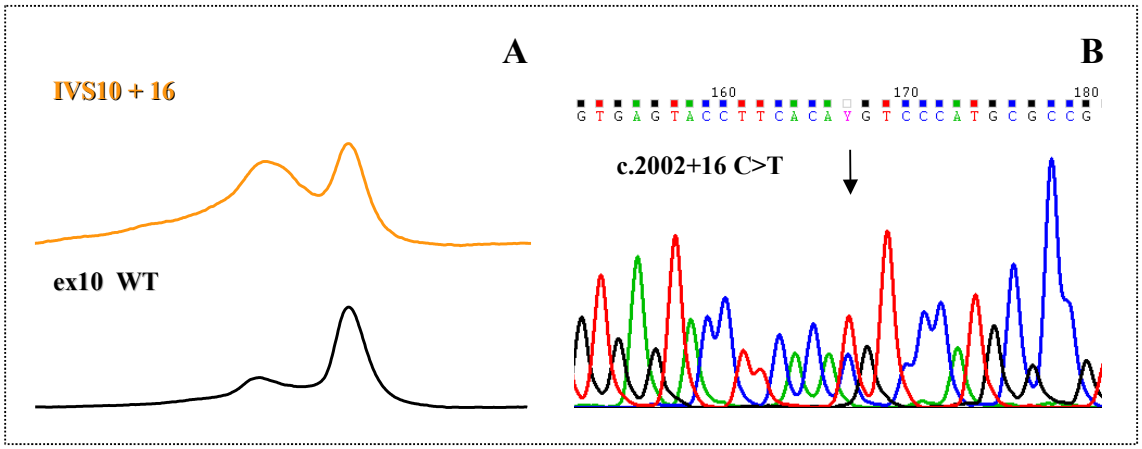

Fig. 39. F4 case: DHPLC and sequencing analysis results.
A: MAPT ex10-IVS10 chromatographic profiles in F4 patient (upper) and wild-type control (lower). B: direct sequence of ex10 in F4 patient disclosing the c.2002+16 C>T heterozygous nucleotide transition (arrow) in intron 10 (IVS10).

7.1.2.5 FTD-MND pedigree

In the analyzed FTLD series 5 unrelated clinically diagnoses FTD-MND patients were included and, among these cases only one belonged to a family characterized by an autosomal dominant

pattern of inheritance of the disease.

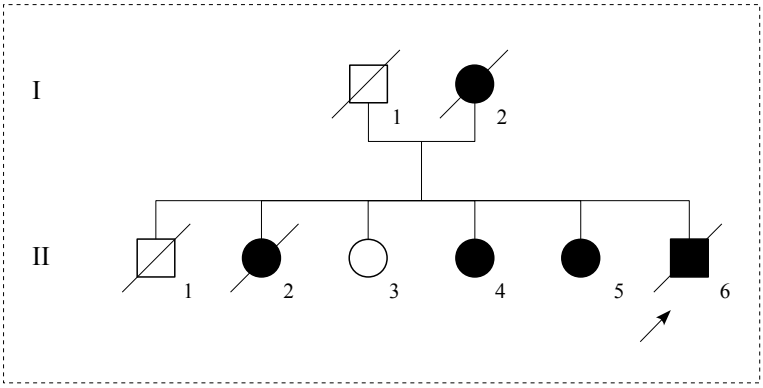

Fig. 40. FTD-MND pedigree.
The arrow indicates the proband; circles, females; squares, male; black symbols, affected family members; slashed symbols, deceased family members. Individual I-2 deceased at age 65 of heart disease but she presented a cognitive decline from age 63. The proband oldest sister (II-2) deceased at age 54 with a four years history of Alzheimer's disease. Since age 62, individual II-4 (a 68 years old unmarried accountant) began to manifest progressive cognitive decline with temporal disorientation, executive dysfunctions in daily tasks (e.g., cooking) and language deterioration. The younger sibling (II-5), a maiden 66 years old, began to display memory deficits associated to depression with lack of appetite at age 56. A few months after the onset of first symptoms she manifested disequilibrium, progressive purposeless behaviours, pauperization of language and echolalia. From the age of 65 years she not longer ambulate and she has become mute.

7.1.2.5.1 Clinical presentation and neuroradiological features

The proband (II.6), an unmarried farmer, deceased at age 58. When he was 48, he started to exhibit a progressive psyco-motor deterioration, accompanied by urinary incontinence. He underwent neurological examination that showed a parkinsonian syndrome with rigidity and bradykinesia. Neuropsychological examination revealed no clear cognitive deficits (MMSE:30/30). He was subjected to CT scan which pointed out a mild degree of cortical atrophy with symmetrical dilatation of ventricular system and third ventricle. Six months later the first evaluation, the patient performed two SPECT assessments: the former showed a bilaterally hypoperfusion of fronto-temporal cortex, basal ganglia and talami while the latter displayed an inhomogeneous uptake for dopamine receptors at basal ganglia (> on right side). After one year from first symptoms, his clinical conditions has worsened: while the parkinsonian syndrome had a discrete entity, the patient was disoriented in time not in space,

with absence of criticisms and lack of awareness of the disease. Sometimes, behaviour was inadequate at circumstances, associated to a moderate cognitive decline (MMSE:20/30). During the following years memory deficit worsened, frequently accompanied by confusional episodes. From age 52 the patient was no longer autonomous and two years later he could not longer ambulate. At age 54 he was hospitalized for fever-associated confusional state and during clinical investigations, he performed a CT scan that revealed a severe triventricular hydrocephalus. He was discharged from hospital with the diagnosis of familial FTD-MND, in advanced aphasic-apraxic state. The patients died at age 58 and, family members gave informed consent to perform a brain autopsy.

7.1.2.5.2 Neuropathological findings

Macroscopical observations revealed a markedly dilated, aligned and symmetrical, ventricular system; a prominent bilaterally cerebral atrophy, with thinning of convolutions and deepening of frontotemporal grooves and, a symmetric atrophy of central gray nuclei, of both the caudatum and putamen-pallido.

The substantia nigra and locus coeruleus appeared depigmented whereas bulbar olives had normal conformation. No atrophy of cerebellar folia was evident and dentate nucleus were well defined. Microscopic examinations revealed neuronal loss, spongiosis of neuropil, most prominent and sometimes confluent in the superficial layers. Pathological process was more widespread at the level of gray matter of frontotemporal convolutions and it was associated to an astrocytic reaction of the white matter. Neuronal loss and reactive astrocytes were also present in gray matter of basal ganglia, particularly in the putamen. Free melanin pigment was widespread in the substantia nigra and locus ceruleus.

Immunohistochemical studies excluded the presence of amyloid plaques and tangles deposits;

conversely tau-negative, ubiquitin-positive inclusion bodies were present in the cytoplasm of granular cells in dentata fascia of hippocampus and in neurons of cortex superficial layers. In affected areas there were also ubiquitin-positive dystrophic neurites.

Immunostaining with TDP-43 antibody also showed a strong presence of different neuronal cytoplasmic inclusions in the superficial cortical layers, with a pattern of distribution typical of FTLD-TDP neuropathological subtype.

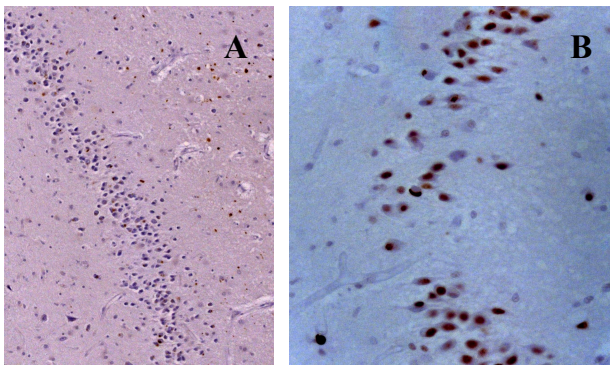

Fig. 41. Brain pathology in proband II-6 of FTD-MND family
A: Ubiquitinated cytoplasmatic inclusions were observed in cerebral cortex and in dentate granular cells of hippocampus. No tau immunopositive deposits were detected.
B: TDP-43 inclusions colocalized with ubiquitin-immunoreactivity.

7.1.2.5.3 Molecular genetics

DNA sample for mutational analysis was available not for the proband but for three family members of the same generation: two affected (individuals II.4 and II.5) and one asymptomatic sisters (II.3).

The mutational screening failed to find any pathogenetic mutations in FTLD-associated genes, including *PGRN* copy number variations. For this reason and considering the occurrence of Alzheimer's Disease in the family, the analysis was extended to autosomal dominant AD-associated genes but, without positive results. This outcome was in agreement with the neuropathological pattern identified in the proband, which had ruled out a diagnosis of Alzheimer's Disease in favour of a FTLD syndrome.

7.1.2.5.4 Linkage and haplotype analysis

Considering the absence of mutations in FTLD known genes and, the clinical presentations and the neuropathological features fulfilling with a diagnosis of FTD-MND, the other possible molecular base to be evaluated was the association to the 9p21.3-13.3 locus on chromosome 9.

Twenty-seven STR markers were analyzed in an interval of 43,36 cM (36,5 Mb), between D9S285 and D9S1780. Although haplotype reconstruction was difficult due to lack of informativity, the two affected sibs (II.4 and II.5) share chromosome 9 haplotypes on both their chromosomes, while the asymptomatic sibling most likely inherited the 2 other haplotypes. Thus, this family is compatible with linkage to the 9p21.3-13.3 locus on chromosome 9.

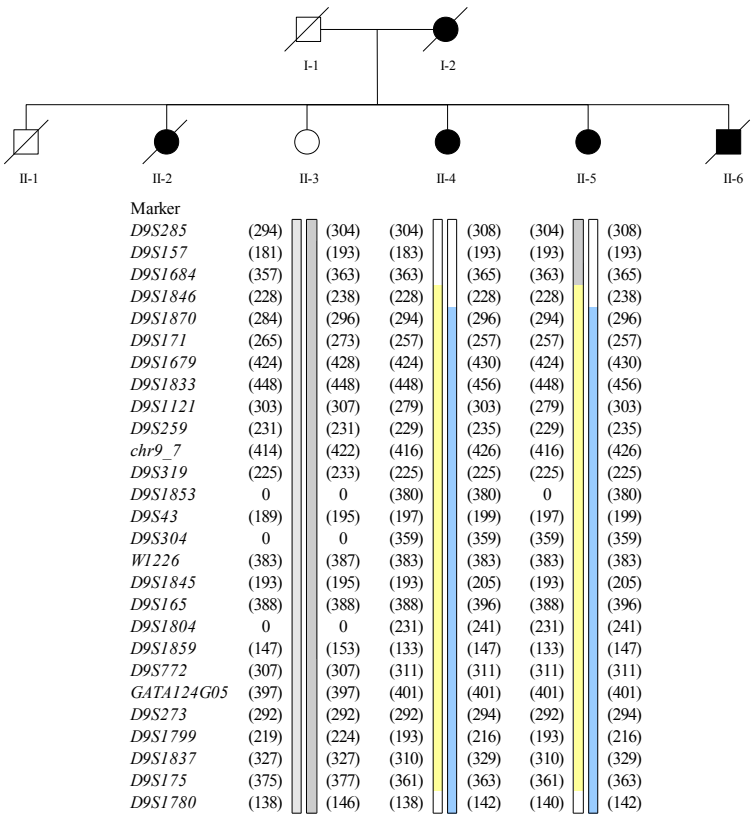

Fig. 42. Segregation of the 9p21.3-13.3 haplotype in the FTD-MND family.
Haplotypes are based on a selection of 27 informative short tandem repeat markers at chromosome 9. The yellow and blue light haplotypes represents the the two possible disease haplotype. Haplotypes for other family members were not inferred due to the lack of informativity within the family.

7.2 CADASIL

7.2.1 NOTCH3 mutational analysis

Twenty-one different *NOTCH3* mutations were identified in the 53 analyzed unrelated index cases, including seven novel variations: Cys108Ser in exon 3, Cys366Trp and Ser396Cys in exon 7, Arg592Cys and Cys606Arg in exon 11, Cys939Arg in exon 18 and Gly1013Cys in exon 19 (Table 19).

Exon	Nucleotide Change	Aminoacid Change	EGF domain	Number of index cases	Mutation for Exon No. (%)
3	c.346C>T	p.R90C	2	3	4 (7,56%)
	c.400T>A	p.C108S*	2	1	
4	c.475C>T	p.R133C	3	2	15 (28,3%)
	c.499C>T	p.R141C	3	3	
	c.514T>C	p.C146R	3	4	
	c.583C>T	p.R169C	4	1	
	c.599G>A	p.C174Y	4	1	
	c.679T>C	p.C201R	5	1	
	c.697C>T	p.R207C	5	3	
5	c.829T>C	p.C251R	6	1	1 (1,9%)
6	c.890G>T	p.C271R	6	1	1 (1,9%)
7	c.998T>G	p.C366W*	9	1	11 (20,75%)
	c.1265C>G	p.S396C*	10	10	
10	c.1660G>T	p.G528C	13	2	2 (3,77%)
11	c.1852C>T	p.R592C*	15	1	3 (5,66%)
	c.1895T>C	p.C606R*	15	1	
	c.1898C>T	p.R607C	15	1	
18	c.2893T>C	p.C939R*	24	1	1 (1,9%)
19	c.3094C>T	p.R1006C	26	12	13 (24,53%)
	c.3115G>T	p.G1013C*	26	1	
22	c.3769C>T	p.R1231C	31	2	2 (3,78%)

Table 19. The spectrum of NOTCH3 mutations.
Notch3 mutations in 53 CADASIL index cases. An asterisk indicates novel

All these substitutions, not observed in healthy control subjects, are missense mutations that lead to an odd number of cysteine residues, affecting EGF-like repeats by causing the loss or gain of one cysteine. Although mutations were distributed unevenly over 10 exons, exons 4, 19 and 7 represented the most frequently affected mutation sites accounting together for 74% of the affected individuals (Table 19). Several mutations seem to cluster in specific geographical regions of Italy (Fig. 43). In particular, 11 mutations (R90C, C146R, R169C, C174Y, C201R, S396C, R592C, C606R, R607C, C939R and G1013C) were identified only in patients from North-East Italy , 4 (C251R, C271F, C366W and R1231C) only in patients from North-West Italy and 2 (C108S and G528C) solely in patients from Central Italy. The novel Ser396Cys substitution was observed in 10 index cases living in the neighboring provinces of Verona, Vicenza, Padua, Treviso and Venice (North-East Italy). Moreover, the Arg1006Cys mutation occurred mainly in patients (9 index cases) from Ascoli Piceno and Chieti or nearby villages (Central Italy), with the exception of three individuals living in Northern Italy for whom no information about the origins of grandparents was available.

Fig. 43. Geographical distribution of NOTCH3 mutations in studied series.
Novel mutations are reported in bold character. Underline variations represent mutations indentified only in patients from a definite geographical area. Number of index cases are reported in bracket when major than a single case. Three main clusters are detectable: North-East Italy, North-West Italy and Central Italy.

7.2.2 Tagging-SNP and *NOTCH3* Haplotype analysis

Allele and 5 SNP haplotype frequencies, estimated from the probands of the 22 pedigrees, the 31 unrelated index cases and the 50 controls are reported in Table 20 and Table 21, respectively. All the 5 SNPs showed to be in Hardy-Weinberg equilibrium. Haplotype analysis showed the 10 haplotypes estimated from the sample set. The 4 most common haplotypes in control population (H1, H2, H3, H4) account for nearly 89% of the observed haplotypes (see table 21 for haplotype coding). In 17 pedigrees the mutations were observed to be linked to the most common haplotype H1. The Arg141Cys mutation was linked to H1 and H5 haplotypes (in 1 index case and 2 families respectively) whereas the H4 was associated to the Cys271Phe variation. The Ser396Cys mutation was observed in two different haplotypes: H1 (in 3 families and 5 index cases) or H2 (1 family). In one of the Ser396Cys families, where experimental data were not completely available, either H1 or H2 were compatible.

In the 31 unrelated all the mutations were also compatible with the hypothesis of mapping on the most common haplotype H1 with the exception of Arg207Cys. that was observed in two index unrelated patients originating in North-Easter Italy, whose haplotypes are likely to be H1 and H2, and H4 and H9, respectively.

SNP	Minor allele (m)	Major allele (M)	Affected			Controls			p-value
			mm	mM	MM	mm	mM	MM	
rs1044009	C	T	2	19	32	10	18	21	0.022
rs10426042	G	C	0	10	40	0	13	37	0.48
rs10423702	A	G	1	12	40	0	11	39	1
rs4809030	T	C	1	12	40	0	12	38	1
rs3815188	T	C	1	16	35	1	15	34	1

Table 20. Genotypes and allele distribution among affected and controls.
p-value: significance of genotype distribution frequencies between affected and controls individuals.

Haplotype	rs3815188	rs1043702	rs10426042	rs4809030	rs1044009	Affected	Controls	χ^2	p-value
H1	C	G	C	C	T	64.17	53.63	2.29	0.1302
H2	C	G	C	C	C	4.02	15.88	7.88	0.0049
H3	T	G	G	C	C	5.97	9.57	0.90	0.3414
H4	C	A	C	T	C	6.04	8.66	0.50	0.4774
H5	T	G	C	C	T	7.06	3.16	1.55	0.2121
H6	T	G	G	C	T	1.24	2.38	0.36	0.5459
H7	C	G	C	T	C	3.77	2.21	0.42	0.5180
H8	T	G	C	C	C	0.60	2.10	0.81	0.3681
H9	C	A	C	T	T	1.42	1.25	0.01	0.9142
H10	C	A	C	C	T	5.71	1.20	3.03	0.0818

Table 21. Haplotypes frequencies (%) estimated in 50 healthy control individuals and in the 53 affected patients (22 pedigree probands and 31 unrelated index cases).
p-value: significance of difference individual haplotype frequencies between affected and controls subjects.

7.2.3 Scalpel skin biopsy

Electron microscopy detected GOM in all 16 patients examined (Table 22). Ultrastructurally typical material accumulated mostly within the basal lamina indenting smooth muscle cells of small dermal arteries (Fig. 44). GOM were also detectable in the basal lamina of pericytes and endothelial cells of some capillaries.

Table 22. GOM detection in skin biopsy.

Case	Sex	Mutation	Age at autopsy	GOM
1	M	R141C	48	+
2	F	C146R	57	+
3	M	C146R	28	+
4	M	C146R	37	+
5	F	C146R	48	+
6	F	R169C	34	+
7	M	R207C	49	+
8	M	S396C	52	+
9	F	S396C	71	+
10	M	S396C	58	+
11	M	S396C	62	+
12	F	G528C	60	+
13	M	R1006C	65	+
14	M	R1006C	52	+
15	M	R1006C	57	+
16	M	G1013C	35	+

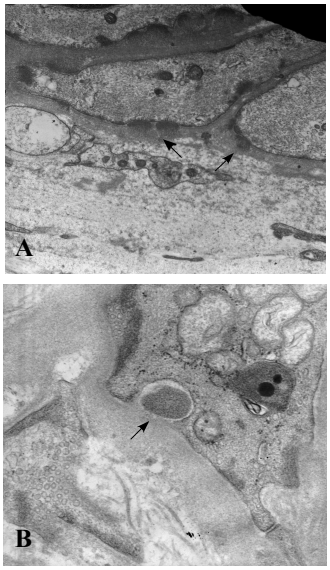

Fig. 44. Electron microscopy of skin biopsy in a NOTCH3 mutation carrier.
A: the arteries with several GOM deposits (arrows).
B: a GOM shown at higher magnification.

7.2.4 A selected case

Among the 575 patients with clinical suspicion of CADASIL but without typical *NOTCH3* mutations (characterized by loss or gain of one residue of cysteine), the *NOTCH3* c.3057delG frameshift mutation (p.Gly994AlafsX277) was identified in one index case (Fig. 45). The patient, a 38 years old woman, was referred to the attention of G.B. Rossi Hospital neurologists because of recurrent headache episodes by the age of 12-18 years, a pattern of MRI characterized by white matter T2-hyperintensities and a positive family history for cognitive decline and psychiatric disorders (Fig. 46). She also underwent a skin biopsy for electron microscopy analysis which revealed the absence of GOM deposits (Fig. 47).

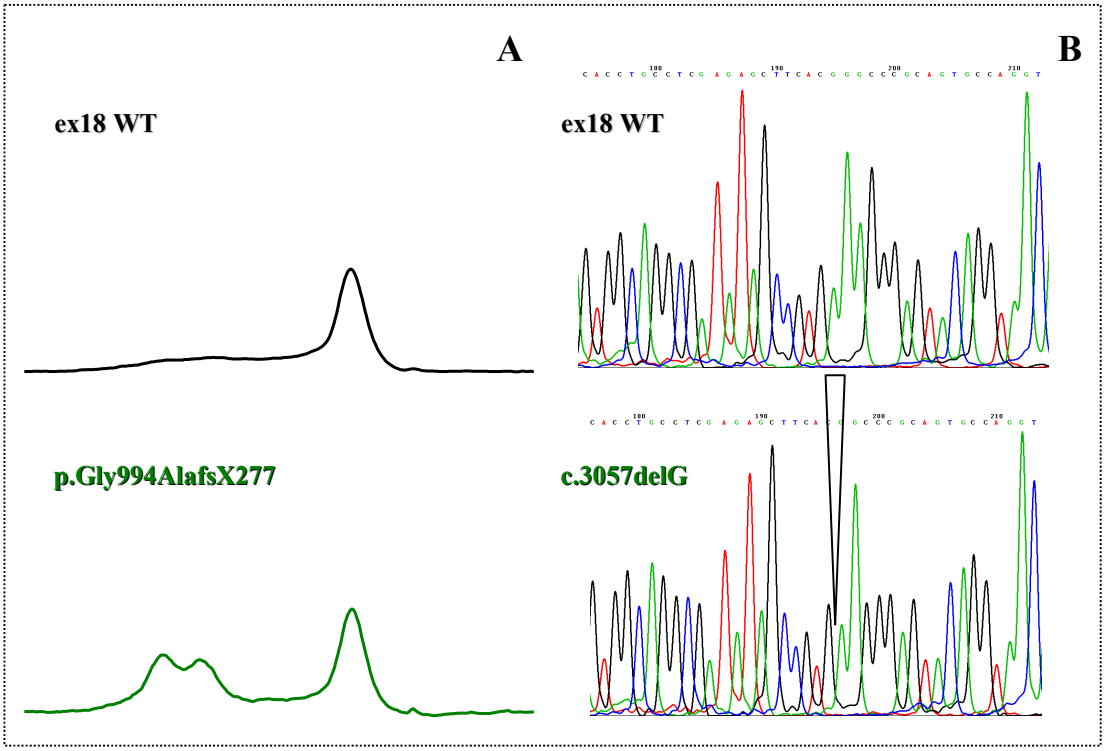

Fig. 45. NOTCH3 frameshift mutation: DHPLC and sequencing analysis results.
A: NOTCH3 ex18 chromatographic profiles in a wild-type control (upper) and affected patient (lower). B: direct sequence of wild-type (upper) and mutated (lower) alleles of affected patient disclosing the c.3057delG heterozygous single nucleotides deletion..

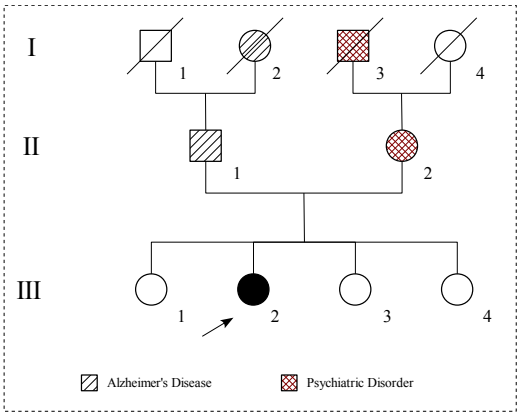

Fig. 46. NOTCH3 ex18 pedigree.
The arrow indicates the proband; circles, females; squares, male; black symbols, affected family members; slashed symbols, deceased family members. Individuals I.2 affected by AD by the age 60 years; II.1 affected by memory deficit and depression by the age 62 years; I.3 and II.2 affected by psychiatric disorder.

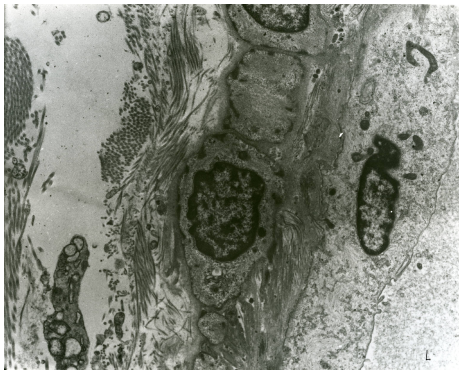

Fig. 47. Electron microscopy in skin biopsy of NOTCH3 p.Gly994AlafsX277 mutation carrier.
GOM deposits were absent also in subsequent investigation of other vessels and in a second

8. Discussion

8.1 Alzheimer's Disease and Frontotemporal Lobar Degeneration

Alzheimer's Disease and Frontotemporal Lobar Degeneration fall into the same category of primary cortical dementia, sharing the general etiological process represented by progressive neurodegeneration. Despite these two forms of dementia can, in principle, be distinguished according to different onset symptoms and neuroradiological imaging, in clinical practice is not always so straightforward and simple because of atypical clinical presentations. For this reason, the entire panel of AD and FTLD associated genes was analyzed in all recruited patients, starting with the investigation of those genes associated with the clinical subtype of dementia and then extended to the other genes. The mutational analysis led to the identification of 8 probably pathogenetic mutations in 8 out of 210 unrelated index cases with a molecular yield of approximately 4% (Table 17). This low mutational frequency may be attributed to the approach used in patients recruitment and to the limits of diagnostic criteria nowadays available to distinguish different forms of dementia.

Two important informations to be collected during the patient examination, are the presence of familiarity for dementia within the family and presumed age of onset of the disease. Actually, the genetic forms of Alzheimer's Disease and Frontotemporal Lobar Degeneration are mainly inherited as an autosomal dominant traits, which means that the disease must occur in many individuals over several generations. This is a very important element that might suggest the existence of a possible genetic basis for the disease, addressing the clinician to advise a genetic analysis to the family. In this study informations about disease familiarity are often missing (not available in 144 out of 210 cases), especially those for patients not visited in G.B. Rossi Hospital (Table 1-2). Moreover, it is also difficult to state how many of the referred familial cases

(50/210) represent Mendelian pathway of inheritance. The absence of these data may explain the overall low mutational yield, since many of analyzed cases are probably sporadic form of AD or FTLD with no Mendelian inheritance pattern.

The other important information which may suggest a possible genetic base is the age of onset of the disease. Unlike literature data, where mean ages of onset in autosomal dominant forms of AD and FTLD range from 30 to 60 years and 45 to 65 years respectively, in this study the mean age at onset tends to be higher (62,5 ± 9,5 years), probably reflecting the inclusion of several sporadic cases. Therefore age of onset may be useful to discriminate genetic forms of AD and FTLD, usually associated to an earlier onset, even though variability in first symptoms manifestation and incomplete penetrance may occur especially in *PSEN2* and *PGRN* mutation carriers.

These considerations highlight the relevance of a thorough clinical assessment as it may allow to identify, with more confidence, those patients with a genetic form of AD or FTLD, reducing the waste of time and money entailed by the mutational screening adopted in this study. In fact, Table 18 shows how analyzed genes are polymorphic: many SNPs have been identified (mostly in *PGRN*, *MAPT*, *VCP*, *PSEN1* and *PSEN2* genes) occurring with an high frequency in the whole series, even in more than 50% of cases. The presence of these SNPs makes the mutational screening more laborious, time-consuming and expensive. In fact, although the first mutational step consisting in DHPLC analysis is rapid, highly sensible and cheap, it only detects the occurrence of a nucleotide change but it does not characterized its entity. For this reason, direct sequencing is necessary to define the occurred nucleotide variation, differentiating SNPs from mutations, with an inevitable overload of work and costs. This, in turn, strengthens the necessity to enrol a selected series. In this study, the clinical diagnosis of included patients is very heterogeneous because of, not only the recurrent atypical presentations of AD and FTLD (as

mentioned upon and in chapters 2 and 3), but also as a consequence of the limitation of diagnostic tools available to make a differential diagnosis of dementia. Nowadays, despite of the improvements in neuropsychological tests, neuroimaging studies and biologic fluids (serum, plasma, CSF) biochemical analyses, these diagnostic approaches are not themselves enough to write out a clinical diagnosis of a particular subtype of dementia while, the only available tool which allows a definite diagnosis of AD or FTLD (or other dementias) is represented mainly by neuropathological examination. The need to distinguish different form of dementia *ante mortem*, is emphasised by the possibility to apply *ad hoc* pharmacological treatments when they would be available. This justifies the spread research in the last years of easy, quick and inexpensive peripheral hallmarks specific of a particular type of dementia in order to make a definite clinical diagnosis. This is the case of PGRN serum or plasma levels which have been demonstrated to be a useful tool for the identification of *PGRN* frameshift mutations carriers, with specificity and sensitivity of 100% [154].

8.1.1 Alzheimer's Disease

In this study 41 patients had a clinical diagnosis of AD while in other 9 cases it was supported by neuropathological findings. No mutations in AD-associated genes were identified in the second group for which the greater part of clinical informations was unavailable, mostly due to the fact that this samples were enrolled in the 1980s when clinicians were not used to collect exhaustive informations but, brain autopsy was carried out only to confirmed or excluded a clinical diagnosis of Creutzfeldt-Jacob Disease.

In four unrelated familial cases of clinically diagnosed AD, two already described PSEN2 non-synonymous changes (p.Arg71Trp and p.Met174Val) and two novel missense variations, one in

PSEN1 (p.Ile437Asn) and the other in PSEN2 (p.Thr18Met) were identified (Table 17).

8.1.1.1 A1 case: PSEN1 p.Ile437Asn

The *PSEN1* transition c.1310 T>A is predicted to cause the substitution of an high hydrophobic isoleucine with an high hydrophilic asparagine, at codon 437 (Fig. 17B). Considering that this residue is conserved between PSEN1s and PSEN2s and it is located in the putative transmenbrane domain TM-IX (Fig. 48), the introduction of an hydrophilic aminoacid in a hydrophobic core could destabilize and alter the physical-chemical interactions between adjacent aminoacids, affecting the organization of the transmembrane domain and maybe impairing the protein function, as predicted by *in silico* analysis.

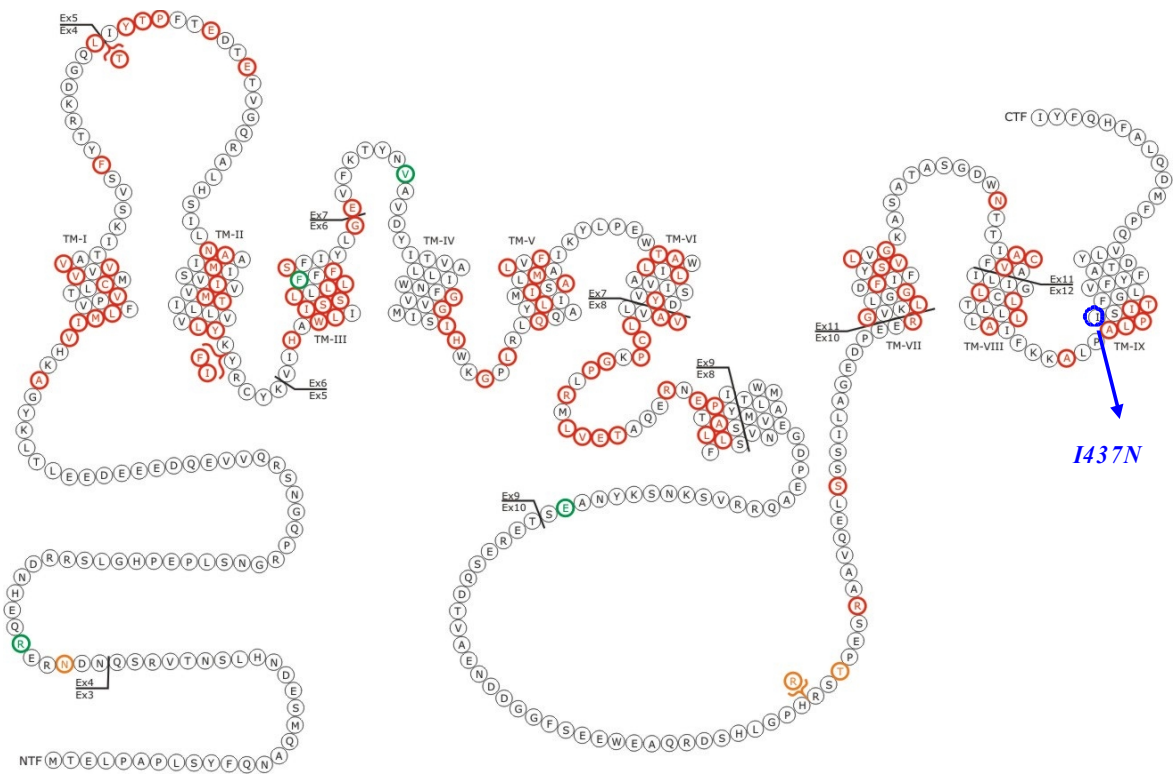

Fig. 48. Schematic representation of putative PSEN1 structure.
Each PSEN1 residue is represented by a circle marked by one-letter aminoacid symbol. Green outlined circle: not pathogenic aminoacid substitution; orange outlined circle: aminoacid substitution with not well-defined pathogenetic role; red outlined circle: pathogenetic aminoacid substitution. Blue outlined circle: aminoacid substitution identified in

Such speculations may be indirectly supported by the identification of few *PSEN1* mutations (reported in literature) affecting other isoleucine residues located in putative transmembrane domains of the protein, which are conserved between presenilins and replaced by an asparagine or other hydrophilic amino acids such as serine or threonine (eg.: p.Ile439Ser in TM-IX or p.Ile143Thr in TM-II). Furthermore, the p.Ile437Asn does not represent a polymorphism since it was excluded in 492 healthy control subjects and in the other 209 analyzed patients. These data argue in favour of a probable pathogenetic role for this *PSEN1* variation, even though DNA samples of other family members were not available to test its cosegregation with the disease.

Considering the shortage of clinical informations about the mutation carrier, it is difficult to define possible genotype-phenotype correlations; the only possible consideration regards the first manifestation of symptoms (over 65 years) that differ from most *PSEN1* mutations, usually associated to an earlier onset.

8.1.1.2 A2 case: PSEN2 p.Thr18Met

The novel *PSEN2* c.53 C>T nucleotide transition was identified in a patient with positive family history for dementia. Both clinical phenotype and neuroimaging features were compatible with a clinical diagnosis of Alzheimer's Disease in the proband. This nucleotide substitution is predicted to cause the aminoacidic replacement p.Thr18Met. This residue, located in the putative N-terminal cytoplasmatic domain of the protein (Fig. 49), is high phylogenetic conserved among PSEN2s, but it is not conserved in PSEN1s; by *in silico* analysis, this substitution is predicted to be not tolerated probably because the threonine is replaced by a more hydrophobic aminoacid (methionine) (Fig. 21B). In PSEN1s this position is occupied by another hydrophilic residue, a phylogenetic conserved asparagine while hydrophobic aminoacids seem to be not tolerated. Even this *PSEN2* substitutions does not represent a polymorphism in the studied population since it

was excluded in 492 healthy control subjects and in the other 209 analyzed patients. These data and the fact that it was identified in a FAD case, devoid of *APP* or *PSEN1* mutations, militate in favour of a possible pathogenetic role for this variation.

8.1.1.3 A4 case: PSEN2 p.Arg71Trp

The *PSEN2* c.211 C>T nucleotide variation was identified in a patient with early onset FAD (59 years) with clinical manifestations and disease evolution fulfilling with a clinical diagnosis of AD. This change affects an arginine residue at codon 71 which is located in the putative N-terminal cytoplasmatic domain of the protein (Fig.49) and conserved among not all but many PSEN2s of different species, not in PSEN1s (Fig. 24A). The predicted aminoacid substitution involves the replacement of a positive charged hydrophilic residue (arginine) with an apolar hydrophobic aromatic aminoacid, tryptophan (Fig. 24B). In a few PSEN2s and PSEN1s the alternative residue at codon 71 is a serine which is probably tolerated within the protein given its hydrophilic polar nature. Therefore, considering the difference in physical-chemical and hydrophobicity properties of involved aminoacids, the substitution p.Arg71Trp may lead to a local conformational change of the protein (predicted not tolerated by *in silico* analysis) which in turn may affect the protein function. Furthermore, the c.211 C>T transition was absent in 801 unrelated index cases (209 affected and 492 controls) excluding its possible role as a polymorphism.

8.1.1.4 A4 case: PSEN2 p.Met174Val

The *PSEN2* c.520 A>G transition was identified in a FAD case with late onset, a rapid progression of the disease (illness duration: 4 years) with typical memory deficits as first clinical presentation. This nucleotide substitution affects a Methionine residue at codon 174, located

within the putative transmembrane domain TM-III of the protein (Fig. 49), which is partially conserved only among PSEN2s (Fig. 28A). This aminoacid is predicted to be replaced by a more hydrophobic residue of Valine (Fig. 28B) with probably no appreciable variation in steric hindrance within the protein. Moreover, Valine is present at position 174 in a few PSEN1s, probably indicating that it may be tolerated within the protein, as predicted by *in silico* analysis, even though the p.Met174Val does not represent a polymorphism since it was absent in all other analyzed cases.

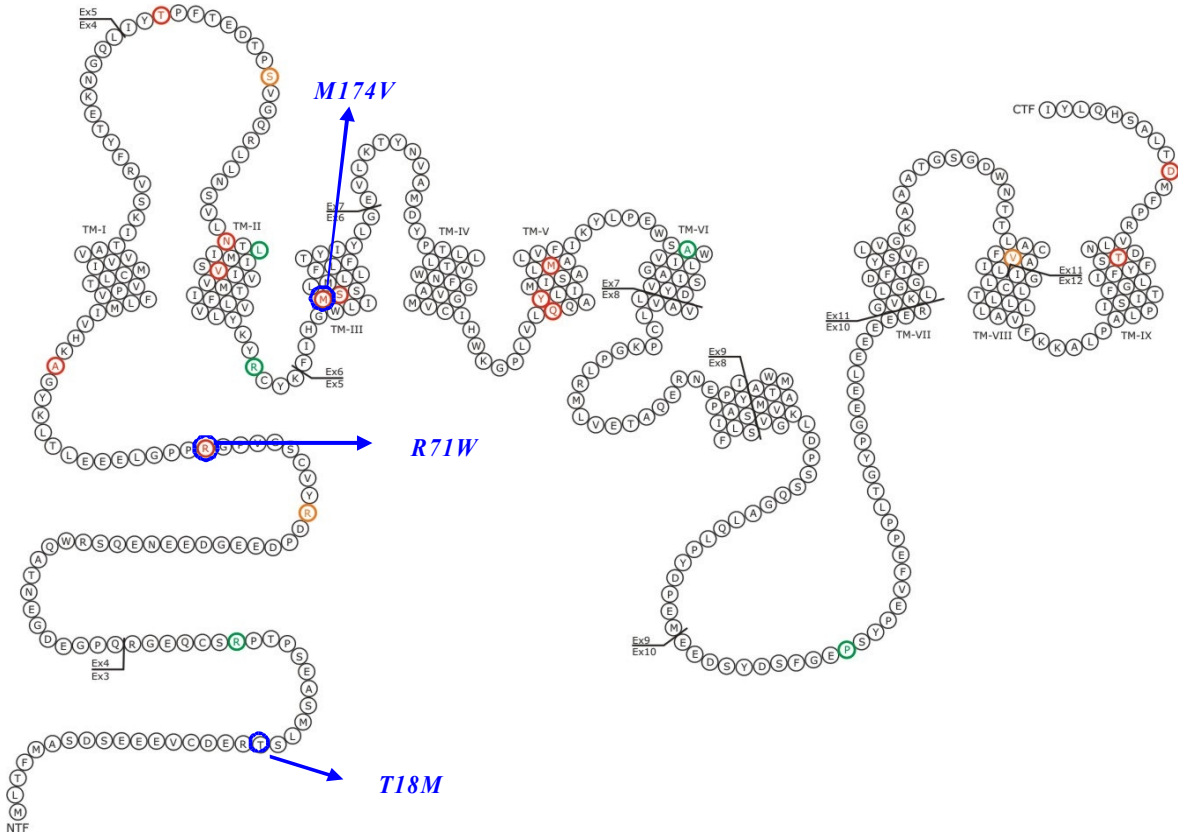

Fig. 49. Schematic representation of putative PSEN2 structure.
Each PSEN2 residue is represented by a circle marked by one-letter aminoacid symbol. Green outlined circle: not pathogenic aminoacid substitution; orange outlined circle: aminoacid substitution with not well-defined pathogenetic role; red outlined circle: pathogenetic aminoacid substitution. Blue outlined circle: aminoacid

8.1.1.5 Genotype-phenotype correlations and literature data

The PSEN2 p.Arg71Trp and p.Met174Val substitutions have been previously identified by Guerreiro et al in two sporadic index cases of Alzheimer's disease and excluded in 251 healthy control subjects [247]. The authors classified these variations as possibly pathogenic on the basis of a well defined pathogenicity algorithm, including criteria such as cosegregation with the disease, absence in healthy controls, phylogenetic conservation among different species and alteration of *in vitro* Aβ peptides levels (as *PSENs* mutations cause an increase in Aβ42/Aβ40 ratio). In the herein reported series these aminoacid replacements were detected in two unrelated index cases of clinically diagnosed Alzheimer's Disease with positive family history for dementia and they were excluded in nearly 500 healthy control subjects. These data argue in favour of a possible pathogenetic role for the p.Arg71Trp and p.Met174Val variations, which in the first case were also supported by *in silico* and phylogenetic analyses while in the second they do not correlate. These results stress the necessity to perform biochemical studies in order to assess possible functional changes in the proteins and in particular, variations in Aβ42/Aβ40 ratio production.

Noteworthy, only 23 *PSEN2* non-synonymous nucleotide variations were already reported in literature and among this group, only 7 were considered definite pathogenetic mutations (Table 22), suggesting a low mutational frequency for *PSEN2* gene, considered the rarest cause of EOFAD [248].

In the present study 2 already reported and one novel *PSEN2* variations have been identified, with a possible pathogenic role. If further analyses will confirm these data, the mutational frequency of *PSEN2* in this series will account for 17,65% of all analyzed FAD cases. This prevalence would be greater than that of *PSEN1* (5,88%), in contrast with literature data. This result may be partially ascribed to the late mean age of onset in the considered series (64,89 ±

9,64) which fulfils with the range associated to *PSEN2* mutations (while *PSEN1* mutations usually correlate with an earlier manifestation of first symptoms). An alternative explanation may be an underestimation of *PSEN2* mutational frequency in literature even if the findings in this study might be related to the small size of AD clinical series. Another possibility to consider could be that these variations, despite molecular and *in silico* results, are not mutations but rare polymorphisms, an hypothesis which may be rule out only by a cosegregation analysis in the families and by testing their ability *in vitro* to increase the secreted Aβ42/Aβ40 peptide ratio.

Literature data

Aminoacid Variation	*protein domain*	*clinical diagnosis*	*familiarity*	*Cosegregation*	*phylogenetic conservation*	*absence in control population*	*In vitro Aβ42/Aβ40 assay*
Polymorphisms							
Arg29His	N-Term	healthy			+/-	observed in 1 chr of CEPH-HGDP	
Leu143His	TM-II	healthy			+++/-	observed in 1 chr of CEPH-HGDP	
Arg163His	HL-II	PD	F	no segregate	+++/+	observed in 1 affected and 1 healthy chr	
Ala252Thr	TM-VI	healthy			+++/+	observed in 2 unrelated chrs of CEPH-HGDP	
Pro334Arg	HL-VIb	AD	F	no segregate	+/-	observed in 67 AD chrs and in 100 healthy chrs	
Pathogenetic mutations							
Ala85Val	N-Term	AD/PK	F	segregate	+++/+	absent in 424 healthy chrs	
Thr122Pro	HL-I	AD	F	segregate	+++/+	absent in 100 healthy chrs	↑ Aβ42/Aβ40
Thr122Arg	HL-I	AD/FTD	F	segregate	+++/+		
Asn141Ile	TM-II	AD	F	segregate	+++/+		↑ Aβ42/Aβ40
Met239Val	TM-V	AD/bd	F	segregate	+++/+		↑ Aβ42/Aβ40
Met239Ile	TM-V	AD	F	segregate	+++/+	absent in 100 healthy chrs	↑ Aβ42/Aβ40
Thr430Met	TM-IX	AD	F	segregate	+++/+	absent in 260 healthy chrs	
Pathogenetic nature debated							
Arg62His	N-Term	AD	S		+/-	observed in 20 unrelated chrs of CEPH-HGDP	↔ Aβ42/Aβ40
Arg71Trp	*N-Term*	*AD*	*S*		++/-	*absent in 502 healthy chrs*	
Ser130Leu	HL-I	AD	F	segregate	+++/-	absent in 220 healthy chrs and in 200 AD chrs	↔ Aβ42/Aβ40
Val139Met	HL-I	AD	F		+++/-	absent in 200 healthy chrs and in 200 AD chrs	
Val148Ile	TM-II	AD			+++/+	absent in 190 healthy chrs and in 256 AD chrs	↔ Aβ42/Aβ40
Met174Val	*TM-III*	*AD*	*S*		+/-	*absent in 502 healthy chrs*	
Ser175Cys	TM-III	AD	F		+++/+		
Gln228Leu	TM-V	AD	F		+++/+	absent in 200 healthy chrs and in 200 AD chrs	
Tyr231Cys	TM-V	FTD	S		+++/+	absent in 200 healthy chrs and in 200 AD chrs	
Val393Met	TM-VIII	AD	F		+++/+	absent in 768 healthy chrs	↔ Aβ42/Aβ40
Asp439Ala	C-Term	AD	F	segregate	+++/+	absent in 100 healthy chrs and in 160 AD chrs	↔ Aβ42/Aβ40

This study

Aminoacid variation	*protein domain*	*clinical diagnosis*	*familiarity*	*cosegregation*	*phylogenetic conservation*	*absence in control population*	*In vitro Aβ42/Aβ40 assay*
Thr18Met	N-Term	AD	F		+++/-	absent in 984 healthy chrs	
Arg71Trp	N-Term	AD	F		++/-	absent in 984 healthy chrs	
Met174Val	TM-III	AD	F		+/-	absent in 984 healthy chrs	

Table 22. PSEN2 non-synonymous nucleotide variations reported in literature and identified in this study.
+++/+ high phylogenetic conserved in PSEN2s and in human PSEN1; +++/- high phylogenetic conserved in PSEN2s not in human PSEN1; ++/- phylogenetic conserved in PSEN2s of many different species not in PSEN1; +/- phylogenetic conserved in PSEN2s of a few different species not in PSEN1; ↑ Aβ42/Aβ40 increased Aβ42/Aβ40 ratio; ↔ Aβ42/Aβ40 no significant alteration of Aβ42/Aβ40 ratio; CEPH-HGDP Centre d'Etude du Polymorphisme

As regards the clinical phenotypes, there is not an evident univocal correlation with the associated mutation; despite of the differences in first clinical symptoms (memory and language impairment in A2 patient, multiple cognitive domains deficits in A3 and behavioural changes in A4), there was a common disease evolution characterized by severe deficit in memory and executive functions coupled to language impairment and loss of autonomy in daily life activities. Moreover, the age of onset and illness duration fall within the range reported for *PSEN2* mutation carriers (with the exception of A3 case who disclosed the first symptoms by the age 59).

8.1.2 Frontotemporal Lobar Degeneration

In this study 71 patients had a clinical syndrome of FTLD while in other 5 cases it was supported by neuropathological findings. No mutations in FTLD-associated genes were identified in the second group for which the greater part of clinical informations was unavailable (for the same reasons reported for cases with a neuropathological diagnosis of AD) but, it is significant that almost all cases were referred as sporadic.

Three already reported (*PGRN* c.378delC and c.813_816delCACT and, *MAPT* c.2002+16 C>T) and one novel (*PGRN* c.1197delC) mutations were identified in 3 FTD and in one PNFA unrelated patients respectively (Table 17). All this cases presented positive family history with a Mendelin pattern of inheritance, even though DNA samples of family members were not available to prove the cosegregation of the disease.

8.1.2.1 Progranulin Mutations

The three identified *PGRN* frameshift mutations are predicted to cause the premature termination of the coding sequence which leads to degradation of the mutant *PGRN* mRNA by Non-sense

Mediated Decay (NMD) [169, 170]. The absence of mutant *PGRN* allele brings a state of haploinsufficiency that was demonstrated to be sufficient to give rise to FTLD [240]. Considering that the majority of *PGRN* pathogenic variations are frameshift null mutations, predicted to act through a mechanism of haploinsufficiency, it would be expected that associated clinical and pathological phenotypes were common to all these changes. Nevertheless, a variability in clinical manifestations (clinical phenotype, age of onset, illness duration, etc.) and neuropathological findings is reported in literature, even within the same family.

Despite the presence of the three mutations in probands relatives have not been molecularly confirmed but only presumed, the clinical phenotype disclosed by the affected individuals was very variable.

Both a wide range in age of onset (48-71) and illness duration (3-20) were observed (Table 23), probably because of incomplete or age-related penetrance of *PGRN* mutations, with a 95% of mutation carriers affected at the age 75 years [171].

Family	*Mutation*	*Clinical phenotype*	*Mean age at onset years (range)*	*Mean Disease duration years (range)*
F1	p.Phe86SerfsX170	FTD/AD	64 *	6 *
F2	p.Thr272SerfsX10	FTD/PD/md	61 (52-71)	15 (10-20)
F3	p.His400ThrfsX12	PNFA/md/ld	49 (48-50)	5 (3-7)

Table 23. Genetic and clinical characteristics of PGRN FTLD families.
*FTD, Frontotemporal Dementia; AD Alzheimer's Disease; PNFA Progressive Non-Fluent Aphasia; md, memory deficits; ld, language dysfunctions; PD, Parkinson Disease; * data available only for*

The clinical presentations associated to these mutations is highly heterogeneous, even within the same family, including Frontotemporal Dementia, Progressive Non-Fluent Aphasia, but also Alzheimer's Disease and Parkinson Disease. Language dysfunctions, encompassing impairment in phonetic verbal fluency, agrammatisms and reduction in spontaneous speech, represent a

prominent finding whether as onset symptoms (in F1 and F3 probands) or in later stages of the disorder (F2 proband) (Table 24). In the p.His400ThrfsX12 mutation carrier language deficits constitute the main symptom which undergoes a progressive deterioration during illness course, corresponding to clinical diagnostic criteria for PNFA syndrome. Behavioural changes are also common in the clinical presentations, especially in the form of apathetic state, carelessness and loss of interests, becoming relevant in the p.Phe86SerfsX170 and p.Thr272SerfsX10 mutation carriers to the point of fulfilling with clinical manifestations of FTD. The F3 proband manifested apathy from the first stages according to literature data where it represents the most prevalent behavioural change in PNFA-*PGRN* mutations carriers [249]. Another clinical feature in common to all three analyzed individuals is the loss of autonomy in daily life activities as has been above reported for AD-affected patients.

Table 24. Clinical presentation and illness evolution in PGRN mutation carriers probands.

Proband	*Mutation*	*Clinical diagnosis*	*Age of onset*	*Clinical presentation*	*Disease Evolution*	*Last Evaluation*
F1	p.Phe86SerfsX170	FTD	64	apathy, language impairment	cognitive decline, executive deficits, impairment of phonemic	behavioural changes, loss of autonomy
F2	p.Thr272SerfsX10	FTD	68	mild deficit in working memory and attention	cognitive decline, episodic temporal and spatial disorientation	apathy, impairment of phonemic, deficit in executive functions, loss of autonomy
F3	p.His400ThrfsX12	PNFA	49	language dysfunction, apathetic state	decline of language function, memory and attention	deficit in comprehension, behavioural changes, inhibition, loss of autonomy, death

Noteworthy are the first disease manifestations in p.Thr272SerfsX10 carrier, characterized by memory impairment and attentional deficits which have been lasted unchanged for some years falling within a clinical state of Mild Cognitive Impairment. That is, for a long time the patient was thought to be in the prodromal phase of Alzheimer's disease, indeed only after the appearance of frontal type symptoms and implementation of clinical informations with neuroimaging and genetic analyses, clinicians made a clinical diagnosis of FTD. This was further supported by detection of low PGRN protein levels in serum (45,42 ng/ml), which differed in a statistically significant manner from control values, well below the cutoff previously proposed

by Ghidoni et al. (a cutoff of 74.4 ng/ml separates *PGRN* mutation carriers from non carriers with a specificity and sensitivity of 100%) (Fig. 34) [154]. Find a MCI clinical phenotype in this patient did not surprise because, the p.Thr272SerfsX10 mutation has already been reported in more than 36 families associated with different syndromes, such as FTD, PNFA, CBD, FTD-MND, LBD and not least MCI and then AD. Other *PGRN* mutations have been described in patients with MCI, such as the variation c.388_391delCAGT (Gln130Serfsx125) identified in a case who then converted to Alzheimer's Disease and only subsequently disclosed behavioural changes and parkinsonian features characteristically observed in *PGRN* mutation carriers [250]. Therefore, these literature data and the results of this study further stress the importance and usefulness to have rapid, inexpensive and sensitive non-invasive tests able to identify biomarker of a specific type of dementia (as is the case of PGRN serum or plasma levels), to perform also in patient with an early atypical clinical presentation.

8.1.2.2 Microtubule associated protein tau mutation

The *MAPT* IVS10+16 C>T have been detected in more than 26 families, disclosing heterogeneous clinical presentations, including FTD, FTD combined with Parkinson Disease, FTD with AD and PSP. Considerable variations in age of onset (range 37-66 years) and illness duration (2-22 years) were described, also within the same family. This nucleotide variation, like other *MAPT* 5'-splice site exon 10 mutations, are predicted to disrupt a stem-loop that regulates alternative splicing of exon 10 causing a two- to six-fold increase in the ratio of 4R/3R tau isoforms (increased levels of exon 10+ RNA) which in turn result in a process of neurodegeneration, by a pathogenic mechanism not fully known [254, 246].

With regard to the F4 patient, in which this mutation was identified, the only possible consideration pertain to the age of onset (59 years) and duration of the disease (5 years) which

fall within the reported range of value. The clinical presentation is also typical of this MAPT mutation carriers, mainly characterized by behaviour disorders.

8.1.2.3 Chromosome 9p-linked FTD-MND family

A linkage to 9p21.3-13.3 locus on chromosome 9 was detected in a FTD-MND Italian kindred with five affected individuals over two generations (Fig. 40). A few clinical informations about deceased family members were collected from the only healthy individuals (II.3) whereas the proband and his two affected siblings were visited by clinicians at G.B. Rossi Hospital.

Table 25. Clinical features in affected individuals

Individuals	*Age of onset*	*Disease duration*	*Clinical presentation*
I.2	63	2	cognitive decline
II.2	50	4	Alzheimer's Disease
II.4	62	6	cognitive decline, executive dysfunctions, language impairment
II.5	56	10	memory deficit, depression, mutism, loss of autonomy
II.6	48	10	parkinsonian syndrome, cognitive decline, memory deficit, absence of criticism, loss of autonomy

The clinical phenotypes within this family was very variable including not only FTD with MND (in the proband) but also atypical presentations characterized by AD-like syndrome, where memory deficit represents the recurrent manifestation also in disease evolution (individuals II.2 and II.5) (Table 25). This is in contrast to clinical findings described in 27 already reported chromosome 9p-linked families, where the main presenting features encompass MND with or without FTD and executive dysfunctions [278, 251-257]. Despite not all clinical manifestations fit with diagnostic criteria for FTD or MND, the mean age of onset (55.8 years) and disease duration (6,4 years) observed in affected individuals were within the range reported in literature (onset: 42.2-60.3; duration: 3-8,6). Furthermore, post-mortem examination of proband brain

disclosed neuropathological characteristics of FTLD-TDP subtype which is the only pathological pattern nowadays reported in FTD-MND chromosome 9p-linked patients. Besides this finding, also microsatellite and haplotype analyses performed in DNA samples of the two affected and the one unaffected alive siblings are compatible with linkage of this family to the 9p21.3-13.3 locus on chromosome 9. Unfortunately, given the data limitations, it was not possible to reduce the linked region in order to identify the candidate disease gene. The only certain thing is that haplotypes shared by the two affected siblings differ from that identified in the Belgian FTD-MND chromosome 9-linked families that have been analyzed by the same research group in Antwerp [253]. This means that the disease in Italian and Belgian families is most likely caused by different mutations of the same not yet identified gene. In none of the 10 already reported papers about this topic the candidate disease gene was identified in spite of the entire coding region mapping in this locus has been almost completely sequenced. These results may suggest that the pathogenic mechanism may relay on variations in gene or protein expression due to genetic defects localized in non-coding regulatory genome regions as guessed by Pearson et al [257].

8.2 CADASIL

8.2.1 *NOTCH3* Mutational analysis

Twenty-one different *NOTCH3* mutations were identified in 22 pedigrees with an autosomal dominant inheritance and 31 unrelated index cases. Seven mutations were not previously reported (Table 19). Fifteen patients had a mutation in exon 4 which accounted for 28,3% in this series confirming its role as a mutational hot spot although its frequency was lower than those reported by Oberstein et al (50%), Joutel et al (55%), Peters et al (58%) and Markus et al (73%). The second most frequent mutation site in this study was exon 19 (24,53%) followed by exon 7

(20,75%). These data confirm the wide variability in the mutational map of *NOTCH3* indeed, the second mutational hot spot was represented by exon 3 in French, German and British series and exon 11 in Dutch series [258-261]. These differences point out the heterogeneity in mutations distribution along the gene, that may reflect a different history of the populations and might be related to the different geographical areas (founder effect) where the mutations appeared for the first time. In fact differences in the geographical distribution of the mutations can also be observed within the same country as the case of Italian sample here reported. Mutational frequencies markedly diverge depending on the living Region of mutation carriers. In the study of Ungaro et al, *NOTCH3* screening was performed on patients from South-Italy where exon 3 represented the mutational hot spot (8 families out of 30 analyzed) followed by exon 8 (4/30) and exon 4 and 22 (4/30) [262].

In Dotti et al series, including patients from Central- and South-Italy, the most mutated exons were exon 11 (21,4%) followed by exons 3 and 4 (17,8%) and exon 8 (14,3%) [263]. CADASIL subjects from more or less the same geographical areas were analyzed by Cappelli et al but, obtained results were different indeed, exon 19 was the most affected exon with a unique mutation, R1006C, recurring in ten out of fifteen analyzed families [264]. This result was explained by the finding that all those families originated in a restricted geographical area near Ascoli Piceno (Region Marche, Central-Italy). In the series reported by Bianchi et al, exon 10 showed an high mutational frequency (11%), representing the second hot spot site in Central-Italy [265]. The results of Cappelli and Bianchi are confirmed by the study herein reported where nine out of twelve R1006C carriers and the two exon10 G528C affected unrelated individuals come from Central-Italy (4 from Chieti and 7 from Ascoli Piceno). In this series a differential distribution of mutation between North-East and North-West Italy was also observed: while in North-East two clusters, exon 4 (in 11 out of 29 index cases from thus area) and exon 7 (10 out

of 29) have been , in North-West mutation were widespread across several exons (exon 4, 19, 22, 5, 6 and 7). Interestingly, the novel S396C mutation was identified in patients originated in a restricted geographical area of Region Veneto (5 families and 5 unrelated index cases from the neighboring provinces of Verona, Vicenza, Padua, Treviso and Venice in North-East) suggesting a common ancestor and hence a possible founder effect as previously demonstrated for the R133C mutation in 18 Finnish families [266] and, as was postulated for the R1006C mutation in Central-Italy [264].

8.2.2 NOTCH3 haplotypes analysis

Each of the reported mutations was linked to an haplotype by following the segregation of the mutation (see Appendix 1-6) and the haplotype in the pedigrees or by probabilistic methods in the unrelated affected individuals. Sixteen of the 21 mutations were linked to the most common haplotype H1.

Mutation Arg141Cys was found to be linked to haplotype H5 (tgcct) in two pedigrees and might be linked to haplotype H1 (cgcct) in one unrelated affected individual that however was heterozygote for 3 SNPs and incompatible for carrying H5 haplotype. Since haplotype H1 and H5 differ for the allele at marker rs3815188 it is plausible that mutation Arg141Cys arose once on haplotype H1 or H5 and that the chromosome carrying the mutation underwent to an intragenic recombination. Despite this speculation, since this NOTCH3 variation was also observed in Chinese affected individuals [267], it can not be excluded that it is an old mutation or more likely that has arisen several times during human history.

Mutation Arg207Cys was linked to haplotype H1 and to other haplotypes since it was found in affected individuals homozygote for the allele opposite to the one contained in the haplotype H1

at marker rs10423702. This mutation has also been described in the Chinese population [267] suggesting that it might have arosen several times in several populations due to independet mutational events.

The novel mutation Ser396Cys was found in individuals from North-Eastern Italy and resulted to be linked either to haplotype H1(cgcct) or haplotype H2(cgccc). Since haplotype H1 and H2 differ for the allele at marker rs1044009 we can argue that mutation Ser396Cys arose once on haplotype H1 or H2 and that the chromosome carrying the mutation underwent an intragenic recombination. This would indicate that mutation Ser396Cys is an old mutation typical of individuals from Northen Italy.

Overall while a few variations were observed in minor haplotypes (H2, H4, H5 and H9), many of the identified mutations are linked to the most common haplotype H1; for this reason a founder effect was not confirmed even though it is compatible. Moreover, 16 mutations were found to be linked to haplotype H1 and this is uncertain for other 3 mutations (R141C, R207C e S396C). Assuming the less stringent hypothesis that 16 over 21 mutations were linked only to haplotype H1, having a frequency equal to 54% (see Table 21) in the general population (estimated from the 50 non affected individuals), haplotype H1 presents more mutations than expected by chance ($p=0.029$). However, this intruding hypothesis should be investigated in a larger sample to be confirmed.

8.2.3 Diagnostic yield of skin biopsy

GOM deposits were identified in all 16 available skin biopsies in patients with a *NOTCH3* mutation causing an odd number of cysteine residues, with a 100% of both specificity and sensitivity. This last value differs from data reported by Markus et al. and Malandrini et al. who

found a lower sensitivity (45% and 57% respectively) [258, 268] whereas it is in agreement with other reports [268-271]. The explanations for these divergences are unclear since no relationship have been detected between the presence or absence of GOM and age [258]. Furthermore, no variations in GOM amount were observed among different *NOTCH3* mutations [260], nor correlations with disease progression [258, 268]. A plausible explanation may relay on a methodological limit intrinsic to skin biopsy: the deepness of biopsy influences the number of useful observable vessels. Recent published data emphasize the necessity to mainly investigate the presence of GOM in arterioles rather than vein or capillaries where they are not always detectable [271]. Moreover, if the first examination is negative, it is important to repeat the investigation in additional vessels since GOM deposition may be a focal process. Scalpel skin biopsy performed in this study is deeper than the punch biopsy reported in other studies [258], providing a higher number of analyzable dermal small arterioles, maybe explaining the high observed sensitivity without excluding a possible sample size effect.

8.2.4 *NOTCH3* frameshift mutation

The *NOTCH3* c.3057delG frameshift mutation (p.Gly994AlafsX277) is predicted to introduce a premature stop codon in mRNA which is probably degraded by a mechanism of NMD. This may indirectly imply that the mutant allele does not exert a negative effect inducing the vessels pathological changes usually detected on skin biopsy electron microscopy of *NOTCH3* mutation carriers. Actually, no GOM deposits were identified in several examinations (more than ten vessels) and in two different skin biopsies, apparently excluding a CADASIL diagnosis. In agreement with this finding, clinical presentation and neuroimaging pattern assessed in this patient were not fully comparable with CADASIL diagnostic criteria: recurrent headache not migraine and a few small subcortical signal alterations on brain MRI not properly specific of

CADASIL. Even family history had disclosed the occurrence of cognitive decline but not stroke or TIA (suggestive of CADASIL). These findings, together seem to exclude a pathogenic role for this variation, further supported by literature data where the only few reported *NOTCH3* deletions are small in-frame deletions, identified in patients with typical clinical and neuroradiological CADASIL presentations, which are predicted to cause the deletion and loss of one cysteine residue [272].

9. Conclusions

9.1 AD and FTLD

9.1.1 Alzheimer's Disease

PSEN2 mutations are considered the rarest cause of familial Early-Onset AD. Several *PSEN2* non-synonymous nucleotide variations whose pathogenetic role is unclear are reported in literature. The result described in this study diverge from literature because they show a more likely pathogenic role for some of the already reported variations, giving *PSEN2* a higher mutational frequency. If these data were not reflected in functional analysis (Aβ42/40 ratio) or replicated in larger sample, these substitutions might act as risk factors rather then pathogenic mutations. That is, these aminoacid replacements, which do not appear to be neutral polymorphisms, might be associated with familial Late-Onset AD, promoting its manifestation (as in the case of *APOE*).

9.1.2 Frontotemporal Lobar Degeneration

The mutational screening of FTLD-associated genes confirmed the genetic heterogeneity of this disorder. The detected mutational frequencies are consistent with literature data, confirming *PGRN* and *MAPT* gene as the main causes of familial FTLD (with *PGRN* mutations more frequent than in *MAPT*). This genetic heterogeneity is further emphasized by the failure to find pathogenic mutations in familial cases of FTLD and by the identification of a family linkaged to chromosome 9; data implying the existence of other FTLD genes not yet identified. In addition to genetic heterogeneity, also observed clinical phenotypes were variable (even within the same family), overlapping with parkinsonism- and AD-like syndromes. Finally, the availability of a serum sample for a patient with a *PGRN* frameshift mutation stressed the utility to assess a

peripheral marker as an indirect indicator of a degenerative process of the central nervous system. Quantification of PGRN serum levels represents a fast and reliable tool to identify *PGRN* mutation carriers and to exclude or confirm the pathogenic role of non-frameshift variations which therefore, might escape a mechanism of action based on a state of haploinsufficiency.

On the basis of obtained results and, in particular, considering the low mutational yield of AD- and FTLD-associated genes (whose mutations accounted for less than 4% of entire series), two diagnostic algorithms (Fig. 50 and 51) are proposed below for the selection of a small group of patients highly suggestive of a genetic basis. These algorithms might help to refine the clinical diagnosis in early stages of these disorders, which represents the starting point for the application of future therapeutic treatments.

The starting point of these algorithms is the clinical diagnosis (as a result of the integration of several informations derived from the neurological examination, neuropsychological tests and neuroimaging) of AD or FTLD. The crucial factor in choosing whether to refer a patient for genetic analysis is the family history for dementia and, in particular, the presence of a pattern of autosomal dominant inheritance within the family.

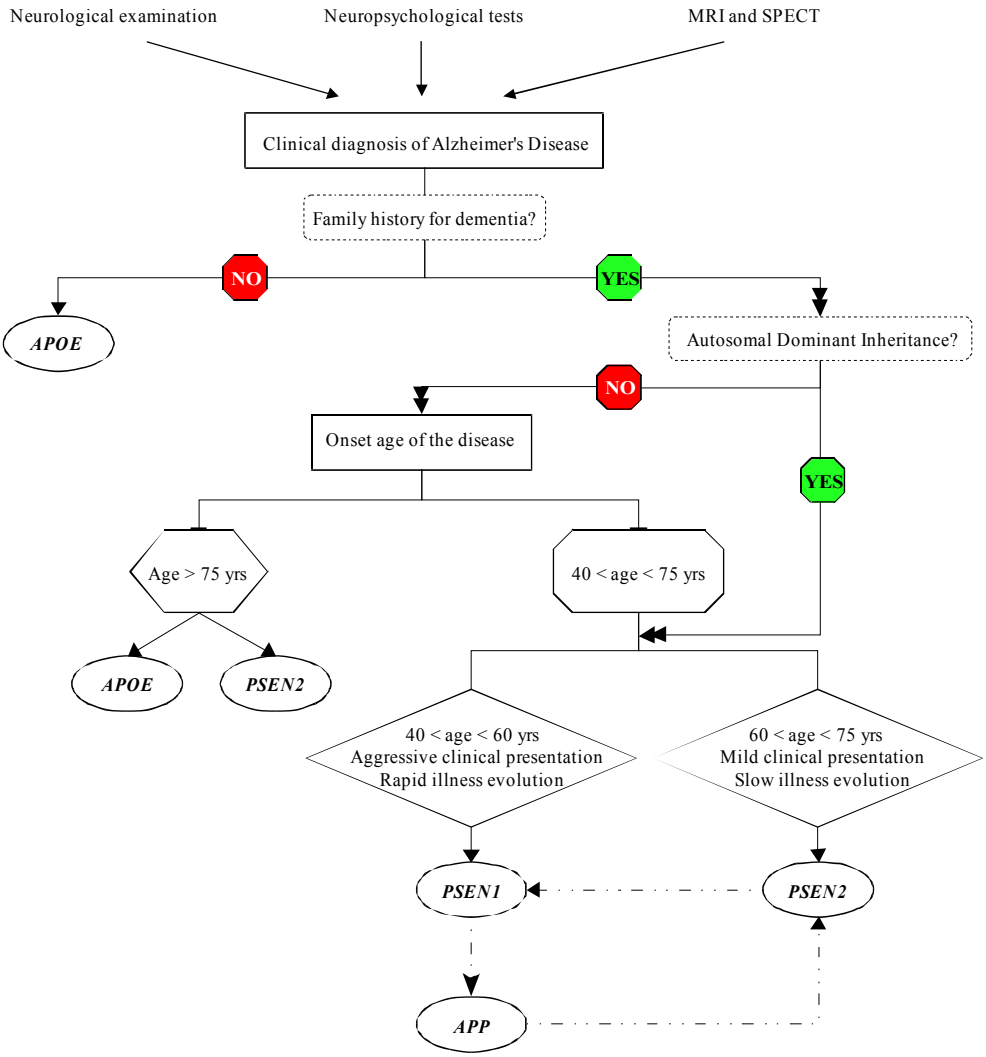

Fig. 50. Alzheimer's Disease diagnostic algorithm for genetic testing.
Abbreviations: MRI, Magnetic Resonance Imaging; SPECT; Single Photon Emission Computed Tomography; APOE, Apolipoprotein E; PSEN1, Presenilin1; PSEN2, Presenilin2; APP, Amyloid Precursor Protein; dashed arrows; genes being analyzed if no mutation is identified in the preceding.

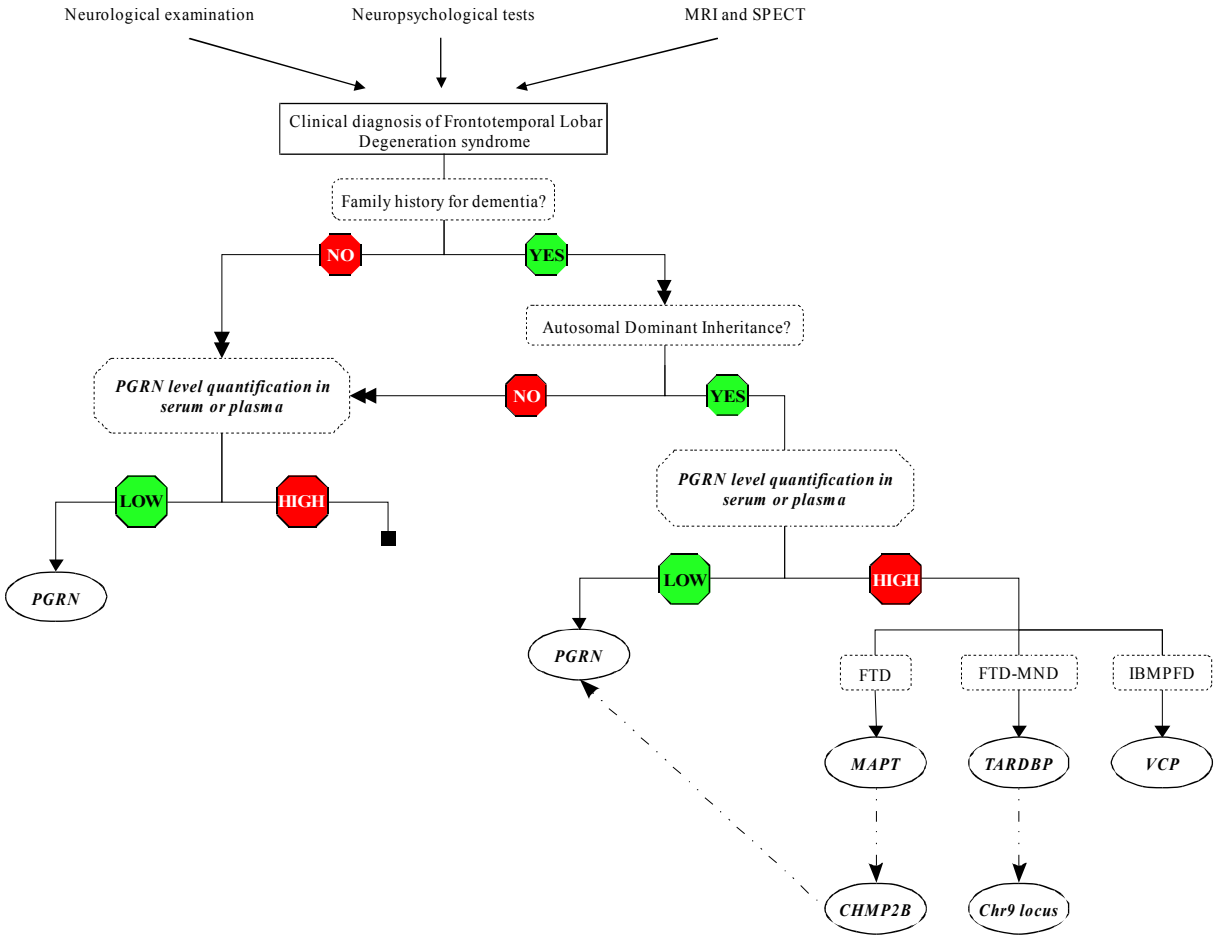

Fig. 51. Frontotemporal Lobar Degeneration diagnostic algorithm for genetic testing.
Abbreviations: MRI, Magnetic Resonance Imaging; SPECT; Single Photon Emission Computed Tomography; PGRN, Progranulin; MAPT, Microtubule Associated Protein Tau; TARDBP, TAR DNA Binding Protein; VCP, Valosin Containing Protein; CHMP2B, Charged Multivesicular Body Protein 2B; Chr, chromosome; FTD, Frontotemporal Dementia; MND, Motor Neuron Disease; IBMPFD; Inclusion Body Myopathy with Paget's Disease of Bone and Frontotemporal Dementia; dashed

9.2 CADASIL

The results of *NOTCH3* mutational analysis showed a wide variation in the distribution of mutations along the gene; heterogeneity observed either within the same population or in comparison to others (French, German, British, Dutch, Italian). In Italy, in particular, there is a clustering of mutations which affect distinct exons in patients living in different geographical areas. For this reason is difficult to define a sole diagnostic algorithm but, the best genetic approach is the one that takes into account these differences (Fig. 52). This reduces the substantial costs that would incur if all *NOTCH3* exons were analyzed. In patients with a negative result at first genetic screening, the analysis extension to other exons may be taken into account in pedigree with a clear pattern of Mendelian inheritance of the disease, after the identification of GOM deposits in skin biopsy that closely correlate with the presence of *NOTCH3* mutations.

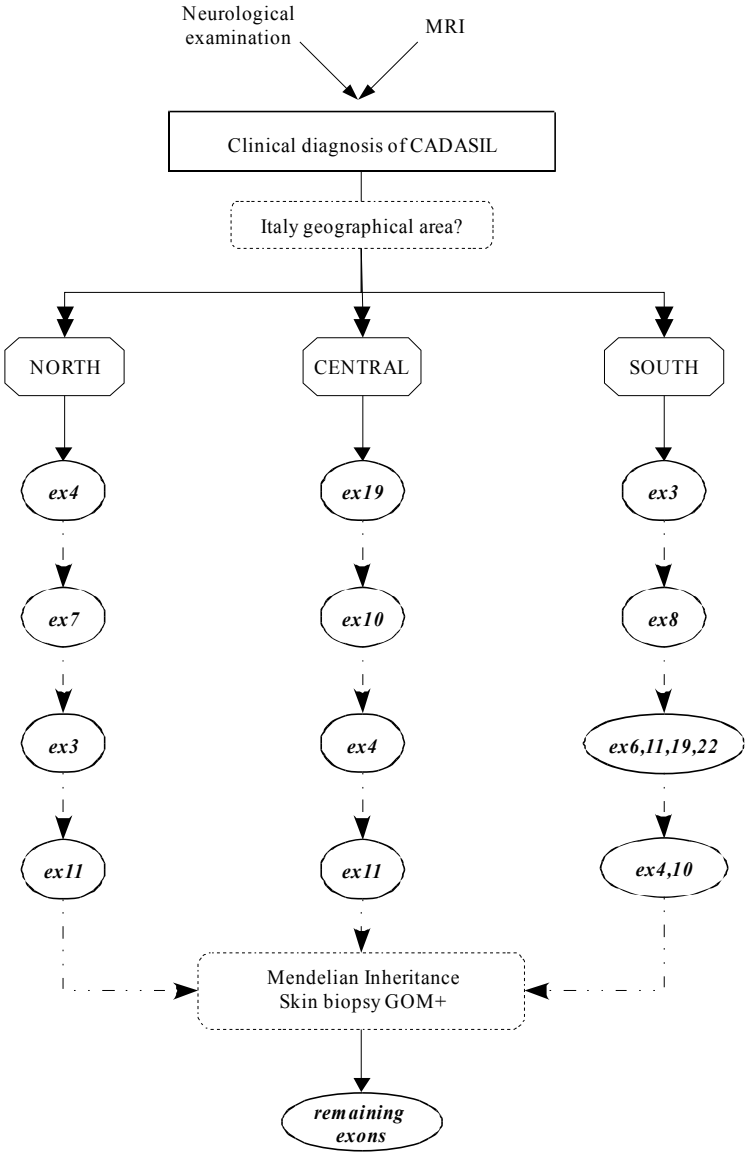

Fig. 52. CADASIL diagnostic algorithm for genetic testing.
Abbreviations: MRI, Magnetic Resonance Imaging; ex, exon; GOM, Granular osmiophilic Material; dashed arrows; genes being analyzed if no mutation is identified in the preceding

Appendix 1: *cerebral lobes*

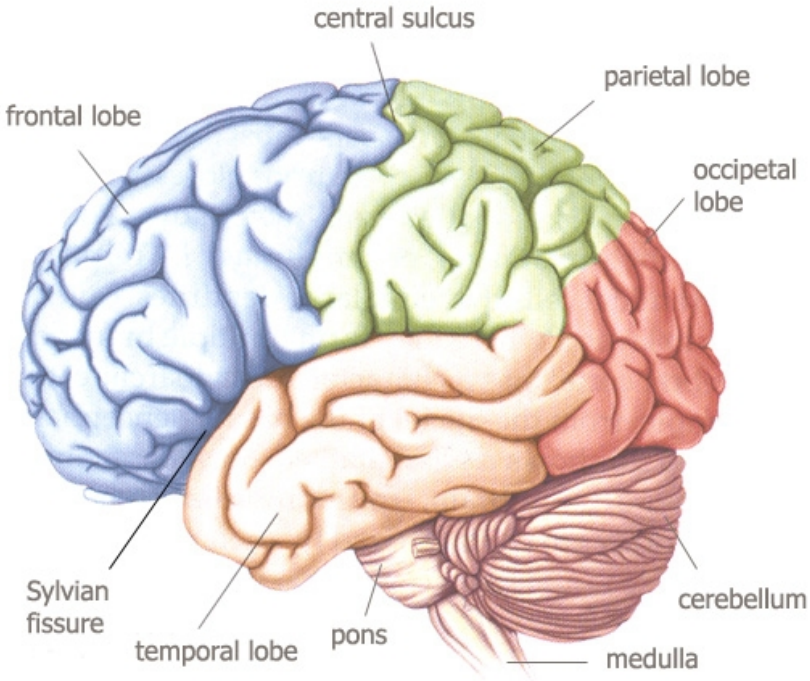

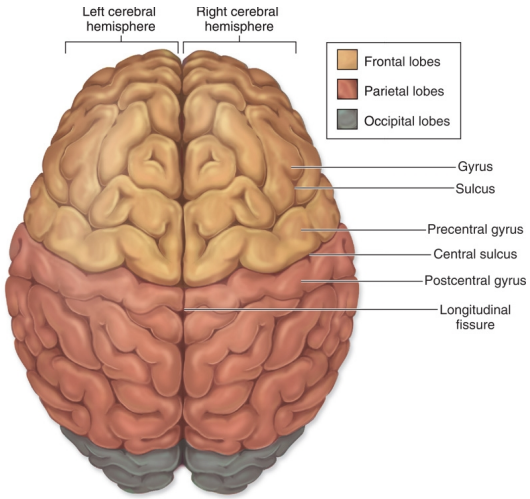

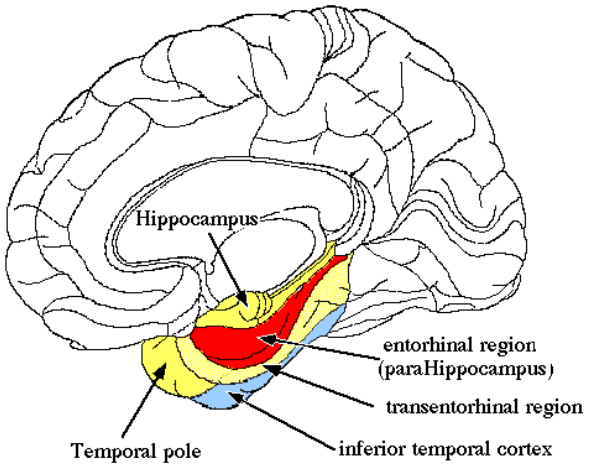

Appendix 2: haplotype reconstruction for CADASIL families

CAD13: R133C

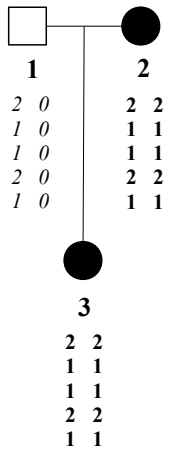

CAD12: R141C

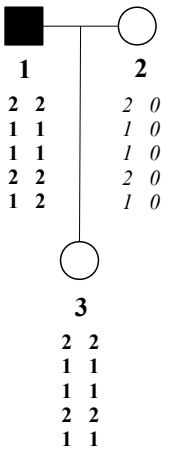

CAD19: C146R

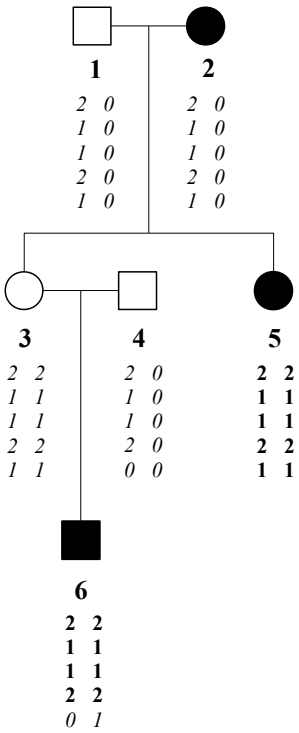

CAD2: C146R

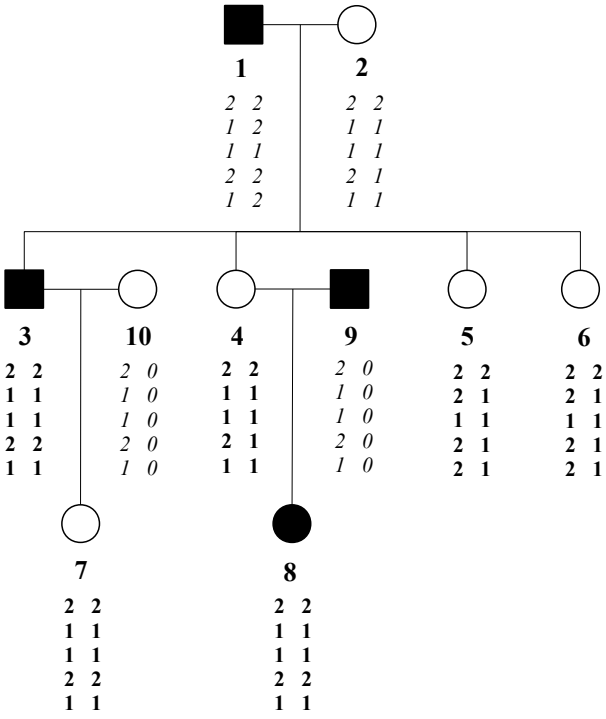

Legend

The circles indicate females; squares, male; black symbols, affected family members; grey symbols, affected status not available; CAD followed by a number, CADASIL families for which haplotype was reconstructed. Inferred haplotypes are reported in italic character.

CAD1: C146R

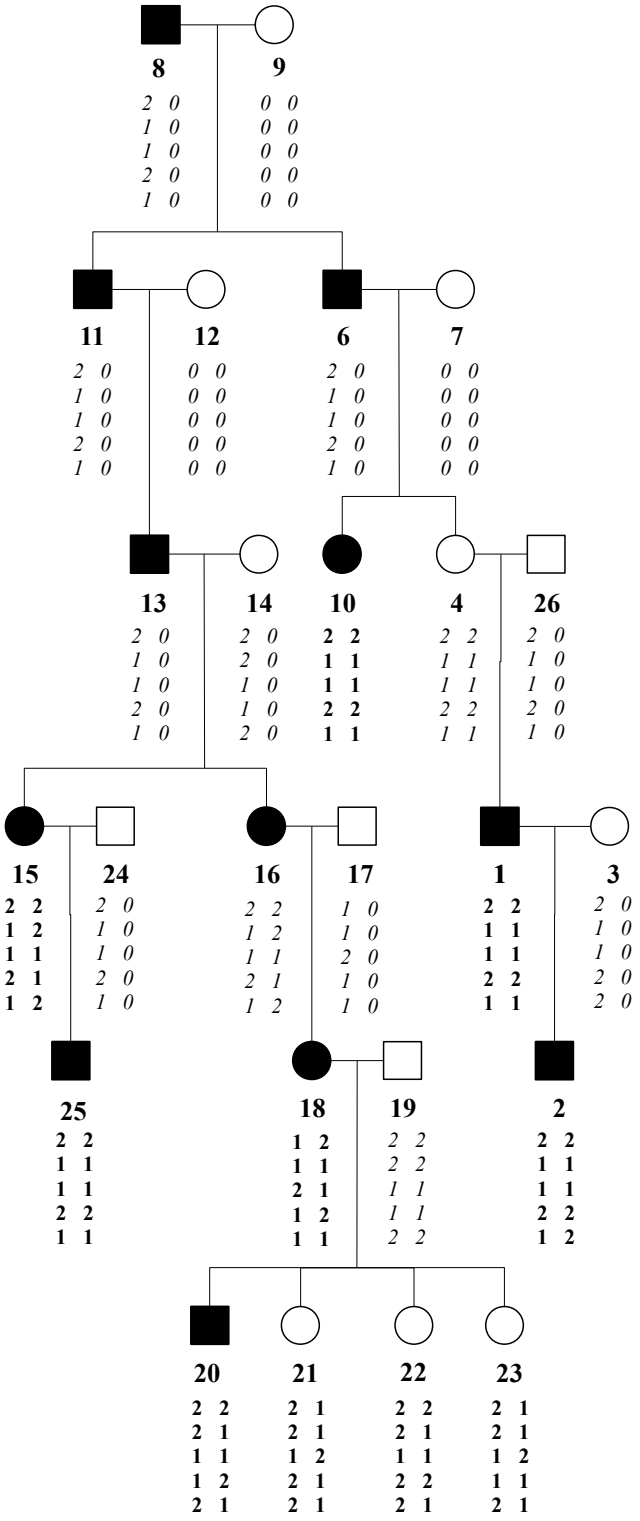
8
2 0
1 0
1 0
2 0
1 0
9
0 0
0 0
0 0
0 0
0 0
11
2 0
1 0
1 0
2 0
1 0
12
0 0
0 0
0 0
0 0
0 0
6
2 0
1 0
1 0
2 0
1 0
7
0 0
0 0
0 0
0 0
0 0
13
2 0
1 0
1 0
2 0
1 0
14
2 0
2 0
1 0
1 0
2 0
10
2 2
1 1
1 1
2 2
1 1
4
2 2
1 1
1 1
2 2
1 1
26
2 0
1 0
1 0
2 0
1 0
15
2 2
1 2
1 1
2 1
1 2
24
2 0
1 0
1 0
2 0
1 0
16
2 2
1 2
1 1
2 1
1 2
17
1 0
1 0
2 0
1 0
1 0
1
2 2
1 1
1 1
2 2
1 1
3
2 0
1 0
1 0
2 0
2 0
25
2 2
1 1
1 1
2 2
1 1
18
1 2
1 1
2 1
1 2
1 1
19
2 2
2 2
1 1
1 1
2 2
2
2 2
1 1
1 1
2 2
1 2
20
2 2
2 1
1 1
1 2
2 1
21
2 1
2 1
1 2
2 1
2 1
22
2 2
2 1
1 1
2 2
2 1
23
2 1
2 1
1 2
1 1
2 1

CAD11: C174Y

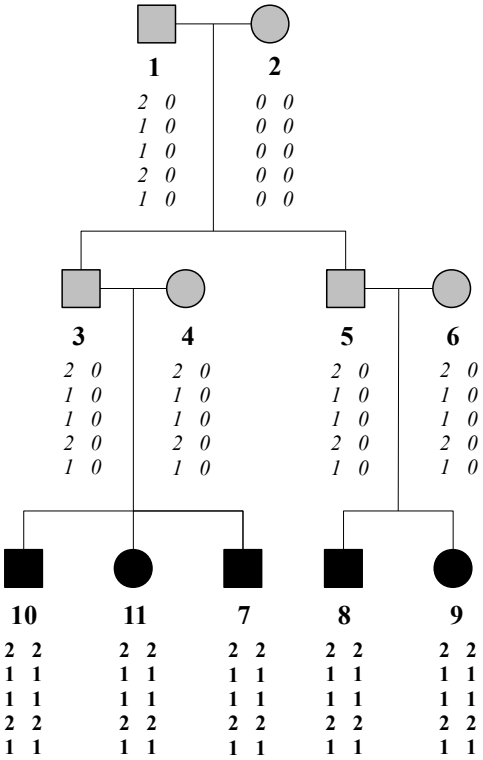

CAD14: C201R

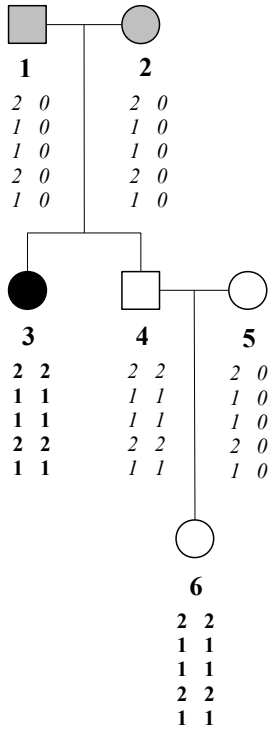

CAD10: C201R

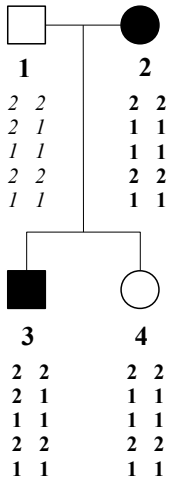

CAD4: S396C

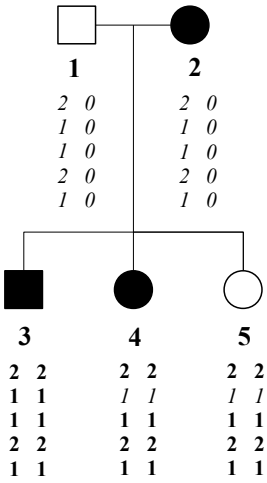

CAD17: S396C

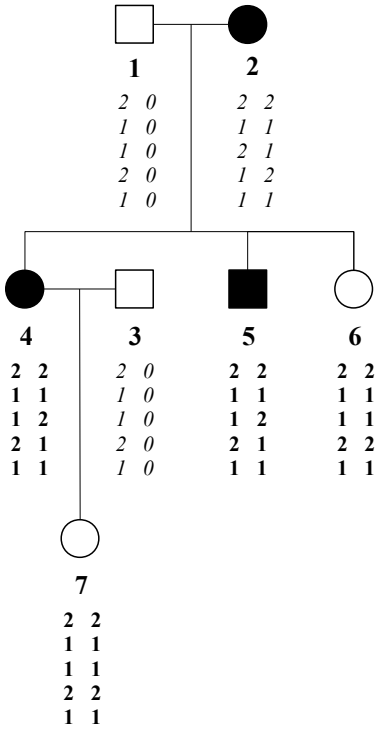

CAD20: S396C

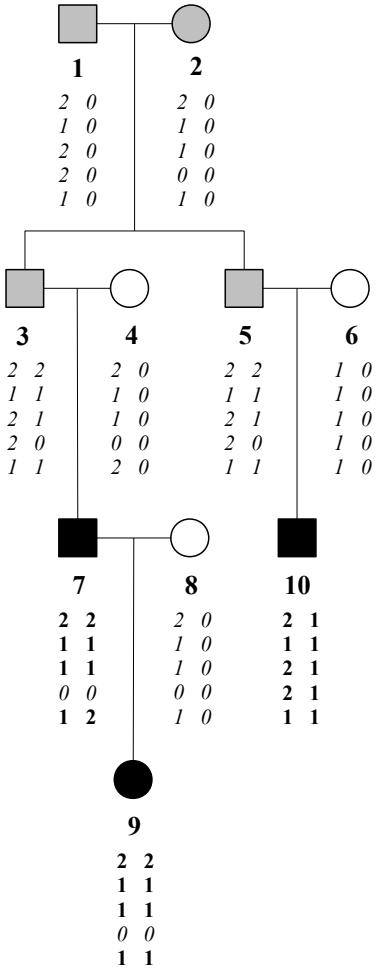

CAD3: S396C

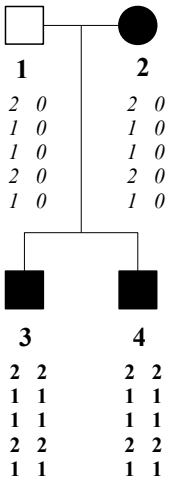

CAD16: S396C

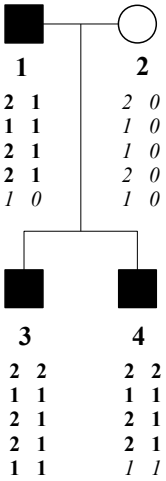

CAD18: R592C

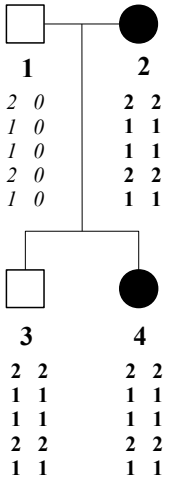

CAD8: G528C

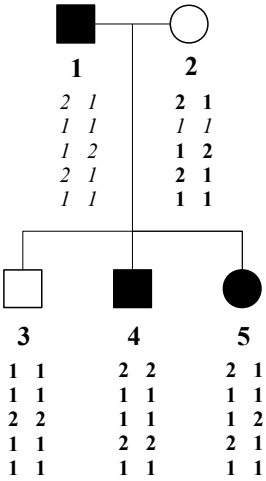

CAD15: R607C

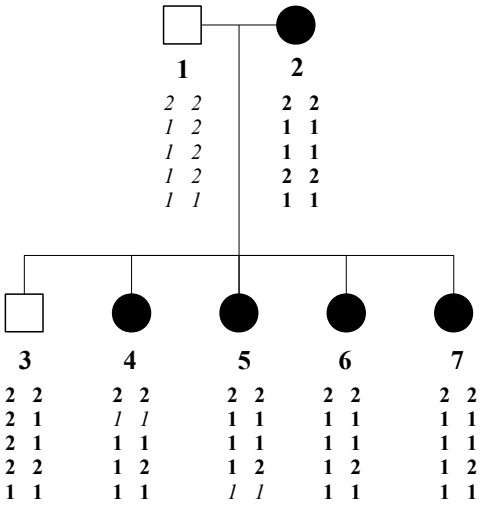

CAD9: R1006C

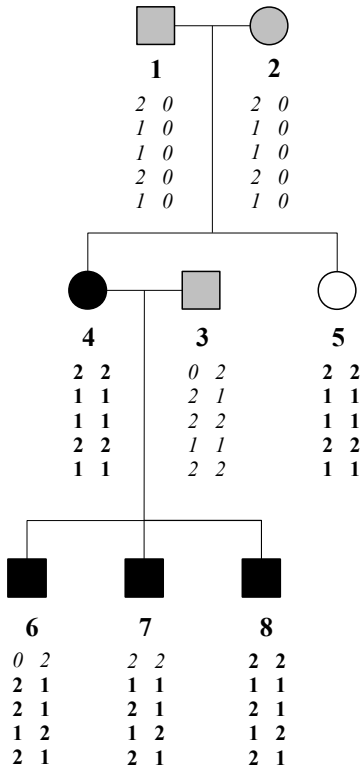

CAD6: R1006C

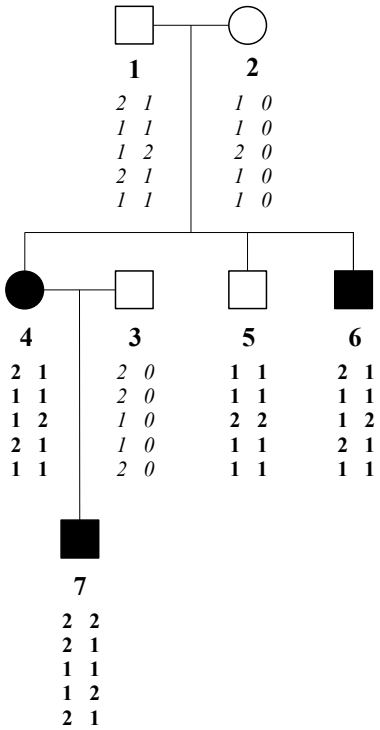

CAD7: R1006C

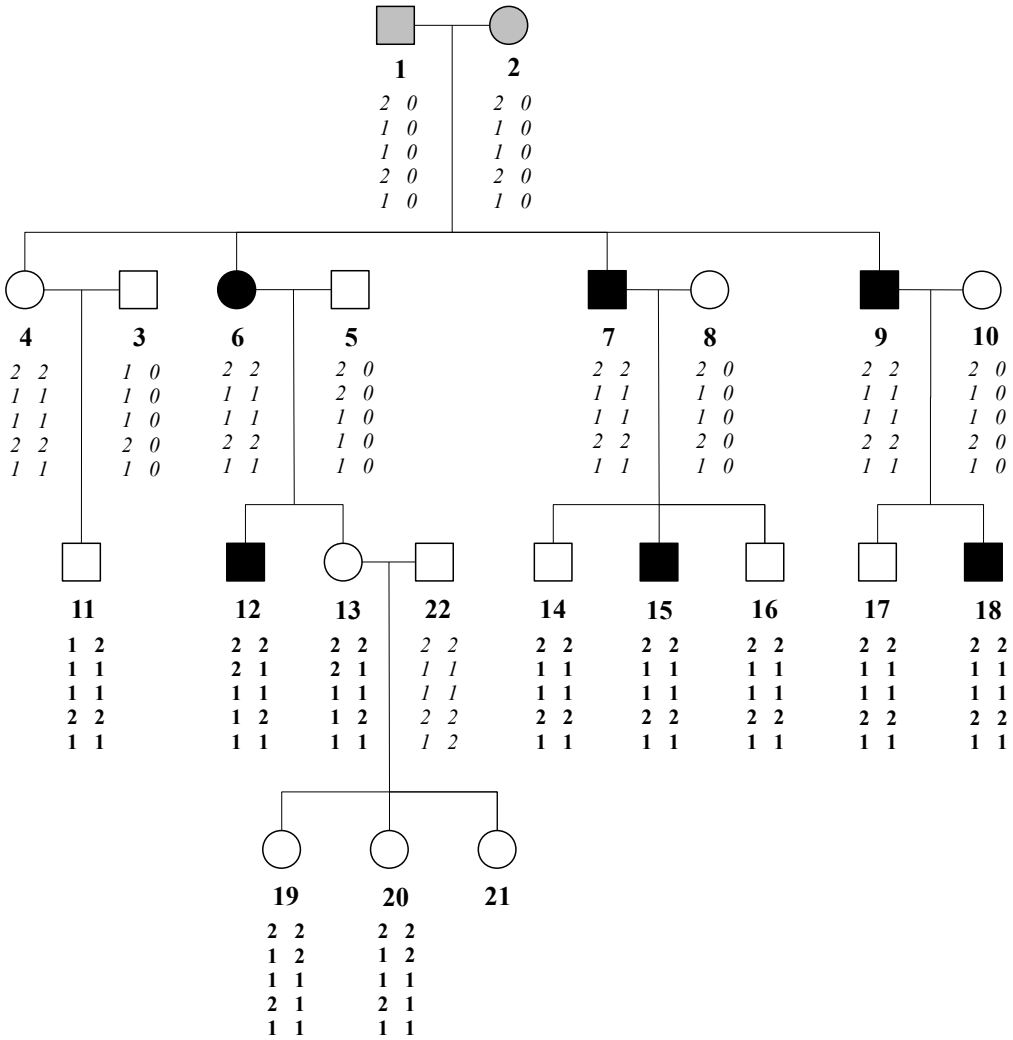
1
2 0
1 0
1 0
2 0
1 0
2
2 0
1 0
1 0
2 0
1 0
4
2 2
1 1
1 1
2 2
1 1
3
1 0
1 0
1 0
2 0
1 0
6
2 2
1 1
1 1
2 2
1 1
5
2 0
2 0
1 0
1 0
1 0
7
2 2
1 1
1 1
2 2
1 1
8
2 0
1 0
1 0
2 0
1 0
9
2 2
1 1
1 1
2 2
1 1
10
2 0
1 0
1 0
2 0
1 0
11
1 2
1 1
1 1
2 2
1 1
12
2 2
2 1
1 1
1 2
1 1
13
2 2
2 1
1 1
1 2
1 1
22
2 2
1 1
1 1
2 2
1 2
14
2 2
1 1
1 1
2 2
1 1
15
2 2
1 1
1 1
2 2
1 1
16
2 2
1 1
1 1
2 2
1 1
17
2 2
1 1
1 1
2 2
1 1
18
2 2
1 1
1 1
2 2
1 1
19
2 2
1 2
1 1
2 1
1 1
20
2 2
1 2
1 1
2 1
1 1
21

CAD5: R1006C

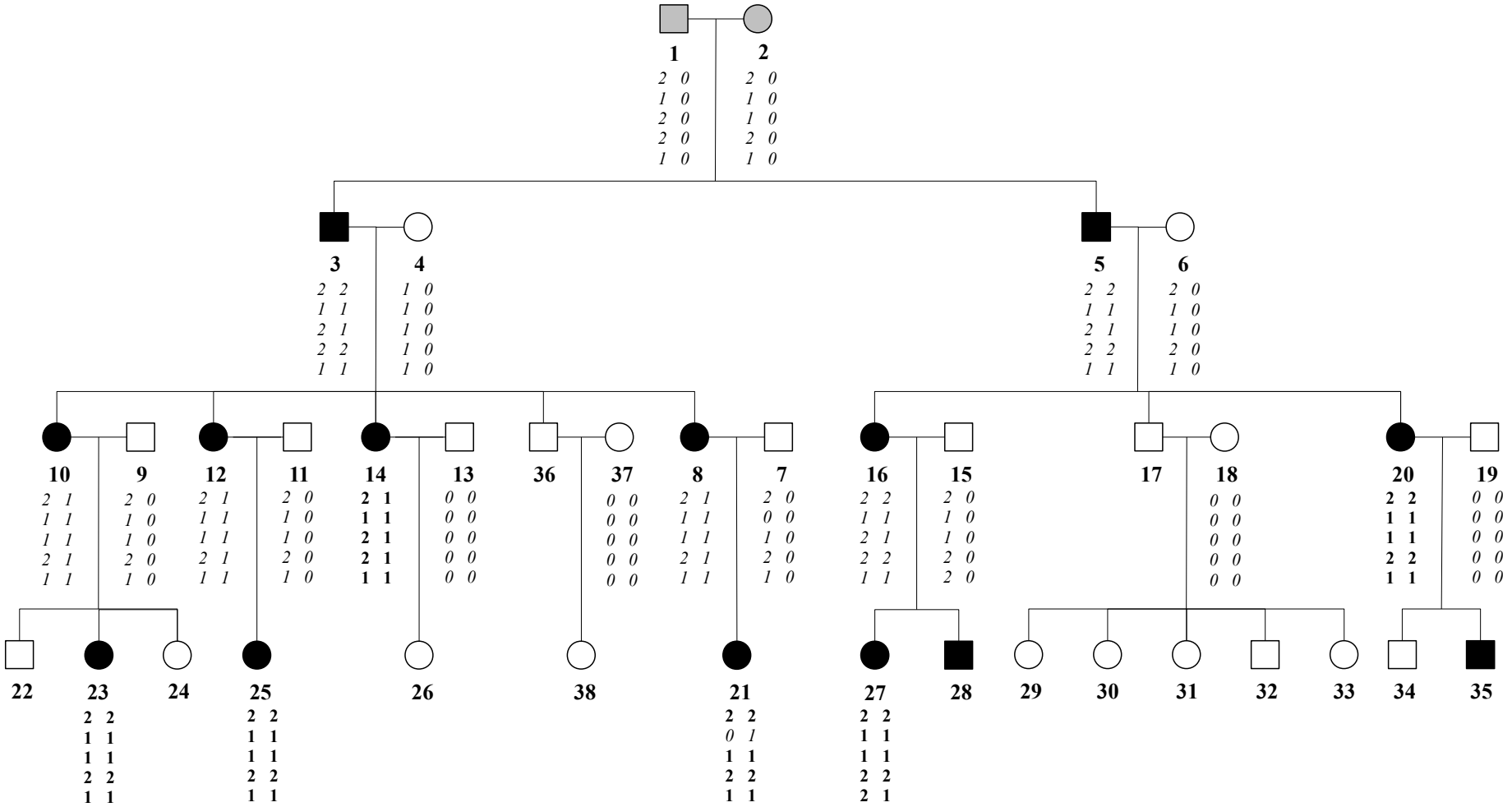
1
2 0
1 0
2 0
2 0
1 0
2
2 0
1 0
1 0
2 0
1 0
3
2 2
1 1
2 1
2 2
1 1
4
1 0
1 0
1 0
1 0
1 0
5
2 2
1 1
2 1
2 2
1 1
6
2 0
1 0
1 0
2 0
1 0
10
2 1
1 1
1 1
2 1
1 1
9
2 0
1 0
1 0
2 0
1 0
12
2 1
1 1
1 1
2 1
1 1
11
2 0
1 0
1 0
2 0
1 0
14
2 1
1 1
2 1
2 1
1 1
13
0 0
0 0
0 0
0 0
0 0
36
37
0 0
0 0
0 0
0 0
0 0
8
2 1
1 1
1 1
2 1
1 1
7
2 0
0 0
1 0
2 0
1 0
16
2 2
1 1
2 1
2 2
1 1
15
2 0
1 0
1 0
2 0
2 0
17
18
0 0
0 0
0 0
0 0
0 0
20
2 2
1 1
1 1
2 2
1 1
19
0 0
0 0
0 0
0 0
0 0
22
23
2 2
1 1
1 1
2 2
1 1
24
25
2 2
1 1
1 1
2 2
1 1
26
38
21
2 2
0 1
1 1
2 2
1 1
27
2 2
1 1
1 1
2 2
2 1
28
29
30
31
32
33
34
35

Bibliography

[1] Kraepelin E. Lehrbuch der Psychiatrie. 4th ed. Leipzig: Abel Meixner; 1893.

[2] Mayer-Gross W, Guttmann K. Schema for the examination of organic cases. *J Ment Sci.* 1937;83:440-51.

[3] World Health Organization. ICD-10, World Health Organization Tenth Revision of the International Classification of Diseases. Geneva: WHO; 1992.

[4] Gustafson L, Hagberg B. Dementia with onset in the presenile period. A crosssectional study. *Acta Psychiatr Scand Suppl.* 1975;257:3-71.

[5] Gustafson L, Hagberg B. Dementia with onset in the presenile period. A crosssectional study. *Acta Psychiatr Scand Suppl.* 1975;257:3-71.

[6] Reisberg B, Ferris SH, de Leon MJ, Crook T. The Global Deterioration Scale for assessment of primary degenerative dementia. *Am J Psychiatry.* 1982;139: 1136-9.

[7] Fratiglioni L, De Ronchi D, Aguero-Torres H. Worldwide prevalence and incidence of dementia. *Drugs Aging.* 1999;15:365-75.

[8] Riedel-Heller SG, Busse A, Aurich C, Matschinger H, Angermeyer MC. Incidence of dementia according to DSM-III-R and ICD-10: results of the Leipzig Longitudinal Study of the Aged (LEILA75+), Part 2. *Br J Psychiatry* 2001;179:255-60; 40.

[9] Ruitenberg A, Ott A, van Swieten JC, Hofman A, Breteler MM. Incidence of dementia: does gender make a difference? *Neurobiol Aging.* 2001;22:575-80.

[10] Wimo A, Winblad B, Aguero-Torres H, von Strauss E. The magnitude of dementia occurrence in the world. *Alzheimer Dis Assoc Disord.* 2003;17:63-7.

[11] Brookmeyer R, Corrada MM, Curriero FC, Kawas C. Survival following a diagnosis of Alzheimer disease. *Arch Neurol.* 2002;59:1764-7.

[12] Hui JS, Wilson RS, Bennett DA, Bienias JL, Gilley DW, Evans DA. Rate of cognitive

decline and mortality in Alzheimer's disease. *Neurology.* 2003; 61:1356-61.

[13] Banerjee S, Murray J, Foley B, Atkins L, Schneider J, Mann A. Predictors of institutionalisation in people with dementia. *J Neurol Neurosurg Psychiatry.* 2003;74:1315-6.

[14] Frikke-Schmidt R, Nordestgaard BG, Thudium D, Moes Gronholdt ML, Tybjaerg-Hansen A. APOE genotype predicts AD and other dementia but not ischemic cerebrovascular disease. *Neurology.* 2001;56:194-200.

[15] Myers RH, Schaefer EJ, Wilson PW, D'Agostino R, Ordovas JM, Espino A, et al. Apolipoprotein E epsilon4 association with dementia in a population-based study: The Framingham study. *Neurology.* 1996;46:673-7.

[16] Hebert LE, Scherr PA, Beckett LA, Funkenstein HH, Albert MS, Chown MJ, et al. Relation of smoking and alcohol consumption to incident Alzheimer's disease. *Am J Epidemiol.* 1992;135:347-55.

[17] Ott A, Slooter AJ, Hofman A, van Harskamp F, Witteman JC, Van Broeckhoven C, et al. Smoking and risk of dementia and Alzheimer's disease in a population-based cohort study: the Rotterdam Study. *Lancet.* 1998;351:1840-3.

[18] Tyas SL, White LR, Petrovitch H, Webster Ross G, Foley DJ, Heimovitz HK, et al. Mid-life smoking and late-life dementia: the Honolulu-Asia Aging Study. *Neurobiol Aging.* 2003;24:589-96.

[19] Anttila T, Helkala EL, Viitanen M, Kareholt I, Fratiglioni L, Winblad B, et al. Alcohol drinking in middle age and subsequent risk of mild cognitive impairment and dementia in old age: a prospective population based study. *BMJ.* 2004;329:539.

[20] Ott A, Stolk RP, van Harskamp F, Pols HA, Hofman A, Breteler MM. Diabetes mellitus and the risk of dementia: The Rotterdam Study. *Neurology.* 1999;53:1937-42.

[21] Peila R, Rodriguez BL, Launer LJ. Type 2 diabetes, APOE gene, and the risk for dementia

and related pathologies: The Honolulu-Asia Aging Study. *Diabetes.* 2002;51:1256-62.

[22] Schnaider Beeri M, Goldbourt U, Silverman JM, Noy S, Schmeidler J, Ravona-Springer R, et al. Diabetes mellitus in midlife and the risk of dementia three decades later. *Neurology.* 2004;63:1902-7.

[23] Ott A, Stolk RP, Hofman A, van Harskamp F, Grobbee DE, Breteler MM. Association of diabetes mellitus and dementia: the Rotterdam Study. *Diabetologia.* 1996;39:1392-7.

[24] Kivipelto M, Helkala EL, Laakso MP, Hanninen T, Hallikainen M, Alhainen K, et al. Apolipoprotein E epsilon4 allele, elevated midlife total cholesterol level, and high midlife systolic blood pressure are independent risk factors for late-life Alzheimer disease. *Ann Intern Med.* 2002;137:149-55.

[25] Tan ZS, Seshadri S, Beiser A, Wilson PW, Kiel DP, Tocco M, et al. Plasma total cholesterol level as a risk factor for Alzheimer disease: the Framingham Study. *Arch Intern Med.* 2003;163:1053-7.

[26] Pappolla MA, Bryant-Thomas TK, Herbert D, Pacheco J, Fabra Garcia M, Manjon M, et al. Mild hypercholesterolemia is an early risk factor for the development of Alzheimer amyloid pathology. *Neurology.* 2003;61:199-205.

[27] Moroney JT, Tang MX, Berglund L, Small S, Merchant C, Bell K, et al. Low-density lipoprotein cholesterol and the risk of dementia with stroke. *JAMA.* 1999;282:254-60.

[28] Seshadri S, Beiser A, Selhub J, Jacques PF, Rosenberg IH, D'Agostino RB, et al. Plasma homocysteine as a risk factor for dementia and Alzheimer's disease. *N Engl J Med.* 2002;346:476-83.

[29] Quadri P, Fragiacomo C, Pezzati R, Zanda E, Forloni G, Tettamanti M, et al. Homocysteine, folate, and vitamin B-12 in mild cognitive impairment, Alzheimer disease, and vascular dementia. *Am J Clin Nutr.* 2004;80:114-22.

[30] in't Veld BA, Ruitenberg A, Hofman A, Stricker BH, Breteler MM. Antihypertensive drugs and incidence of dementia: the Rotterdam Study. *Neurobiol Aging.* 2001;22:407-12.

[31] Jick H, Zornberg GL, Jick SS, Seshadri S, Drachman DA. Statins and the risk of dementia. *Lancet.* 2000;356:1627-31.

[32] Zamrini E, McGwin G, Roseman JM. Association between statin use and Alzheimer's disease. *Neuroepidemiology* 2004;23:94-8.

[33] Li G, Higdon R, Kukull WA, Peskind E, Van Valen Moore K, Tsuang D, et al. Statin therapy and risk of dementia in the elderly: a community-based prospective cohort study. *Neurology.* 2004;63:1624-8.

[34] Zandi PP, Sparks DL, Khachaturian AS, Tschanz J, Norton M, Steinberg M, et al. Do statins reduce risk of incident dementia and Alzheimer disease? The Cache County Study. *Arch Gen Psychiatry.* 2005;62:217-24.

[35] Anthony JC, Breitner JC, Zandi PP, Meyer MR, Jurasova I, Norton MC, et al. Reduced prevalence of AD in users of NSAIDs and H2 receptor antagonists: the Cache County study. *Neurology.* 2000;54:2066-71.

[36] Cornelius C, Fastbom J, Winblad B, Viitanen M. Aspirin, NSAIDs, risk of dementia, and influence of the apolipoprotein E epsilon 4 allele in an elderly population. *Neuroepidemiology.* 2004;23:135-43.

[37] Stern Y, Gurland B, Tatemichi TK, Tang MX, Wilder D, Mayeux R. Influence of education and occupation on the incidence of Alzheimer's disease. *JAMA.* 1994;271:1004-10.

[38] Ott A, Breteler MM, van Harskamp F, Claus JJ, van der Cammen TJ, Grobbee DE, et al. Prevalence of Alzheimer's disease and vascular dementia: association with education. The Rotterdam study. *BMJ.* 1995;310:970-3.

[39] De Ronchi D, Fratiglioni L, Rucci P, Paternico A, Graziani S, Dalmonte E. The effect of

education on dementia occurrence in an Italian population with middle to high socioeconomic status. *Neurology.* 1998;50:1231-8.

[40] Karp A, Kareholt I, Qiu C, Bellander T, Winblad B, Fratiglioni L. Relation of education and occupation-based socioeconomic status to incident Alzheimer's disease. *Am J Epidemiol.* 2004;159:175-83.

[41] Wallin A, Brun A, Gustafson L and the Swedish Consensus Group. Swedish consensus on dementia diseases. Wallin A, Brun A, Gustafson L, eds. *Acta Neurol Scand* 1994;(Suppl 157) 90:1-31.

[42] Maurer K, Volk S and Gerbaldo H. Auguste D and Alzheimer's disease. *Lancet*. 1997;349:1546-1549.

[43] Alzheimer A. Uber Einen eigenartigen schweren Erkrankungsprozeb der Hirnrinde. *Neurologisches cenrealblatt.* 1906;23:1129-1136.

[44] Evans DA, Funkenstein HH, Albert MS, et al. Prevalence of Alzheimer's disease in a community population of older persons. Higher than previously reported. *JAMA*. 1989;262:2551-2556.

[45] Gurland BJ, Wilder DE, Lantigua R, et al. Rates of dementia in three ethnoracial groups. *Int J Geriatr Psychiatry.* 1999;14:481-493.

[46] Ganguli M, Dodge HH, Chen P, et al. Ten-year incidence in a rural elderly US community population: the movies project. *Neurology.* 2000;54:1109-1116.

[47] Perkins P, Annegers JF, Doody RS, et al. Incidence and prevalence of dementia in a multiethnic cohort of municipal retirees. *Neurology.* 1997;49:44-50.

[48] Corder EH, Saunders AM, Strittmatter WJ, et al. Gene dosage of apolipoprotein E type 4 allele and the risk of Alzheimer's disease in late onset families. *Science*. 1993;261:921-923.

[49] Martins CA, Oulhaj A, de Jager CA, Williams JH. APOE alleles predict the rate of cognitve

decline in Alzheimer disease: a nonlinear model. *Neurology.* 2005;65:1888-1893.

[50] Mayeux R, Saunders AM, Shea S, Mirra S, Evans D, Roses AD, Hyman BT, Crain B, Tang MX, Phelps Ch. Utility of the apolipoprotein E genotype in the diangnosis of Alzheimer's disease. Alzhemer's Disease Centers Consortium on Apolipoprotein E and Alzheimer's Disease. *N Engl J Med.* 1998;338:506-511.

[51] Holland AJ, Hon J, Huppert FA, et al. Incidence and course of dementia in people with Down's syndrome: findings from a population-based study. *J Intellect Disabil Res.* 2000;44:138-146.

[52] Ownby RL, Crocco E, Acevedo A, et al. Depression and risk for Alzheimer disease: systematic review, meta-analysis, and metaregression analysis. *Arch Gen Psychiatry.* 2006;63:530-538.

[53] Jellinger KA. Head injury and dementia. *Curr Opin Neurol.* 2004;17:719-723.

[54] Borenstein AR, Wu Y, Mortimer JA, et al. Developmental and vascular risk factors for Alzheimer's disease. *Neurobiol Aging*. 2005;26:325-334.

[55] Newman AB, Fitzpatrick AL, Lopez O, et al. Dementia and Alzheimer's disease incidence in relationship to cardiovascular disease in the Cardiovascular Health Study cohort. *J Am Geriatr Soc.* 2005;53:1101-1107.

[56] Merchant C, Tang MX, Albert S, et al. The influence of smoking on the risk of Alzheimer's disease. *Neurology.* 1999;52:1408-1412.

[57] Fritsch T, Smyth KA, Debanne SM, et al. Participation in novelty-seeking leisure activities and Alzheimer's disease. *J Geriatr Psychiatry Neurol.* 2005;18:134-141.

[58] Manly JJ, Schupf N, Tang MX, et al. Cognitive decline and literacy among ethnically diverse elders. *J Geriatr Psychiatry Neurol.* 2005;18:213-217.

[59] Townsend KP, Pratico D. Novel therapeutic opportunities for Alzheimer's disease: focus on

nonsteroidal anti-inflammatory drugs. *Faseb J.* 2005;19:1592-1601.

[60] McKhann G, Drachman Da, Folstein M, Katzman R, Price DL, Stadlan EM. Clinical diagnosis of Alzheimer's disease – report of the NINCDS-ADRDA work group under the auspices of Department of Health and Human Services Task Force on Alzheimer's disease. *Neurology.* 1984;43:939-944.

[61] Folstein MF, Folstein SE, McHugh PR. "Mini-mental state". A practical method for grading the cognitive state of patients for the clinician. *J Psychiatr Res.* 1975;12:189-98.

[62] Blessed G, Tomlinson BE, Roth M. The association between quantitative measures of dementia and of senile change in the cerebral grey matter of elderly subjects. *Br J Psychiatry.* 1968;114:797-811.

[63] Cahn DA, Salmon DP, Bondi MW, et al. A population-based analysis of qualitative features of the neuropsychological test performance of individuals with dementia of the Alzheimer type: implications for individuals with questionable dementia. *J Int Neuropsychol Soc.* 1997;3:387-393.

[64] Becker JT, Boller F, Lopez OL, et al. The natural history of Alzheimer's disease: Description of study cohort and accuracy of diagnosis. *Arch Neurol.* 1994;51:585-594.

[65] Lopez OL, Becker JT, Somsak D, et al. Awareness of cognitive deficits and anosoagnosia in Probable Alzheimer's disease. *Eur Neurol.* 1994;34:277-282.

[66] Stern Y, Albert M, Brandt J, et al. Utility of extrapyramindal signs and psychosis as predictors of cognitive and functional decline, nursing home admission, and death in Alzheimer's disease: Prospective analyses from the Predictors Study. *Neurology.* 1994;44:2300-2307.

[67] Wragg RE, Jeste DV. Overview of depression and psychosis in Alzheimer's disease. *Am J Psychiat.* 1989;146:577-587.

[68] Jagust W. Positron emission tomography and magnetic resonance imaging in the diagnosis

and prediction of dementia. *Alzheimers Dement.* 2006;2:36-42.

[69] deToledo-Morrell L, Stoub TR, Bulgakova M, et al. MRI-derived entorhinal volume is a good predictor of conversion from MCI to AD. *Neurobiol Aging.* 2004;25:1197-1203.

[70] Pennanen C, Kivipelto M, Tuomainen S, et al. Hippocampus and entorhinal cortex in mild cognitive impairment and early AD. *Neurobiol Aging*. 2004;25:303-310.

[71] Herholz K, Salmon E, Perani D, et al. Discrimination between Alzheimer dementia and controls by automated analysis of multicenter FDG PET. *Neuroimage*. 2002;17:302-316.

[72] Motter R, Vigo-Pelfrey C, Kholodenko D, et al. Reduction of beta-amyloid peptide42 in the cerebrospinal fluid of patients with Alzheimer's disease. *Ann Neurol.* 1995;38:643-648.

[73] Vandermeeren M, Mercken M, Vanmechelen E, et al. Detection of tau proteins in normal and Alzheimer's diseasde cerebrospinal fluid with a sensitive sandwich enzyme-linked immunosorbent assay. *J Neurochem*. 1993;61:1828-1834.

[74] Hu YY, He SS, Wang XC, et al. Elevated levels of phosphorylated neurofilament proteins in cerebrospinal fluid of Alzheimer's disease patients. *Neurosci Lett*. 2002;320:156-160.

[75] Ishiguro K, Ohno H, Arai H, et al. Phosphorylated tau in human cerebrospinal fluid is a diagnostic marker fro Alzheimer's disease. *Neurosci Lett.* 1999;270:91-94.

[76] Buerger K, Zinkowski R, Teipel SJ, et al. Differential diagnosis of Alzheimer disease with cerebrospinal fluid levels of tau protein phosphorylated at threonine 231. *Arch Neurol.* 2002;59:1267-1272.

[77] Blennow K. Cerebrospinal fluid protein biomarkers for Alzheimer's disease. *NeuroRx*. 2004;1:213-225.

[78] Maddalena A, Papassotiropoulos A, Muller-Tillmanns B, et al. Biochemical diagnosis of Alzheimer disease measuring the cerebrospinal fluid ratio of phpsphorylated tau protein to beta-amyloid peptide42. Arch Neurol. 2003;60:1202-1206.

[79] Birks J. Cholinesterase inhibitors for Alzheimer 's disease. *Cochrane Database Syst Rev.* 2006;1:CD005593.

[80] Tariot PN, Farlow MR, Grossberg GT, Graham SM, McDonald S, Gergel I. Memantine treatment in patients with moderate to severe Alzheimer disease already receiving donepezil: a randomized controlled trial. *JAMA*. 2004;291:317-324.

[81] Brodaty H, Ames D, Snowdon J, et al. A randomized placebo-controlled trial of risperidone for the treatment of aggression, agitation, and psychosis of dementia. *J Clin Psychiatry.* 2003;64:134-143.

[82] Street JS, Clark WS, Gannon KS, et al. Olanzapine treatment of psychotic and behavioural sumptoms in patients with Alzheimer disease in nursing care facilities. A double-blind, randomized, placebo-controlled trial. The HGEU Study Group. *Arch Gen Psychiatry.* 2000;57:968-976.

[83] Klafki HW, Staufenbiel M, Kornhuber J, Wiltfang J. therapeutic approaches to Alzheimer's disease. *Brain*. 2006;129:2840-2855.

[84] Schenk D, Barbour R, Dunn W, et al. Immunization with amyloid-beta attenuates Alzheimer- disease-like pathology in the PDAPP mouse. *Nature*. 1999;400:173-177.

[85] Orgogozo JM, Gilman S, Dartigues JF, et al. Subacute meningoencephalitis in a subset of patients with AD after Abeta42 immunisation. *Neurology.* 2003;61:46-54.

[86] Tanzi RE, Gusella JF, Watkins PC, et al. Amyloid beta protein gene: cdna, mrna distribution, and genetic linkage near the Alzheimer locus. *Science*. 1987;235:880-884.

[87] Sherrington R, Rogaev EI, Liang Y, et al. Cloning of a gene bearing missense mutations in early-onset familial Alzheimer's disease. *Nature*. 1995;375:754-760.

[88] Rogaev EI, Sherrington R, Rogaeva EA, et al. Familial Alzheimer's disease in kindreds with missense mutations in a gene on chromosome 1 related to the Alzheimer's disease type 3 gene.

Nature. 1995;376:775-778.

[89] Turner PR, O'Connor K, Tate WP, Abraham WC. Roles of amyloid precursor protein and its fragments in regulating neural activity, plasticity and memory. *Prog Neurobiol.* 2003;70(1):1-32.

[90] Priller C, Bauer T, Mitteregger G, Krebs B, Kretzschmar HA, Herms J. Synapse formation and function is modulated by the amyloid precursor protein. *J Neurosci.* 2006;26(27):7212-7221.

[91] Mullan M, Crawford F, Axelman K, Houlden H, Lilius L, Winblad B, Lannfelt L. A pathogenic mutation for probable Alzheimer's disease in the APP gene at the N-terminus of beta-amyloid. *Nature Genetics.* 1992;1:345-347.

[92] Hendriks L, van Duijn CM, Cras P, Cruts M, Van Hul W, van Harskamp F, Warren A, McInnis MG, Antonarakis SE, Martin JJ, Hofman A, Van Broeckhoven C. Presenile dementia and cerebral haemorrhage linked to a mutation at codon 692 of the beta-amyloid precursor protein gene. *Nature Genetics.* 1992;1:218-221.

[93] Levy E, Carman MD, Fernandez-Madrid IJ, Power MD, Lieberburg I, van Duinen SG, Bots GT, Luyendijk W, Frangione B. Mutations of the Alzheimer's disease amyloid gene in hereditary cerebral haemorrhage, Dutch type. *Science*. 1990;248:1124-1126.

[94] Eckman CB, Mehta ND, Crook R, Perez-tur J, Prihar G, Pfeiffer E, Graff-Radford N, Hinder P, Yager D, Zenk B, Refolo LM, Prada CM, Younkin SG, Hutton M, Hardy J. A new pathogenic mutation in the APP gene (I716V) increases the relative proportion of A beta 42(43). *Human Molecular Genetics.* 1997;6:2087-2089.

[95] Goate A, Chartier-Harlin MC, Mullan M, Brown J, Crawford F, Fidani L, Giuffra L, Haynes A, Irving N, James L, Mant R, Newton P, Rooke K, Roques P, Talbot C, Pericak-Vance M, Roses A, Williamson R, Rossor M, Owen M, Hardy J. Segregation of a missense mutation in the amyloid precursor protein gene with familial Alzheimer's disease. *Nature*. 1991;349:704-706.

[96] Rovelet-Lecrux A, Hannequin D, Raux G, Meur NL, Laquerriere A, Vital A, Dumanchin C,

Feuillette S, Brice A, Vercelletto M, Dubas F, Frebourg T, Campion D. APP locus duplication causes autosomal dominant early-onset Alzheimer disease with cerebral amyloid angiopathy. *Nature Genetics*. 2006;38:24-26.

[97] Wolfe MS, De Los Angeles J, Miller DD, Xia W, Selkoe DJ. Are presenilins intramembrane-cleaving proteases? Implications for the molecular mechanism of Alzheimer's disease. *Biochemistry.* 1999;38(35):11223-11230.

[98] Kovacs DM, Fausett HJ, Page KJ, et al. Alzheimer-associated presenilin 1 and 2: neuronal expression in brain and localization to intracellular membranes in mammalian cells. *Nat Med*. 1996;2(2).224-229.

[99] Takasugi N, Tomita T, Hayashi I, et al. The role of presenilin cofactors in the gamma-secretase complex. *Nature*. 2003;422(6930):438-441.

[100] Scheuner D, Eckman C, Jensen M, et al. Secreted amyloid beta-protein similar to that in tha senile plaques of Alzheimer's disease is increased in vivo by the presenilin 1 and 2 and APP mutations linked to familial Alzheimer's disease. *Nat Med.* 1996;2(8):864-870.

[101] Saunders AM, Strittmatter WJ, Schmechel D, et al. Association of apolipoprotein E allele epsilon 4 with late-onset familial and sporadic Alzheimer's disease. *Neurology.* 1993;43:1467-1472.

[102] Strittmatter WJ, Saunders AM, Schmechel D, et al. Apolipoprotein E: high-avidity, binding to beta-amyloid and increased frequency of type 4 allele in late-onset familial Alzheimer disease. *Proc Natl Acad Sci USA.* 1993;90:1977-1981.

[103] Bertram L, McQueen MB, Mullin K, et al. Systematic Meta-Analyses of Alzheimer Disease Genetic Association Studies: The AlzGene Database. *Nat Genet.* 2007;39:17-23.

[104] Mahley RW, Weisgraber KH, Huang Y. Apolipoprotein E4: a causative factor and therapeutic target in neuropathology, including Alzheimer's disease. *Proc Natl Acad Sci USA.*

2006;103(15):5644-5651.

[105] Corder EH, Saunders AM, Risch NJ, et al. Protective effect of apolipoprotein E type 2 allele for late onset Alzheimer disease. *Nat Genet.* 1994;7:180-184.

[106] Bales KR, Verina T, Cummins DJ, et al. Apolipoprotein E is essential for amyloid deposition in the APP(V717F) transgenic mouse model of Alzheimer's disease. *Proc Natl Acad Sci USA*. 1999;96:15233-15238.

[107] Beffert U, Cohn JS, Petit-Turcotte C, et al. Apolipoprotein E and beta-amyloid levels in the hippocampus and frontal cortex of Alzheimer's disease subjects are disease-related and apolipoprotein E genotype dependent. *Brain Res.* 1999;843:87-94.

[108] Poirier J. Apolipoprotein E and Alzheimer's disease. A role in amyloid catabolism. *Ann N Y Acad Sci.* 2000;924:81-90.

[109] Bertram L, Lill CM, Tanzi RE. The Genetics of Alzheimer Disease: Back to the Future. *Neuron*. 2010;68:270-281.

[110] Harold D, Abraham R, Hollingworth P, Sims R, Gerrish A, Hamshere ML, Pahwa JS, Moskvina V, Dowzell K, Williams A, et al. Genome-wide association study identifies variants at CLU and PICALM associated with Alzheimer's disease. *Nat Genet.* 2009;41:1088-1093.

[111] Lambert JC, Heath S, Even G, Campion D, Sleegers K, Hiltunen M, Combarros O, Zelenika D, Bullido MJ, Tavernier B, et al; European Alzheimer's Disease Initiative Investigators. Genome-wide association study identifies variants at CLU and CR1 associated with Alzheimer's Disease. *Nat Genet*. 2009;41:1094-1099.

[112] Seshadri S, Fitzpatrick AL, Ikram MA, DeStefano AL, Gudnason V, Boada M, Bis JC, Smith AV, Carassquillo MM, Lambert JC, et al; CHARGE Consortium; GERAD1 Consortium; EADI1 Consortium. Genome-wide analysis of genetic loci associated with Alzheimer disease. *JAMA*. 2010:303:1832-1840.

[113] DeMattos RB, O'dell MA, Parsadanian M, Taylor JM, Harmony JA, Bales KR, Paul SM, Aronow BJ and Holtzman DM. Clusterin promotes amyloid plaque formation and is critical for neuritic toxicity in a mouse model of Alzheimer's disease. *Proc Natl Acad Sci USA*. 2002;99:10843-10848.

[114] Rogers J, Li R, Mastroeni D, Grover A, Leonard B, Ahern G, Cao P, Kolody H, Vedders L, Kolb WP and Sabbagh M. Peripheral clearance of amyloid beta peptide by complement C3-dependent adherence to erythrocytes. *Neurobiol Aging. 2006*;27:1733-1739.

[115] Baig S, Joseph SA, Tayler H, Abraham R, Owen MJ, Williams J, Kehoe PG and Love S. Distribution and expression of picalm in Alzheimer disease. *J Neuropathol Exp Neurol*. 2010;69:1071-1077.

[116] Wigge P, Kőhler K, Vallis Y, Doyle CA, Owen D, Hunt SP and McMahon HT. Amphiphysin heterodimers: Potential role in clathrin-mediated endocytosis. *Mol Biol Cell.* 1997;8:2003-2015.

[117] Hubbard BM and Anderson JM. Age, senile dementia and ventricular enlargement. *J Neurol Neurosurg Psychiatry.* 1981;44:631-635.

[118] de la Monte SM. Quantitation of cerebral atrophy in preclinical and and-stage Alzheimer's disease. Ann Neurol. 1989;25:450-459.

[119] Ratnavalli E, Brayne C, Dawson K, et al. The prevalence of frontotemporal dementia. *Neurology*. 2002;58:1615-1621.

[120] Harvey RJ, Skelton-Robinson M, Rossor MN. The prevalence and causes of dementia in people under the age of 65 years. *J Neurol Neurosurg Psychiatry.* 2003;74:1206-1209.

[121] Borroni B, Alberici A, Grassi M, et al. Is frontotemporal lobar degeneration a rare disorder? Evidence from a preliminary study in Brescia County, Italy. *J Alzheimers Dis.* 2010;19:11-16.

[122] Rosso SM, Donker Kaat L, Baks T, et al. Frontotemporal dementia in The Netherlands: patient characteristics and prevalence estimates from a population-based study. *Brain*. 2003;126:2016-2022.

[123] Knopman DS, Petersen RC, Edland DS, et al. The incidence of frontotemporal lobar degeneration in Rochester, Minnesota, 1990 through 1994. *Neurology*. 2004;62:506-508.

[124] Mercy L, Hodges JR, Dawson K, et al. Incidence of early-onset dementias in Cambridgeshire, United Kingdom. *Neurology*. 2008;71:1496-1499.

[125] Rademakers R, Eriksen JL, Baker M, et al. Common variation in the miR-659 binding-site of GRN is a major risk factor for TDP-43 positive frontotemporal dementia. *Hum Mol Genet.* 2008;17: 3631-3642.

[126] Simon-Sanchez J, Seelaar H, Bochdanovits Z, et al. Variation at GRN 3'-UTR rs5848 is not associated with a risk of frontotemporal lobar degeneration in Dutch population. *PloS One.* 2009:4:e7494.

[127] Rollinson S, Rohrer JD, van der Zee J. No association of PGRN 3'-UTR rs5848 in frontotemporal lobar degeneration. *Neurobiol Aging*. Published Online First: 13 May 2009.

[128] Benussi L, Ghidoni R, Galimberti D, et al. The CST3 B haplotype is associated with frontotemporal lobar degeneration. *Eur J Neurol.* 2010;17:143-146.

[129] Srinivasan R, Davidson Y, Gibbons L, et al. The apolipoprotein E epsilon4 allele selectively increases the risk of frontotemporal lobar degeneration in males. *J Neurol Neurosurg Psychiatry*. 2006;77:154-158.

[130] Li X, Rowland LP, Mitsumoto H, et al. Prion protein codon 129 genotype prevalence is altered in primary progressive aphasia. *Ann Neurol.* 2005;58:858-864.

[131] Verpillat P, Camuzat A, Hannequin D, et al. Association between the extended tau haplotype and frontotemporal dementia. *Arch Neurol.* 2002;59:935-939.

[132] Rollinson S, Rizzu P, Sikkink S, et al. Ubiquitin associated protein 1 is a risk factor for frontotemporal lobar degeneration. *Neurobiol Aging.* 2009;30:656-665.

[133] Van Deerlin VM, Sleiman PMA, Martinez-Lage M, et al. Common genetic variants at 7p21 show strong association with frontotemporal lobar degeneration with TDP-43 inclusions. *Nat Genet.* 2010;42:234-239.

[134] The Lund and Manchester Groups. Consensus Statement. Clinical and neuropathological criteria for frontotemporal dementia: *J Neurol Neurosurg Psychiatry.* 1994;57:416-418.

[135] Nearly D, Snowden JS, Gustafson L, Passant U, Stuss D, Black S, Freedman M, Kertesz A, Robert PH, Albert M, Boone K, Miller BL, Cummings J, Benson DF. *Neurology.* 1998;51:1546-1554.

[136] Liu W, Miller BL, Kramer JH, et al. Behavioural disorders in the frontal and temporal variants of frontotemporal dementia. *Neurology.* 2004;62:742-748.

[137] Miller BL, Cummings JL, Villanueva-Meyer J, et al. Frontal lobe degeneration: clinical, neuropsychological, and SPECT characteristics. *Dementia*. 1993;4:1374-1382.

[138] Ames D, Cummings JL, Wirshing WC, et al. Repetitive and compulsive behaviour in frontal lobe degenerations. *J Neuropsychiatry Clin Neurosci.* 1994;6:100-113.

[139] Kramer JH, Jurik J, Sha SJ, et al. Distinctive neuropsychological patterns in frontotemporal dementia, semantic dementia, and Alzheimer disease. *Cogn Behav Neurol.* 2003;16:211-218.

[140] Turner RS, Kenyon LC, Trojanowski JQ, et al. Clinical, neuroimaging, and pathologic features of progressive nonfluent aphasia. *Ann Neurol*. 1996;39:166-173.

[141] Mesulam MM. Primary progressive aphasia-a-language-based dementia. *N Engl J Med.* 2003;349:1535-1542.

[142] Hodhes JR, Bozeat S, Lambon Ralph MA, et al. The role of conceptual knowledge in

object use evidence from semantic dementia. *Brain*. 2000;123:1913-1925.

[143] Snowden JS, Bathgate D, Varma A, et al. Distinct behavioural profiles in frontotemporal dementia and semantic dementia. *J Neurol Neurosurg Psychiatr*y. 2001;70:323-332.

[144] Thompson SA, Patterson K, Hodges JR. Left/right asymmetry of atrophy in semantic dementia: behavioural-cognitive implications. *Neurology*. 2003;61:1196-1203.

[145] Lomen-Hoerth C, Murphy J, Langmore S, et al. Are amyothophic lateral sclerosis patients cognitively normal? *Neurology*. 2003;60:1094-1097.

[146] Seeley WW, Crawford R, Rascovski K, et al. Frontal paralimbic network atrophy in very mild behavioural variant frontotemporal dementia. *Arch Neurol.* 2008;65:249-255.

[147] Gorno-Tempini ML, Dronkers NF, Rankin KP, et al. Cognition and anatomy in three variants of primary progressive aphasia. *Ann Neurol.* 2004;55:335-346.

[148] Mummery CJ, Patterson K, Price CJ, et al. A voxel-based morphometry study of semantic dementia: relationship between temporal lobe atrophy and semantic memory. *Ann Neurol*. 2002;47:36-45.

[149] Chang JL, Lomen-Hoerth C, Murphy J, et al. A voxel-based morphometry study of patterns of brain atrophy in ALS and ALS/FTLD. *Neurology*. 2005;65:75-80.

[150] Kamo H, McGeer PL, Harrop R, et al. Positron emission tomography and histopathology in Pick's disease. *Neurology*. 1987;37:439-445.

[151] Talbot PR, Lloyd JS, Snowden JS, et al. A clinical role for 99mtc-HMPAO SPECT in the investigation of dementia? *J Neurol Neurosurg Psychiatry.* 1998;64:306-313.

[152] Silverman DH, Small GW, Chang CY, et al. Positron emission tomography in evaluation of dementia: Regional brain metabolism and long-term outcome. *JAMA*. 2001;286:2120-2127.

[153] Verwey NA, Kester MI, van der Flier WM, et al. Additional value of CSF amyloid-beta 40 levels in the differentiation between FTLD and control subjects. *J Alzheimers Dis.* 2010;20:445-

452.

[154] Ghidoni R, Benussi L, Glionna M, et al. Low plasma progranulin levels predict progranulin mutations in frontotemporal lobar degeneration. *Neurology*. 2008;71:1235-1239.

[155] Foulds PG, Davidson Y, Mishra M, et al. Plasma phosphorylated TDP-43 protein levels correlate with brain pathology in frontotemporal lobar degeneration. *Acta Neuropathol.* 2009;118:647-658.

[156] Franceschi M, Anchisi D, Pelati O, et al. Glucose metabolism and serotonin receptors in the frontotemporal lobar degeneration. *Ann Neurol.* 2005;57:216-225.

[157] Snowden JS, Nearly D, Mann DMA. Frontotemporal lobar degeneration: frontotemporal dementia, progressive aphasia, semantic dementia. *Churchill-Livingstone, London.* 1996.

[158] Stevens M, van Duijn CM, Kamporst W, et al. Familial aggregation in frontotemporal dementia. *Neurology*. 1998;50:1541-1545.

[159] Rohrer JD, Guerreiro R, Vandrovcova J, et al. The heritability and genetics of frontotemporal lobar degeneration. *Neurology*. 2009;73:1451-1456.

[160] LoPresti P, Szuchet S, Papasozomenos SC, et al. Functional implications for the microtubule-associated protein tau: localization in oligodendrocytes. *Proc Natl Acad Sci USA*. 1995;92:10369-10373.

[161] Goedert M, Spillantini MG, Potier MC, et al. Cloning and sequencing of the cDNA encoding an isoform of microtubule-associated protein tau containing four tandem repeats: differential expression of tau protein mRNAs in human brain. *Embo J.* 1989;8:393-399.

[162] Hutton M, Lendon CL, Rizzu P, et al. Association of missense and 5'-splice-site mutations in tau with the inherited dementia FTDP-17. *Nature*. 1998;393:702-705.

[163] Dayanandan R, van Slegtenhorst M, Mack TG, et al. Mutations in tau reduce its microtubule binding properties in intact cells and affect its phopsphorylation. *FEBS Lett.*

1999;446:228-232.

[164] Nacharaju P, Lewis J, Easson C, et al. Accelerated filament formation from tau protein with specific FTDP.17 missense mutations. *FEBS Lett.* 1999;447:195-199.

[165] He Z, Bateman A. Progranulin (granulin-epithelin precursor, PC-cell-derived growth factor, acrogranin) mediates tissue repair and tumorigenesis. *J Mol Med.* 2003;81:600-612.

[166] He Z, Ong CH, Halper J, et al. Progranulin is a mediator of the wound response. *Nat Med.* 2003;9:225-229.

[167] Ahmed Z, Mackenzie IR, Hutton ML, et al. Progranulin in frontotemporal lobar degeneration and neuroinflammation. *J Neuroinflammation.* 2007;4:7.

[168] Van Damme P, Van Hoecke A, Lambrechts D, et al. Progranulin functions as a neurotrophic factor to regulate neurite outgrowth and enhance neuronal survival. *J Cell Biol*. 2008;181:37-41.

[169] Baker M, Mackenzie IR, Pickering-Brown SM, Gass J, Rademakers R, et al. Mutations in progranulin cause tau-negative frontotemporal dementia linked to chromosome 17. *Nature*. 2007;442: 916-919.

[170] Cruts M, Gijselinck I, Van der Zee J, Engelborghs S, Wils H, et al. Null mutations in progranulin cause ubiquitin-positive frontotemporal dementia linked to chromosome 17q21. *Nature.* 2006;442:920-924.

[171] Gass J, Cannon A, Mackenzie IR, Boeve B, Baker M, Adamson J, et al. Mutations in progranulin are a major cause of ubiquitin-positive frontotemporal lobar degeneration. *Hum Mol Genet.* 2006;15:2988-3001.

[172] Le Ber I, Camuzat A, Hannequin D, et al. Phenotype variability in progranulin mutation carriers: a clinical, neuropsychological, imaging and genetic study. *Brain*. 2008;131:732-746.

[173] Mesulam M, Johnson N, Krefft TA, et al. Progranulin mutations in primary progressive

aphasia: the PPA1 and PPA3 families. *Arch Neurol.* 2007;64:43-47.

[174] Benussi L, Binetti G, Sina E, Gigola L, Bettecken T, Meitinger T, Ghidoni R. A novel deletion in progranulin gene is associated with FTDP-17 and CBS. *Neurobiology of Aging.* 2008;29:427-435.

[175] Kimonis VE, Fulchiero E, Vesa J, et al. VCP disease associated with myophathy, Paget disease of bone and frontotemporal dementia: review of a unique disorder. *Biochim Biophys Acta.* 2008;1782:744-748.

[176] Gydesen S, Brown JM, Brun A, et al. Chromosome 3 linked frontotemporal dementia (FTD-3). *Neurology.* 2002;59:1585-1594.

[177] Parkinson N, Ince PG, Smith MO, et al. ALS phenotypes with mutations in CHMP2B (charged multivesicular protein 2B). *Neurology.* 2006;67:1074-1077.

[178] Le Ber I, Camuzat A, Berger E, et al. Chromosome 9p-linked families with frontotemporal dementia associated with motor neuron disease. *Neurology.* 2009;72:1669-16776.

[179] Benajiba L, Le Ber I, Camuzat A, Lacoste M, Thomas-Anterior C, et al. TARDBP mutations in motoneuron disease with frontotemporal lobar degeneration. *Ann Neurol.* 2009;65(4):470-473.

[180] Kovac GG, Murrell JR, Horvath S, Haraszti L, Majtenyi K, et al. TARDBP variation associated with frontotemporal dementia, supranuclear gaze palsy, and chorea. *Mov Disord.* 2009;24(12):1843-1847.

[181] Van Langenhove T, van der Zee J, Sleegers K, Engelborghs S, Vandenberghe R, et al. Genetic contribution of FUS to frontotemporal lobar degeneration. *Neurology.* 2010;74(5):366-371.

[182] Broe M, Hodges JR, Schofield E, Shepherd CE, Krill JJ, Halliday GM. Staging disease severity in pathologically confirmed cases of frontotemporal dementia. *Neurology.*

2003;60:1005-1011.

[183] Mackenzie IR, Neumann M, Bigio EH, Cairns NJ, Alafuzoff I, et al. Nomenclature for neuropathologic subtypes of frontotemporal lobar degeneration: consensus recommendations. *Acta Neuropathol*. 2009;117:15-18.

[184] Mackenzie IR, Neumann M, Bigio EH, Cairns NJ, Alafuzoff I, et al. Nomenclature and nosology for neuropathologic subtypes of frontotemporal lobar degeneration: an update. *Acta Neuropathol.* 2010;119:1-4.

[185] Arai T, Hasegawa M, Akiyama H, Ikeda K, Nonaka T, Mori H, Mann D, Tsuchiya K, Yoshida M, Hashizume Y, Oda T. TDP-43 is a component of ubiquitin-positive tau-negative inclusions in frontotemporal lobar degeneration and amyotrophic lateral sclerosis. *Biochem Biophys Res Commun.* 2006;351:602-611.

[186] Mackenzie IR, Baborie A, Pickering-Brown S, Du Plessis D, Jaros E, Perry RH, Neary D, Snowden JS, Mann DM. Heterogeneity of ubiquitin pathology in frontotemporal lobar degeneration: classification and relation to clinical phenotype. *Acta Neuropathol.* 2006;112:539-549.

[187] Spillantini MG, Goedert M. Tau protein pathology in neurodegenerative diseases. *Trends Neurosci.* 1998;21:428-433.

[188] Zhukareva V, Mann D, Pickering-Brown S, Uryu K, Shuck T, Shah K, Grossman M, Miller BL, Hulette CM, Feinstein SC, Trojanowski JQ, Lee VM. *Ann Neurol.* 2002;51:730-739.

[189] Bigio EH, Brown DF and White CL 3rd. Progressive supranuclear pulsy with dementia: cortical pathology. *J Neuropathol Exp Neurol.* 1999;58:359-364.

[190] Sha S, Hou C, Viskontas IV, Miller BL. Are frontotemporal lobar degeneration, progressive supranuclear palsy and corticobasal degeneration distinct diseases? *Nat Clin Pract Neurol.* 2006;2:658-665.

[191] Ishihara K, Araki S, Ihori N, Shiota J, Kawamura M, Yoshida M, Hashizume Y, Nakano I. Argyrophilic grain disease presenting with frontotemporal dementia: a neuropsychological and pathological study of an autopsied case with presenile onset. *Neuropathology*. 2005;25:165-170.

[192] Bigio EH, Lipton AM, Yen SH, Hutton ML, Baker M, Nacharaju P, White CL 3rd, Davies P, Lin W, Dickson DW. Frontal lobe dementia with novel tauopathy: sporadic multiple system tauopathy with dementia. *J Neuropathol Exp Neurol.* 2001,60:328-341.

[193] Neumann M, Rademakers R, Roeber S, et al. A new subtype of frontotemporal lobar degeneration with FUS pathology. *Brain*. 2009;132:2922-2931.

[194] Munoz DG, Neumann M, Kusaka H, et al. FUS pathology in basophilic inclusion body disease. *Acta Neuropathol*. 2009;118(5):617-627.

[195] Neumann M, Roeber S, Kretzschmar HA, et al. Abundant FUS-immunoreactive pathology in neuronal intermediate filament inclusion disease. *Acta Neuropathol.* 2009;118(5):605-616.

[196] Pikkarainen M, Hartikainen P and Alafuzoff I. Neuropathologic Features of Frontotemporal Lobar Degeneration With Ubiquitin-Positive Inclusions Visualized With Ubiquitin-Binding Protein p62 Immunohistochemistry. *J Neuropathol Exp Neurol.* 2008;67:280-298.

[197] Holm IE, Isaacs AM, Mackenzie IR. Absence of FUS-immunoreactive pathology in frontotemporal dementia linked to chromosome 3 (FTD-3) caused by mutation in the CHMP2B gene. *Acta Neuropathol.* 2009;118:719-720.

[198] Razvi SS, Davidson R, Bone I, Muir KW. The prevalence of cerebral autosomal dominant arteriopathy with subcortical infarcts and leukoencephalopathy (CADASIL) in the west of Scotland. *J Neurol Neurosurg Psychiatry.* 2005;76(5):739-741.

[199] Joutel A, Dodick DD, Parisi JE, Cecillon M, Tournier-Lasserve E, Bousser MG. De novo mutation in the Notch3 gene causing CADASIL. *Ann Neurol.* 2000;47(3):388-391.

[200] Biessels GJ, Staekenborg S, Brunner E, et al. Risk of dementia in diabetes mellitus: a systematic review. *Lancet Neurol*. 2006;5:64-74.

[201] Seshadri S, Beiser A, Selhub J, et al. Plasma homocysteine as a risk factor for dementia and Alzheimer's disease. *N Engl J Med.* 2002;346:476-483.

[202] Posner HB, Tang MX, Luchsinger J, et al. The relationship of hypertension in the elderly to AD, vascular dementia and cognitive function. *Neurology*. 2002;58:1175-1181.

[203] Tournier-Lasserve E, Joutel A, Melki J, et al. Cerebral autosomal dominant arteriopathy with subcortical infarcts and leukoencephalopathy maps to chromosome 19q12. *Nat Genet.* 1993;3:256-259.

[204] Joutel A, Corpechot C, Ducros A, et al. Notch3 mutations in CADASIL, a hereditary adult-onset condition causing stroke and dementia. *Nature*. 1996;383:707-710.

[205] Gladstone JP, Dodick DW. Migraine and white matter lesions: when to suspect cerebral autosomal dominant arteriopathy with subcortical infarcts and leukoencephalopathy (CADASIL). *Neurologist.* 2005;11:19-29.

[206] Schultz A, Santoianni R, Hewan-Lowe K. Vasculopathic changes of CADASIL can be focal in skin biopsies. *Ultrastruct Pathol.* 1999;23:241-247.

[207] Desmond DW, Moroney JT, Lynch T, et al. The natural history of CADASIL: a pooled analysis of previously published cases. *Stroke*. 1999;30:1230-1233.

[208] Chabriat H, Vahedi K, Iba-Zizen MT, et al. Clinical spectrum of CADASIL: a study of 7 families. Cerebral autosomal dominant arteriopathy with subcortical infarcts and leukoencephalopathy. *Lancet*. 1995;346:934-939.

[209] Valenti R, Poggesi A, Pescini F, Inzitari D, Pantoni L. psychiatric disturbances in CADASIL: a brief review. *Acta Neurol Scand.* 2008;118:291-295.

[210] Buffon F, Porcher R, Hernandez K, et al. Cognitive profile in CADASIL. *J Neurol*

Neurosurg Psychiatry. 2006;77:175-180.

[211] Dichgans M, Mayer M, Uttner I, et al. The phenotypic spectrum of CADASIL: clinical findings in 102 cases. *Ann Neurol.* 1998;44:731-739.

[212] Chabriat H, Levy C, Taillia H, et al. Patterns of MRI lesions in CADASIL. *Neurology.* 1998;51:452-457.

[213] Dichgans M, Filippi M, Bruning R, et al. Quantitative MRI in CADASIL: correlation with disability and cognitive performance. *Neurology.* 1999;52:1361-1367.

[214] Moon SY, Ki CS, Kim JW, Suh YL, Kwon JC, Na DL. Silent infarcts demonstrated by diffusion-weighted MRI in CADASIL. *Eur Neurol.* 2003;49(3):178-180.

[215] Dichgans M, Holtmannspotter M, Hergoz J, et al. Cerebral microbleeds in CADASIL: a gradient-echo magnetic resonance imaging and autopsy study. *Stroke*. 2002;33:67-71.

[216] Tournier-Lasserve E, Iba-Zizen MT, Romero N, et al. Autosomal dominant syndrome with strokelike episodes and leukoencephalopathy. *Stroke*. 1991;22:1297-1302.

[217] Chabriat H, Joutel A, Vahedi K, et al. [CADASIL (cerebral autosomal dominant arteriopathy with subcortical infarcts and leukoencephalopathy)]. *J Mal Vasc.* 1996;21:277-282.

[218] Unlu M, de Lange RP, de Silva R, et al. Detection of complement factor B in the cerebrospinal fluid of patients with cerebral autosomal dominant arteriopathy with subcortical infarcts and leukoencephalopathy disease using two-dimensional gel electrophoresis and mass spectrometry. *Neurosci Lett.* 2000;282:149-152.

[219] Sjögren M, Minthon L, Davidsson P, Granérus A-K, Clarberg A, Vanderstichele H, Vanmechelen E, Wallin A, Blennow K. CSF levels of tau, beta-amyloid (1-42) and GAP-43 in frontotemporal dementia, other types of dementia and normal aging. *J Neural Transm*. 2000;107(5):563-579.

[220] Formichi P, Parnetti L, Radi E, Cevenini G, Dotti MT, Federico A. CSF levels of beta-

amyloid 1-42, tau and phosphorylated tau protein in CADASIL. *Eur J Neurol.* 2008;15(11):1252-1255.

[221] Formichi P, Parnetti L, Radi E, Cevenini G, Dotti MT, Federico A. CSF Biomarkers Profile in CADASIL-A Model of Pure Vascular Dementia: Usefulness in Differential Diagnosis in the Dementia Disorder. *Int J Alzheimers Dis*. 2010.

[222] Forteza AM, Brozman B, Rabinstein AA, Romano JB, Bradley WG. Acetazolamide for the treatment of migraine with aura in CADASIL. *Neurology.* 2001;57:2144-2145.

[223] Ragoschke-Schumm A, Axer H, Witte OW, et al. Intracerebral haemorrhages in CADASIL. *J Neurol Neurosurg Psychiatry.* 2005;76:1606-1607.

[224] Dichgans M, Markus HS, Salloway S, et al. Donepezil in patients with subcortical vascular cognitive impairment: a randomised double-blind trial in CADASIL. *Lancet Neurol.* 2008;7:310-318.

[225] Villa N, Walker L, Lindsell CE, Gasson J, Iruela-Arispe ML, Weinmaster G. Vascular expression of Notch pathway receptors and ligands is restricted to arterial vessels. *Mech Dev.* 2001;108:161-164.

[226] Dubroca C, Lacombe P, Domenga V, Maciazek J, Levy B, Tournier-Lasserve E, Joutel A, Henrion D. Impaired vascular mechanotransduction in a transgenic mouse model of CADASIL arteriopathy. *Stroke*. 2005;36:113-117.

[227] Lacombe P, Oligo C, Domenga V, Tournier-Lasserve E, Joutel A. Impaired cerebral vasoreactivity in a transgenic mouse model of cerebral autosomal dominant arteriopathy with subcortical infarcts and leukoencephalopathy arteriopathy. *Stroke*. 2005;36:1053-1058.

[228] Lacombe P, Oligo C, Domenga V, Tournier-Lasserve E, Joutel A. Impaired cerebral vasoreactivity in a transgenic mouse model of cerebral autosomal dominant arteriopathy with subcortical infarcts and leukoencephalopathy arteriopathy. *Stroke*. 2005;36:1053-1058.

[229] Joutel A, Monet M, Domenga V, Riant F, Tournier-Lasserve E. Pathogenic mutations associated with Cerebral Autosomal Dominant Arteriopathy with Subcortical Infarcts and Leukoencephalopathy differently affect Jagged binding and Notch3 activity via the RBP/JK signaling pathway. *Am J Hum Genet.* 2004;74:338-347.

[230] Monet M, Domenga V, Lemaire B, Souilhol C, Langa F, Babinet C, Gridley T, Tournier-Lasserve E, Cohen-Tannoudji M, Joutel A. The archetypal R90C CADASIL-NOTCH3 mutation retains NOTCH3 function in vivo. *Hum Mol Genet.* 2007;16:982-992.

[231] Donahue CP, Kosik KS. Distribution pattern of *NOTCH3* mutations suggests a gain-of-function mechanism for CADASIL. *Genomics.* 2004;83:59-65.

[232] Rouchoux MM, Maurage CA. CADASIL: Cerebral autosomal dominant arteriopathy with subcortical infarcts and leukoencephalopathy arteriopathy. *J Neuropathol Exp Neurol.* 1997;56:947-964.

[233] Viswanathan A, Gray F, Bousser MG, Baudrimont M, Chabriat H. Cortical neuronal apoptosis in CADASIL. *Stroke*. 2006;37:2690-2695.

[234] Okeda R, Arima K, Kawai M. Arterial changes in cerebral autosomal dominant arteriopathy with subcortical infarcts and leukoencephalopathy arteriopathy (CADASIL) in relation to pathogenesis of diffuse myelin loss of cerebral white matter: examination of cerebral medullary arteries by reconstruction of serial sections of an autopsy case. *Stroke*. 2002;33:2565-2569.

[235] Gutierrez-Molina M, Caminero Rodriguez A, Martinez Garcia C, et al. Small arterial granular degeneration in familial Binswanger's syndrome. *Acta Neuropathol (Berl)*. 1994;87:98-105.

[236] Ebke M, Dichgans M, Bergmann M, et al. CADASIL: skin biopsy allows diagnosis in early stages. *Acta Neurol Scand.* 1997;95:351-357.

[237] Joutel A, Favrole P, Labauge P, et al. Skin biopsy immunostaining with *NOTCH3* monoclonal antibody for CADASIL diagnosis. *Lancet*. 2001;358:2049-2051.

[238] Rovelet-Lecrux A, Hannequin D, Raux G, Meur NL, Laquerriere A, Vital A, Dumanchin C, Feuillette S, Brice A, Vercelletto M, Dubas F, Frebourg T, Campion D. APP locus duplication causes autosomal dominant early-onset Alzheimer disease with cerebral amyloid angiopathy. *Nature Genetics*. 2006;38: 24-26.

[239] Sleegers K, Brouwers N, Gijselinck I, Theuns J, Goossens D, Wauters J, Del-Favero J, Cruts M, van Duijn CM, Van Broeckhoven C. APP duplication is sufficient to cause early onset Alzheimer's dementia with cerebral amyloid angiopathy. *Brain*. 2006;129: 2977-2983.

[240] Gijselinck I, van der Zee J, Engelborghs S, Goossens D, Peeters K, Mattheijssens M, Corsmit E, Del-Favero J, De Deyn PP, Van Broeckhoven C, Cruts M. Progranulin locus deletion in frontotemporal dementia. *Human Mutation*. 2008;29: 53-58.

[241] Deprez L, Peeters K, Van Paesschen W, Claeys KG, Claes LR, Suls A, Audenaert D, Van Dyck T, Goossens D, Del-Favero J, De Jonghe P. Familial occipitotemporal lobe epilepsy and migraine with visual aura: linkage to chromosome 9q. *Neurology*. 2007;68(23):1995-2002.

[242] Gijselinck I, Engelborghs S, Maes G, Cuijt I, Peeters K, Mattheijssens M, Joris G, Cras P, Martin JJ, De Deyn PP, Kumar-Singh S, Van Broeckhoven C, Cruts M. Identification of 2 Loci at chromosomes 9 and 14 in a multiplex family with frontotemporal lobar degeneration and amyotrophic lateral sclerosis. *Arch Neurol*. 2010;67(5):606-16.

[243] Kimmel G, Shamir R. GERBIL: Genotype resolution and block identification using likelihood. *Proc Natl Acad Sci U S A*. 2005;102:158-62.

[244] Sleegers K, Brouwers N, Van Damme P, Engelborghs S, Gijselinck I, van der Zee J, Peeters K, Mattheijssens M, Cruts M, Vandenberghe R, De Deyn PP, Robberecht W, Van Broeckhoven C. Serum biomarker for progranulin-associated frontotemporal lobar degeneration.

Ann Neurol. 2009;65(5):603-9.

[245] Hutton M, Lendon CL, Rizzu P, Baker M, Froelich S, Houlden H, Pickering-Brown S, Chakraverty S, Isaacs A, Grover A, Hackett J, Adamson J, et al. Association of missense and 5-prime-splice-site mutations in tau with the inherited dementia FTDP-17. *Nature*. 1998;393:702-705.

[246] Hutton M. Missense and splice site mutations in tau associated with FTDP-17: multiple pathogenic mechanisms. *Neurology*. 2001;56(suppl.4);S21-S25.

[247] Guerreiro RJ, Baquero M, Blesa R, Boada M, Brás JM, Bullido MJ, Calado A, Crook R, Ferreira C, Frank A, Gómez-Isla T, Hernández I, Lleó A, Machado A, Martínez-Lage P, Masdeu J, Molina-Porcel L, Molinuevo JL, Pastor P, Pérez-Tur J, Relvas R, Oliveira CR, Ribeiro MH, Rogaeva E, Sa A, Samaranch L, Sánchez-Valle R, Santana I, Tàrraga L, Valdivieso F, Singleton A, Hardy J, Clarimón J. Genetic screening of Alzheimer's disease genes in Iberian and African samples yields novel mutations in presenilins and APP. *Neurobiol Aging.* 2010;31(5):725-31. Epub 2008 Jul 30.

[248] Jayadev S, Leverenz JB, Steinbart E, Stahl J, Klunk W, Yu CE, Bird TD. Alzheimer's disease phenotypes and genotypes associated with mutations in presenilin 2. *Brain*. 2010;133:1143-1154.

[249] Rohrer JD, Warren JD. Phenomenology and anatomy of abnormal behaviours in primary progressive aphasia. *J Neurol Sci.* 2010;293:35-38.

[250] Carecchio M, Fenoglio C, De Riz M, Guidi I, Comi C, Cortini F, Venturelli E, Restelli I, Cantoni C, Bresolin N, Monaco F, Scarpini E, Galimberti D. Progranulin plasma levels as potential biomarker for the identification of GRN deletion carriers. A case with atypical onset as clinical amnestic Mild Cognitive Impairment converted to Alzheimer's disease. *J Neurol Sci.* 2009;287:291-293.

[251] Luty AA, Kwok JB, Thompson EM, Blumbergs P, Brooks WS, Loy CT, Dobson-Stone C, Panegyres PK, Hecker J, Nicholson GA, Halliday GM, Schofield PR. Pedigree with frontotemporal lobar degeneration-motor neuron disease and tar DNA binding protein-43 positive neuropathology: genetic linkage to chromosome 9. *BMC Neurol* 2008;8:32.

[252] Boxer AL, Mackenzie IR, Boeve BF, Baker M, Seeley WW, Crook R, Feldman H, Hsiung GY, Rutherford N, Laluz V, Whitwell J, Foti D, McDade E, Molano J, Karydas A, Wojtas A, Goldman J, Mirsky J, Sengdy P, Dearmond S, Miller BL, Rademakers R. Clinical, neuroimaging and neuropathological features of a new chromosome 9p-linked FTD-ALS family. *J Neurol Neurosurg Psychiatry*. 2011;82(2):196-203.

[253] Gijselinck I, Engelborghs S, Maes G, Cuijt I, Peeters K, Mattheijssens M, Joris G, Cras P, Martin JJ, De Deyn PP, Kumar-Singh S, Van Broeckhoven C, Cruts M. Identification of 2 Loci at Chromosome 9 and 14 in a Multiplex Family With Frontotemporal Lobar Degeneration and Amyotrophic Lateral Sclerosis. *Arch Neurol.* 2010;67(5):606-616.

[254] Morita M, Al-Chalabi A, Andersen PM, Hosler B, Sapp P, Englund E, Mitchell JE, Habgood JJ, de Belleroche J, Xi J, Jongjaroenprasert W, Horvitz HR, Gunnarsson LG, Brown RH Jr. A locus on chromosome 9p confers susceptibility to ALS and frontotemporal dementia. *Neurology*. 2006;66(6):839–844.

[255] Valdmanis PN, Dupre N, Bouchard JP, Camu W, Salachas F, Meininger V, Strong M, Rouleau GA. Three families with amyotrophic lateral sclerosis and frontotemporal dementia with evidence of linkage to chromosome 9p. *Arch Neurol.* 2007;64(2):240–245.

[256] Vance C, Al-Chalabi A, Ruddy D, Smith BN, Hu X, Sreedharan J, Siddique T, Schelhaas HJ, Kusters B, Troost D, Baas F, de Jong V, Shaw CE. Familial amyotrophic lateral sclerosis with frontotemporal dementia is linked to a locus on chromosome 9p13.2–21.3. *Brain*. 2006;129(4):868-876.

[257] Pearson JP, Williams NM, Majounie E, Waite A, Stott J, Newsway V, Murray A, Hernandez D, Guerreiro R, Singleton AB, Neal J, Morris HR. Familial frontotemporal dementia with amyotrophic lateral sclerosis and a shared haplotype on chromosome 9p. *J Neurol*. 2010. Nov 12. Epub ahead of print.

[258] Markus HS, Martin RJ, Simpson MA, Dong YB, Ali N, Crosby AH, Powell JF. Diagnostic strategies in CADASIL. *Neurology.* 2002;59: 1134-1138.

[259] Joutel A, Vahedi K, Corpechot C, Troesh A, Chabriat H, Vayssière C, Cruaud C, Maciazek J, Weissenbach J, Bousser MG, Bach JF, Tournier-Lasserve E. Strong clustering and stereotyped nature of Notch3 mutations in CADASIL patients. *Lancet*. 1997;350:1511-1515.

[260] Peters N, Opherk C, Bergmann T, Castro M, Herzog J, Dichgans M. Spectrum of mutations in biopsy-proven CADASIL. Implications for diagnostic strategies. *Arch Neurol.* 2005;62:1091-1094.

[261] Lesnik Oberstein SA. Diagnostic strategies in CADASIL. *Neurology.* 2003;60(12):2020.

[262] Ungaro C, Mazzei R, Conforti FL, Sprovieri T, Servillo P, Liguori M, Citrigno L, Gabriele AL, Magariello A, Patitucci A, Muglia M, Quattrone. Cadasil: Extended Polymorphisms and Mutational analysis of the NOTCH3 Gene. *J Neurosci Res.* 2009;87:1162-1167.

[263] Dotti MT, Federico A, Mazzei R, Bianchi S, Scali O, Conforti FL, Sprovieri T, Guidetti D, Aguglia U, Consoli D, Pantoni L, Sarti C, Inzitari D, Quattrone A. The spectrum of Notch3 mutations in 28 Italian CADASIL families. *J Neurol Neurosurg Psychiatry.* 2005;76:736-738.

[264] Cappelli A, Ragno M, Cacchiò G, Scarcella M, Staffolani P, Pianese L. High recurrence of the P1006C NOTCH3 mutation in central Italian patients with cerebral autosomal dominant arteriopathy with subcortical infarcts and leukoencephalopathy (CADASIL). *Neurosci Lett.* 2009;462:176-178.

[265] Bianchi S, Rufa A, Ragno M, D'Eramo C, Pescini F, Pantoni L, Cappelli A, Perretti A,

Zicari E, Zolo P, Inzitari D, Dotti MT, Federico A. High frequency of exon 10 mutations in the NOTCH3 gene in Italian CADASIL families: phenotype peculiarities. *J Neurol.* 2010;257:1039-1042.

[266] Mykkänen K, Savontaus ML, Juvonen V, Sistonen P, Tuisku S, Tuominen S, Penttinen M, Lundkvist J, Viitanen M, Kalimo H, Pöyhönen M. Detection of the founder effect in Finish CADASIL families. *Eur J Hum Genet.* 2004;12:813-819.

[267] Wang Z, Yuan Y, Zhang W, et al. NOTCH3 mutations and clinical features in 33 mainland Chinese families with CADASIL. J Neurol Neurosurg Psychiatry. 2010;Oct 9. [Epub ahead of print].

[268] Malandrini A, Gaudiano C, Gambelli S, Berti G, Serni G, Bianchi S, Federico A, Dotti MT. Diagnostic value of ultrastructural skin biopsy studis in CADASIL. *Neurology.* 2008;68:1430-1432.

[269] Mayer M, Straube A, Bruening R, Uttner I, Pongrazt D, Gasser T, Dichgans M, Muller-Höcher J. Muscle and skin biopsies are a sensitive diagnostic tool in the diagnosis of CADASIL. *J Neurol.* 1999;246:526-532.

[270] Brulin M, Godfraind C, Leteurtre E, Ruchoux MM. Morphometric analysis of ultrastructural vascular changes in CADASIL: analysis of 50 skin biopsy specimens and pathogenic implications. Acta Neuropathol 2002;104:241-248.

[271] Tikka S, Mykkänen K, Ruchoux MM, Bergholm R, Junna M, Pöyhönen M, Yki-Järvinen H, Houtel A, viitanen M, Baumann M, Kalimo H. Congruence between *NOTCH3* mutations and GOM in 131 CADASIL patients. *Brain*. 2009;132:933-939.

[272] Dichgans M, Ludwing H, M¨uller-H¨ocker J, Messerschmidt A, Gasser T. Small in-frame deletions and missense mutations in CADASIL: 3D models predict misfolding of Notch3 EGF-like repeat domains. *Eur J Human Genet.* 2000;8:280-285.

Acknowledgments

I would like to thank:

- Prof. Gian Maria Fabrizi, who has given me the opportunity to undertake this PhD program and, thanks to his advice, helped me to grow professionally;
- Dott.ssa Tiziana Cavallaro for the time she spent in reviewing the clinical and neuropathological data for the thesis, and for trust me;
- Dott. Moreno Ferrarini who supported me with his competence. He was not just a colleague, but a friend who allowed me to grow up through his disinterested and appropriate advices;
- Dott.ssa Anna Russignan who listened to me even in difficult times and with whom is born a beautiful friendship that I hope will grow even outside work;
- Dott.ssa Ermanna Turano, Dott.ssa Alessia Farinazzo and the other guys of the Neuropatholgy's laboratory because with their serenity and liking they have cheered up my days;
- my parents, because it is through their sacrifices and constant support that I now succeed in this title;
- Federico who encouraged and motivated me in this long career.